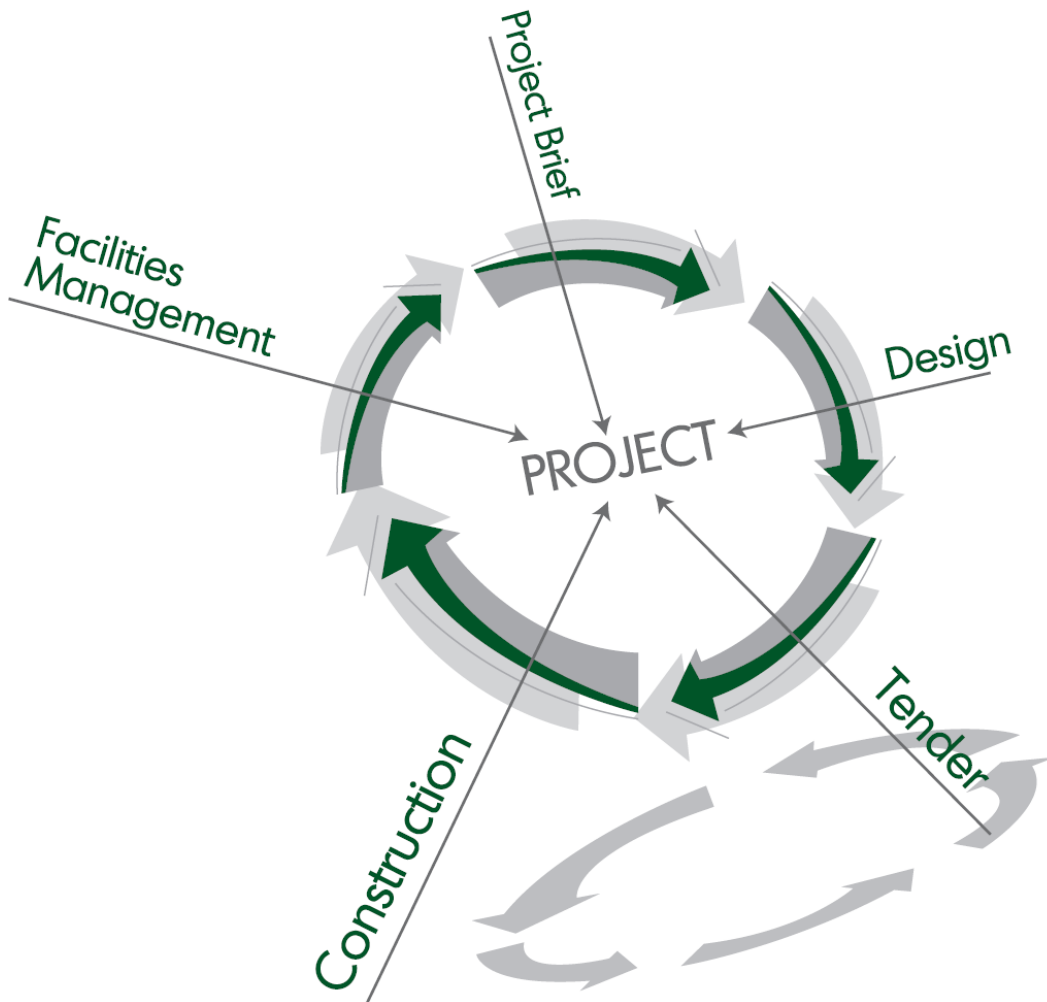


# Malaysian Construction Research Journal



# **MALAYSIAN CONSTRUCTION RESEARCH JOURNAL (MCRJ)**

**Volume 20 | No. 3 | 2016**

The Malaysian Construction Research Journal is indexed in

**Scopus Elsevier**

ISSN No.: 1985 - 3807

Construction Research Institute of Malaysia (CREAM)  
MAKMAL KERJA RAYA MALAYSIA  
1<sup>st</sup> Floor, Block E, Lot 8, Jalan Chan Sow Lin,  
55200 Kuala Lumpur  
MALAYSIA



# Contents

Editorial Advisory Board

Editorial

ANALYSIS OF ROCK BURST EVENT IN DEEP TBM EXCAVATION OF PAHANG-SELANGOR RAW WATER TRANSFER TUNNEL Romziah Azit and Mohd Ashraf Mohamad Ismail	1
PRE-CRACKED RC CONTINUOUS BEAMS STRENGTHENED IN SHEAR USING CFRP STRIPS ORIENTED AT 45°/135° Noorwirdawati Ali, Abdul Aziz Abdul Samad, J. Jayaprakash, Noridah Mohamad and Shahiron Shahidan	15
PERFORMANCE OF INNOVATIVE CELLULAR MAT (NEW LIGHTWEIGHT MATERIAL) USING MINI TRIAL EMBANKMENT Reventheran Ganasan, Alvin John Lim Meng Siang and Devapriya Chitral Wijeyesekera	29
EXPERIMENT AND COMPUTATIONAL FLUID DYNAMICS (CFD) SIMULATION OF FLOW CHARACTERISTICS IN DISSOLVED AIR FLOTATION TANK Nor Azalina Rosli, Mohamad Fared Murshed and Mohd Nordin Adlan	43
THE ADOPTION OF PASSIVE COOLING STRATEGY IN DESIGNING PUBLIC ASSEMBLY BUILDING – A DESIGN TYPOLOGY FOR THE TAOIST ACADEMIC CENTRE IN TROPICAL CLIMATE Loo Kok Hoo, Benson Lau and Foo Chee Hung	63
A REVIEW OF BUILDING INFORMATION MODELING (BIM)–BASED BUILDING CONDITION ASSESSMENT CONCEPT Adi Irfan Che-Ani, Mohd Harris, Muhammad Farihan Irfan Mohd-Nor, Mohd Zulhanif Abd-Razak and Afifuddin Husairi Hussain	85

# Editorial Advisory Board

**Zuhairi Abd. Hamid, Prof., Ir., Dr.,  
Chief Editor**

Construction Research Institute of Malaysia  
(CREAM)

**Mustafa Alshawi, Prof., Dr.**

University of Salford, UK

**Charles Egbu, Prof., Dr.**

University of Salford, UK

**C. S. Poon, Prof., Dr.**

Hong Kong Polytechnic University, Hong Kong

**George Ofori, Prof., Dr.**

National University of Singapore, Singapore

**Vilas Nitivattananon, Dr.**

Asian Institute of Technology (AIT), Thailand

**Abu Bakar Mohamad Diah, Datuk Wira, Dr.**

Deputy Minister of Science, Technology and  
Innovation, Malaysia

**Khairun Azizi Mohd. Azizli, Prof., Dr.**

Universiti Teknologi PETRONAS

**Roslan Zainal Abidin, Prof., Dr.**

Infrastructure University Kuala Lumpur

**Taksiah Abdul Majid, Prof., Dr.**

Universiti Sains Malaysia

**Joy Jacqueline Pereira, Prof., Dr.**

LESTARI, Universiti Kebangsaan Malaysia

**Muhd Fadhil Nuruddin, Prof., Ir., Dr.**

Universiti Teknologi PETRONAS

**Mohd. Saleh Jaafar, Prof., Dato', Ir., Dr.**

Universiti Putra Malaysia

**Norwina Mohd. Nawawi, Assoc. Prof., Ar. Dr.**

International Islamic University Malaysia

**Chan Toong Khuan, Ir., Dr.**

University of Melbourne, Australia

**Ahmad Baharuddin Abd. Rahman,  
Assoc. Prof., Dr.**

Universiti Teknologi Malaysia

**Lee Yee Loon, Prof., Dr.**

Universiti Tun Hussein Onn Malaysia

**Mohamad Omar Bin Mohamad Khaidzir, Dr.**

Forest Research Institute of Malaysia (FRIM)

**Kurian V. John, Prof., Dr.**

Universiti Teknologi PETRONAS

**Paridah Tahir, Prof., Dr.**

Universiti Putra Malaysia

**Roshana Takim, Assoc. Prof., Dr.**

Universiti Teknologi MARA

**Siti Hawa Hamzah, Prof., Ir., Dr.**

Universiti Teknologi MARA

**Mohamad Jamil Sulaiman, Ir., Dr.**

SIRIM Berhad

**Megat Azmi Megat Johari, Assoc. Prof., Dr.**

Universiti Sains Malaysia

**Kamaluddin Abdul Rashid, Mr.**

Jabatan Kerja Raya Malaysia

**Md. Abdul Mannan, Prof., Dr.**

Universiti Malaysia Sarawak

**Mahmood Md Tahir, Prof., Ir., Dr.**

Universiti Teknologi Malaysia

**Nasir Shafiq, Prof., Dr.**

Universiti Teknologi PETRONAS

**Noraini Bahri, Ir.**

Construction Industry Development Board (CIDB)  
Malaysia

**Badorul Hisham Abu Bakar, Prof., Dr.**

Universiti Sains Malaysia

**Zulkifli Mohamed Udin, Assoc. Prof., Dr.**

Universiti Utara Malaysia

**Abdul Rashid Abdul Aziz,  
Prof., Sr, Dr.**

Universiti Sains Malaysia

**Sobri Harun, Assoc. Prof., Dr.**

Universiti Teknologi Malaysia

**Aziz Saim, Assoc. Prof., Dr.**

Universiti Teknologi Malaysia

**Hamimah Adnan, Assoc. Prof., Datin, Sr, Dr.**

Universiti Teknologi MARA

**Abdul Karim Mirasa, Prof., Ir., Dr.**

Universiti Malaysia Sabah

**Wan Hamidon Wan Badaruzzaman,  
Prof., Ir., Dr.**

Universiti Kebangsaan Malaysia

**Hamidah Mohd. Saman, Assoc. Prof., Dr.**

Universiti Teknologi MARA

**Zainal Arifin Ahmad, Prof., Dr.**

Universiti Sains Malaysia

**Azmi Ibrahim, Prof., Dr.**

Universiti Teknologi MARA

**Mahyuddin Ramli, Prof., Dato', Ir., Dr.**  
Universiti Sains Malaysia

**Hajah Faridah Hj. Ismail, Assoc. Prof., Sr, Dr.**  
Universiti Teknologi MARA

**Mohd. Shahir Liew, Assoc. Prof., Ir., Dr.**  
Universiti Teknologi PETRONAS

**Low Kaw Sai, Assoc. Prof., Ir., Dr.**  
The Institution of Engineers Malaysia

**Narayanan Sambu Potty, Prof., Dr.**  
Mohandas College of Engineering and  
Technology, India

**Padzil Fadzil Hassan, Assoc. Prof., Dr.**  
Universiti Teknologi MARA

**Maria Zura Mohd. Zain, Ms.**  
Construction Research Institute of Malaysia  
(CREAM)

**Sugiura, Kunitomo, Dr.**  
Kyoto University, Japan

**Itaru Nishizaki, Dr.**  
Public Works Research Institute (PWRI), Japan

**Low Sui Pheng, Prof., Dr.**  
National University of Singapore, Singapore

**Zhangping You, Prof., Dr.**  
Michigan Technological University, USA

**Norhayati Abdul Hamid, Assoc. Prof., Dr.**  
Universiti Teknologi MARA

**Ahmad Hazim Abdul Rahim, Mr.**  
Construction Research Institute of Malaysia  
(CREAM)

**Mazlin Mokhtar, Prof., Dr.**  
LESTARI, Universiti Kebangsaan Malaysia

**Hassan Basri, Prof., Dato', Ir., Dr.**  
Universiti Kebangsaan Malaysia

**Khairuddin Abdul Rashid, Prof., Sr. Dr.**  
International Islamic University Malaysia

**Foo Chee Hung, Dr.**  
Construction Research Institute of Malaysia  
(CREAM)

**Dongping Fang, Prof. Dr.**  
Tsinghua University, China

**Ibnu Syabri, Prof., Dr.**  
Institut Teknologi Bandung, Indonesia

**Francis K.W. Wong, Prof., Dr.**  
Hong Kong Polytechnic University, Hong Kong

**Kobayashi Kiyoshi, Prof., Dr.**  
Kyoto University, Japan

**Sulaiman Abdulkareem, Dr.**  
University of Ilorin, Nigeria

**Aidah Jumahat, Dr.**  
Universiti Teknologi MARA

**Guest Editor:**

**Haryati Awang, Dr.**  
Universiti Teknologi MARA

**Edy Tonnizam Mohamad Ahmad Zahirani  
Ahmad Azhar, Assoc. Prof., Dr.**  
Universiti Teknologi Malaysia

**Ahmad Zahirani Ahmad Azhar, Dr.**  
International Islamic University Malaysia

**Razman Salim, Prof., Dr.**  
Universiti Teknologi Malaysia

**Mohd Azmi Ismail, Dr.**  
Universiti Sains Malaysia

**Secretariat:**

**Tengku Mohd Hafizi Raja Ahmad, Mr.**  
Construction Research Institute of Malaysia  
(CREAM)

**Nurulhuda Mat Kilau, Ms.**  
Construction Research Institute of Malaysia  
(CREAM)

## Editorial

### Welcome from the Editors

Welcome to the twentieth (20<sup>th</sup>) issue of Malaysian Construction Research Journal (MCRJ). In this issue, we are pleased to include six papers that cover wide range of research area in construction industry. The editorial team would like to express our sincere gratitude to all contributing authors and reviewers for their contributions, continuous support and comments.

In this issue:

**Romziah Azit and Mohd Ashraf Mohamad Ismail** evaluate the rock burst phenomenon at the Pahang-Selangor Raw Water Transfer Tunnel. Stress-strength method was used to analyse the tunnel behaviour under high overburden stress based on strength factor and tangential stress. Analysed results show that section with high overburden have high possibility of rock burst. Furthermore, it allows a reasonable prediction of the tunnel behaviours under different rock conditions, support systems and overburden stress which serves as a tool in the observational design and construction method for the deep tunnel excavation.

**Noorwirdawati Ali, et. al.**, present an experimental work on six full-scale reinforced concrete continuous beams with a size of 150x350x5800mm strengthened in shear using CFRP strips. They found that beams wrapped with CFRP strips recorded shear capacity enhancement of around 19.05% to 43.74% compared to the control specimens. Beams wrapped on four sides showed the highest shear capacity enhancement which was 43.74% compared to the control specimen, while beams wrapped on three sides showed the lowest shear enhancement which was 19.05%. The mode of failure of beams wrapped on four sides was shear with rupture of the CFRP strips. For beams wrapped on three sides, shear failure with CFRP rupture and debonding of CFRP strips from the concrete surface were observed.

**Reventheran Ganasan, et. al.**, investigate a new lightweight material which would minimize both differential and non-uniform settlement in soft ground/soils. The mini trial embankment test was built with the innovative cellular mats place underneath to identify the stiffness of the three different thicknesses. Less settlement was found along the mini trial embankment where the innovative cellular mat was placed. The innovative approach has shown to be able to improve the stiffness of soils as well as helping in allowing water/moisture to flow through in or out without condition of floating due to the porosity characteristics of the cellular structure.

**Nor Azalina Rosli, et. al.**, presents numerical and experimental investigations on the effects of number of nozzles and inlet velocity on the flow characteristics in a dissolved air flotation (DAF) tank pilot plant. The flow characteristics was modelled using a Eulerian multiphase and k- $\epsilon$  turbulence (RNG) model by using GAMBIT 2.3.16 and simulated using FLUENT 6.3.26 (Fluent Inc., Canonsburg, PA, USA) software. The velocity distribution, air injection location and internal baffle

inclination were investigated for 4 different experimental setups. The results indicated that the number of nozzles and inlet velocity were contributed to flow distribution and dispersion inside the tank and thus, influence the efficiency of the solid-liquid separation process in flotation tank.

By adopting an integrated environmental design approach which involved performative analysis through computational studies, **Loo Kok Hoo, et. al.**, successfully explores the workable sustainable architecture prototype for public assembly spaces in the tropical climate. The design scheme was then tested and modified to achieve the optimum spatial and environmental delight for the development of a Taoist Academic Centre (TAC). On a much larger scale, the present study provides a data base for future explorations that emphasized on bioclimatic design. As the study focused on the thermal performance of the public assembly building, future research can investigate further on modular construction system, materials, and even the renewable energy systems of the basic unit, as well as how such unit, in modular system, can be expanded through permutation and combination of various design programs.

Through literature review, covering the previous research, guidelines, reports, and other relevant sources, **Adi Irfan Che-Ani, et. al.**, study the potential of BIM in building condition assessment practice. A framework for building condition assessment via BIM for existing buildings was then proposed, with the aim of demonstrating the implementation of building condition assessment (BCA) toward achieving sufficient facility management practices for preventive maintenance, repair, and upgrading work.

*Editorial Committee*



# ANALYSIS OF ROCK BURST EVENT IN DEEP TBM EXCAVATION OF PAHANG-SELANGOR RAW WATER TRANSFER TUNNEL

**Romziah Azit And Mohd Ashraf Mohamad Ismail**

*School Of Civil Engineering, Engineering Campus, Universiti Sains Malaysia, 14300 Nibong Tebal, Seberang Perai Selatan, Pulau Pinang, Malaysia*

## **Abstract**

Tunnelling under high overburden and high in-situ stress can pose a major threat to the tunnel construction due to the phenomenon of rock burst. Rock burst is a typical phenomenon caused by underground excavation due to stress release and rock explosion where the rock masses broken in large or small pieces. Thus, predicting the occurrence of this phenomenon and its mechanism is important especially in determining suitable tunnel support system. In this study, the event of rock burst phenomenon at the Pahang-Selangor Raw Water Transfer Tunnel which is evaluated between the Chainage of 13 to 27 km beneath the Titiwangsa Main Range. This is the most critical section because of the high overburden up to 1200 m and presence several fault zones. Stress-strength method was used to analyse the tunnel behaviour under high overburden stress based on strength factor and tangential stress. Analysed results show that section with high overburden have high possibility of rock burst. Furthermore, it allows a reasonable prediction of the tunnel behaviours under different rock conditions, support systems and overburden stress which serves as a tool in the observational design and construction method for the deep tunnel excavation.

**Keywords:** *Deep tunnel excavation, high overburden, rock burst, stress-strength, tangential stress*

## **INTRODUCTION**

With worldwide economic and social development, there are more long tunnels at great depth being planned and constructed. Tunnel boring machines (TBMs) are strongly considered for long tunnels due to the schedule and overall cost benefits. Drill and blast excavation has however been adopted for some long tunnels due to geological risks and improved technology for high speed productivity. However, tunnelling under high overburden requires much concern on controlling the rock displacement and deformations around the excavation area. Excavation in rock will disturb the in-situ stress of the rock mass, and might lead to different problems such as rock burst, ground squeezing or rock swelling (Ortlepp, 2001).

Rock burst phenomenon is characterized by violent rock failure, may cause damage to underground opening and equipment include injuries and fatal accidents, construction and production delays and higher cost of construction and operation. Therefore, here is a need for the development of suitable computational methods for the prediction and control of rock bursts particularly for a safe and economical underground excavation (Sharan, 2007).

In many cases, the rock burst phenomenon occurs due to overstressing where the rock surrounding the excavation is brittle and massive (Bhasin and Grimstad, 1996). In the past several decades, a vast majority of work related to mechanism of rock bursts had been undertaken (Zhu *et. al.*, 2010). Instability commonly arises either from the structural features of the rock mass or from the high stress to strength conditions. Hence, it is important to analyse the strength of rock masses for predicting their behaviour in underground excavations. However, a rock burst is one of the most complicated mechanism and numerous affecting factors, which accounts for the difficulty of predicting its characteristics. Besides, the prevention of rock bursts is one of the key problems in the construction of deep tunnels, in which rock burst prediction is a basic problem and the essential reasons of this phenomenon

have not been understood.

This paper attempts to illustrate and interpret the various instability scenarios arising from the stress-strength relationships of the rock in deep tunnel excavation at Pahang-Selangor Raw Water Transfer Project (PSRWTP). The method of stress-strength ratio is a rock mechanic criterion, which makes use of the ratio of the tunnel walls maximum to predict rock burst. This simple and practical method, with definite meaning, has become fairly popular all over the world (Li *et. al.*, 2006).

## LITERATURE REVIEW

Rock burst phenomenon occurs in a brittle and isotropic rock mass when the rock mass strength is less than the magnitude of maximum tangential compressive stress (Panthi, 2012). Many researches based on the field data and theoretical analysis have been conducted to study the rock burst (Dalgöç, 2002; Kumar, 2003; Torabi, 2008; Brox, 2013), some empirical or semi-empirical methods have been proposed and employed extensively in the design or construction. However, no matter how good the site investigation and theoretical analysis, it is very difficult to predict exactly these failures at depth in the complex geological conditions. At present, the mechanism of rock burst is still not very clear and precise forecasting rock burst is the precondition of prevention rock burst. The mechanism of rock burst considered previously results from the constitutive behaviour of the rock material, and may involve shearing, splitting or crushing of the intact rock. Therefore, there is a need for research in this field due to the complexity of the problem and the limitations of predictive methods. Wang and Park (2001) discussed a comprehensive rock burst prediction based on analysis of strain energy in rocks, while Castro *et. al.* (2009) investigated factors Influencing fault-slip in seismically active structures. With regard to the mechanism involved, Manchao *et. al.* (2011) through experimental work, predicted of rock burst based on experimental systems and artificial intelligence techniques and Jiang *et. al.* (2010) provided a theoretical method to simulate the conditions causing rock burst using local energy release rate.

Knowledge of the mechanical and physical properties of the rock mass is of great importance in order to reduce rock burst problems from underground engineering (Zhang *et. al.*, 2012; Panthi, 2012; Li *et. al.*, 2012; Aydin, 2009). A better understanding of the failure process and a better rock mass strength prediction make it possible to reduce rock burst problems by improving design of the underground excavations, improve near surface tunnelling and reduce waste rock extraction. Therefore, it is important to estimate the strength of rock masses for predicting their behaviour and reduce rock burst problems in underground engineering due to deeper excavation. Edelbro (2003) was concluded in his review on rock mass strength that the uniaxial compressive strength, block size and shape, joint strength and a scale factor are the most important parameters that should be used when estimating the rock mass strength. Although the utility of the compressive strength value is limited, the unconfined compressive strength allows comparisons to be made between rocks and provides some indications of rock behaviour under more complex stress systems (Tang *et. al.*, 2000).

The in situ stresses at the deep underground engineering may have great impact on the stability (Zhang *et. al.*, 2012; Li *et. al.*, 2012; Panthi 2012; Hadjigeorgiou, 2012), especially where the stresses set up around it exceed the strength of the rock mass. Knowledge of in situ stress at a site is a key requirement for the information on the magnitudes and orientations of the principal stresses. For instance, the information is used to estimate the rock burst potential (Liu, 2011), to determine underground orientations (Panthi, 2012) and as boundary condition input to numerical modelling (Lehtonen *et. al.*, 2012). Rock at a certain depth is subjected to

stresses caused by the weight of overburden and from locked in original tectonic pressure. In-situ stress included the vertical stress and horizontal stress, where the horizontal stress is dependent on coefficient of lateral stress and vertical stress. Different coefficient of lateral stress will bring different conditions to the excavation opening. For example, differential stress, total displacement and strength factor around an excavated opening will be different for tunnel under same vertical stress but different horizontal stress (Hoek, 2006). The vertical stress can be approximated, to an acceptable level of accuracy, by the product of the depth below surface and the unit weight of the rock mass. However, in complex tectonic environments the vertical stresses may be lower or higher (Stille and Palmström, 2008) than the overburden stress.

Many researchers have investigated the complex rock burst from different points of view (Jin-shan *et al.*, 2007). However, different researchers have different opinions on the interpretation of forecast criteria. Many methods of forecasting rock bursts have been proposed, including rock mechanics assessment, stress detection, modern mathematical theories (Li *et al.*, 2006), some experience expressions, numerical Calculations and integral judgments (Xuan and Xuhui, 2009). At present, different scholars choose different parameters as evaluation index of criterion for rock burst, the classification of rock burst intensity also differed from each scholar (the criteria of rock burst is listed in Table 1). Based on previous researching criteria of rock burst, it chooses maximum tangential stress  $\sigma_{\theta}$ , uniaxial compressive strength  $\sigma_c$ (UCS), uniaxial tensile strength  $\sigma_t$ , ratio of maximum tangential stress to uniaxial compressive strength  $\sigma_{\theta}/\sigma_c$ , ratio of uniaxial compressive strength to uniaxial tensile strength  $\sigma_c/\sigma_t$  and Wet as the input features (Khanlari *et al.*, (2011); Xuan *et al.*, (2009); Le *et al.*, (2005); Wang and Park, 2001).

**Table 1.** Criteria and valuation of qualitative indexes in classification of rock burst category

Author	Rock bursts criteria	None Rock burst	Minor Rock burst	Medium Rock burst	Severe Rock burst
Xuan and Xuhui, 2009	1. Elastic energy index (Wet)	< 2.0	2.0 - 3.5	3.5-5.0	> 5.0
	2. Stress Coefficient ( $\sigma_{\theta}/\sigma_c$ )	< 0.2	0.2 - 0.3	0.3 - 0.55	> 0.55
	3. Rock brittleness Coef. ( $\sigma_c/\sigma_t$ )	> 40	40 - 26.7	26.7 - 14.5	< 14.5
Li <i>et al.</i> , 2005	1. Elastic energy index (Wet)	< 2.0	2.0 - 3.5	3.5 - 5.0	> 5.0
	2. Stress Coefficient ( $\sigma_{\theta}/\sigma_c$ )	< 0.2	0.2 - 0.3	0.3 - 0.55	> 0.55
	3. Rock brittleness Coef. ( $\sigma_c/\sigma_t$ )	> 40	40 - 26.7	26.7 - 14.5	< 14.5
Li <i>et al.</i> , 2006	1. Brittleness coef. of strength	> 40	40 - 26.7	26.7 - 14.5	< 14.5
	2. Stress coef. ( $\sigma_{\theta}/\sigma_c$ )	< 0.3	0.3 - 0.5	0.5 - 0.7	> 0.7
	3. Tendency index	< 2.0	2.0 - 3.5	3.5 - 5.0	> 5.0
	4. Linear elastic energy	< 40	40 - 100	100 - 200	> 200
Khanlari and Ali, 2011	1. Strain energy	50 - 100kJ/m <sup>3</sup>	100 - 150	150 - 200	> 200kJ/m <sup>3</sup>
	2. Rock brittleness( $\sigma_c/\sigma_t$ )	> 40	40 - 26.7	26.7 - 14.5	< 14.5
	3. Seismic energy		< 6.3 x 10 <sup>7</sup>	< 6.3 x 10 <sup>8</sup>	< 6.3 x 10 <sup>10</sup>
	4. Tangential stress ( $\sigma_{\theta}/\sigma_c$ )	< 0.3	0.3 -0.5	0.5 - 0.7	> 0.7

Author	Rock bursts criteria	None Rock burst	Minor Rock burst	Medium Rock burst	Severe Rock burst
Wang and Park, 2001	1. Rock brittleness( $\sigma_c/\sigma_t$ )	> 40	40 - 26.7	26.7 - 14.5	< 14.5
	2. Tangential stress ( $\sigma_\theta/\sigma_c$ )	< 0.3	< $6.3 \times 10^7$	< $6.3 \times 10^8$	< $6.3 \times 10^{10}$
	3. RQD	< 0.25	0.3 - 0.5	0.5 - 0.7	> 0.7

The occurrence of rock burst in deep hard rock tunnels is also important to recognize and evaluate prior to tunnel construction for constructability in terms of minimizing the risk of method of excavation, construction schedule and construction costs. Brox, (2013) has analysed observations and anecdotal information of rock burst and spalling from several deep tunnel projects in relation to an empirical method for the prediction of overstressing to assess the validity of the empirical method for tunnelling practitioners to adopt as a practical approach for assessing the potential for overstressing in deep hard rock tunnels. From his finding, new rock burst classification has been developed based on the overstressing in the form of rock burst and spalling occurred from direct observations in several deep hard rock tunnels around the world as listed in Table 2 below.

**Table 2.** List of rock burst in deep hard rock tunnels around the world (Brox, 2013)

Project	Year	Excavation method	Length (m)	Size (m)	Overburden (m)	Rock burst Condition
Allafal	1990	Drill & Blast	4.5	5	1150	Severe
Lesotho Transfer	1990	TBM	45	5	1300	Minor
Rio Blanco	1990	TBM	11.6	6.5	1200	Minor
Kemano T2	1991	TBM	8	6	650	Minor
Vereina	1996	TBM	21.6	5	1500	Severe
Manapouri	2002	TBM	10	10	1200	Minor
Casecnan	2005	TBM	21.6	5	1400	Moderate
Loetschberg	2008	Drill & Blast /TBM	34	8	2000	Severe
El Platanal	2009	Drill & Blast	12	6	1800	Severe
Ashlu	2010	TBM	44	4.1	600	Minor
Olmos	2000	TBM	14	5	2000	Severe
Jinping	2011	TBM	16	12	2500	Severe
Seymour Capilano	2011	TBM	14	4	550	Severe
Qinling	2012	TBM	28	12	2200	Minor
Pahang Selangor	2014	TBM	45	5.2	1200	Moderate

## PROJECT BACKGROUND

The purpose of the Pahang-Selangor raw water transfer tunnel is to convey raw water from the Semantan River in Pahang State to a water treatment plant in Selangor State, Malaysia. The transfer tunnel is 5.2 m diameter circular tunnel and 44.6 km long with 1/1,900 gradient. Excavation is primarily used a Tunnel Boring Machine (TBM) for about 35 km of the whole route with three TBM sections. Figure 1 shows the location map, the highest peak of tunnel under the Main Range is the border between Pahang and Selangor States. The mountain range forms the backbone of Peninsular Malaysia with the highest peak Mt. Korbu at 2183 m above sea level in Titiwangsa Main Range approximately 150 km north of the project site, and tunnel route crosses below the peak at about 1200m.

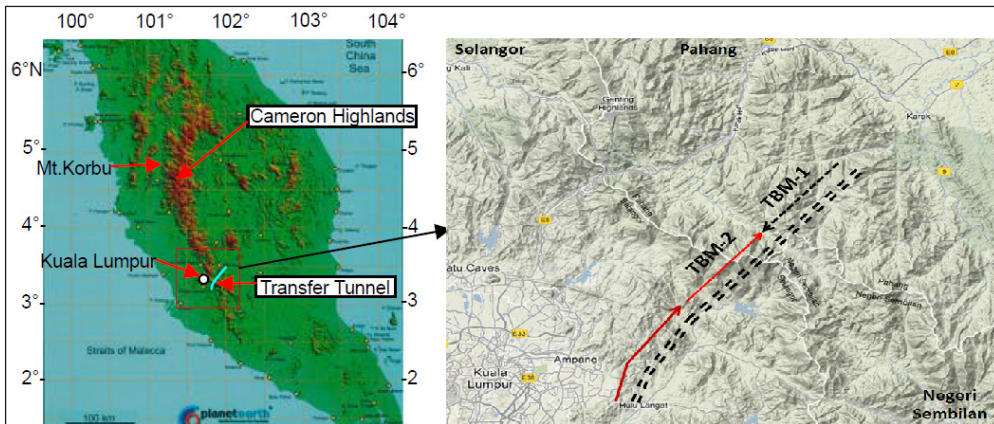


Figure1. Location Map (Shuttle Radar Topography Mission datasets, NASA)

## Geological Description

The project area is composed of Main Range granite and sedimentary rocks of Palaeozoic and Mesozoic age. Figure 2 shows the general geology along the tunnel, consists of Karak Formation (Silurian-Devonian) on the Pahang side (Ch. 0 to 4,000) which is made up of metasediments such as schist, phyllite, and hornfels; from Ch. 4,000 to the other end of the tunnel in Selangor, the geology consists of Granite (Triassic) with small sections of Hawthorndon Schist (Ordovician-Silurian). This rock is mainly black shale to schist, strongly folded by the intrusion of granitic rocks in Triassic age. The Granite is subdivided into 3 sub-types, namely Bukit Tinggi Granite, Genting Sempah micro-Granite and Kuala Lumpur Granite. The tunnel alignment is intersected by several faults with a strike essentially N-S, but with increasing occurrence of NW-SE along the western of the tunnel. The faults are generally indicating a general tensional state of stress in the central part of the range. There are also several lineaments that have been identified from regional topographic trends such as stream channels. The faults and lineament appear to be integral parts of the granite emplacement, uplift and alteration.

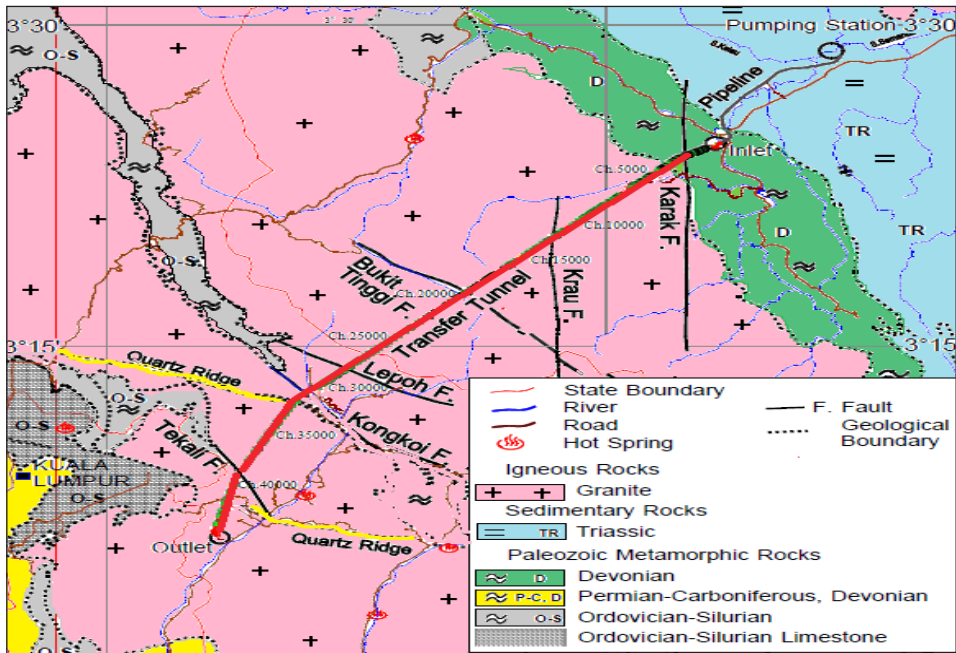


Figure 2. Geological condition along the tunnel alignment

## TBM Excavation

Three main beam type Robbins Tunnel Boring Machines with diameter of 5.2 m were selected for the tunnel excavation. The TBMs were designed to excavate granite with 80% of the excavation length having compressive strength over 200 MPa with; individual tunnel drives lengths of up to 11.7 km; major faults, quartz dikes and several overlying valleys (Kawata *et. al.*, 2014). The actual TBM excavation monthly progress rates achieved ranged from 200 m to 660 m or average 16 m per day. TBM excavation was constantly monitored and controlled from the operation room. The exposed surfaces in the tunnels were mapped continuously by geologists in 10 to 50m sections as excavation progressed and Schmidt rebound hammer value was recorded every 5 m of tunnel to give an approximate measurement of rock strength. The rock was classified into different types by empirical method using the Japan Highway System as a basis for selection of rock support. The rock support was designated into categories consisting of types A, B, CI, CII, D and E; type A requiring no support and E is being the heaviest support (steel rib H-125, 500 mm interval; fibre mortar 20-180 mm thick; steel lagging; backfill grouting and/or forepoling). Figure 3 shows the Installation System on TBM was conducted.

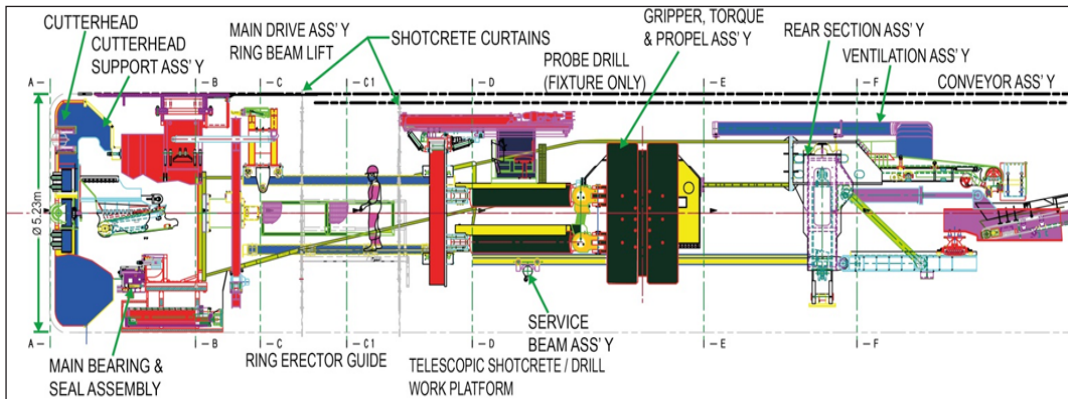


Figure 3. Support Installation System on TBM

## Rock Burst Phenomena

During the excavation below high overburden zones the rock burst and spalling has occurred from Ch. 24610 m to upstream. Main positions of rock burst phenomena are side wall and tunnel face as shown in Figure 4. Serious joint sets such as core disking did not accompany on the wall. Generally, condition of rock is hard and massive without any requirements for special support except shotcrete in moderate rock burst zones. Once rock burst happened, the process of behaviour changed to be stable.



Figure 4. Rock burst in TBM 2 at Ch. 24610

## METDODOLOGY

### In-situ Stress Test

The compact conical-ended borehole overcoring (CCBO) and hydraulic fracturing method were applied as the initial stress measurement for this project which is internationally regarded as the simplest, easiest and highest accuracy of measurement (Obara & Sugawara, 2003; Kang, Ishiguro, & Obara, 2006). The initial stress tensor  $\{\sigma_x, \sigma_y, \sigma_z, \tau_{xy}, \tau_{yz}, \tau_{zx}\}$  is calculated from 24 strain tensor, and an eigenvalue and an eigenvector of these 6 stress components are principal stress. Diameter of drill hole is 76 mm and the tests were done at more than 10 meters depth from the tunnel wall. Figure 5 shows the structural view of cone with 24 gauges strain cell and the stress measurement using CCBO at the PSRWT.

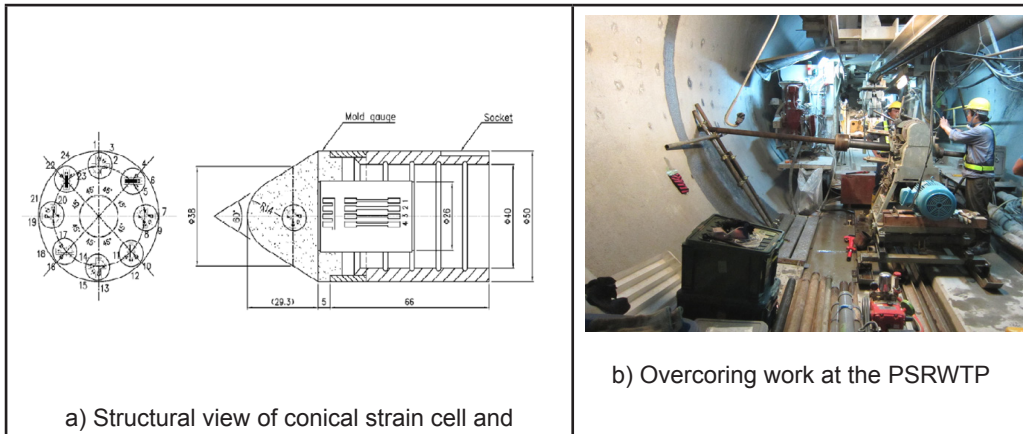


Figure 5. Photo of stress measurement using CCBO

To apply the CCBO, it is necessary to drill borehole with polished and conical shaped borehole bottom, to where be glued strain cell consisted of 8 sets of rosette gauge with three components. Then carrying out overcoring of the borehole at the same diameter caused the stress relief of rock. At that time the released strain is measured and it is used to determine the three-dimensional initial stress (six independent stress components) by stress analysis based on the theory of elasticity. CCBO is applicable to medium-hard and hard rock in isotropic homogeneous with over 100mm intervals of fracture and it is possible to apply in case there is no water seep out or spring from the borehole bottom. The borehole should be drilled with 5 degrees upwards on the horizontal plane and the limit of measurement depth is about 30m from the borehole mouth because of equipment specification.

In this study to assess the stress conditions below high overburden, in-situ stress test was carried out at three locations in a tunnel, at which overburdens are 227 m, 1130 m and 157 m respectively as shows in Figure 6.

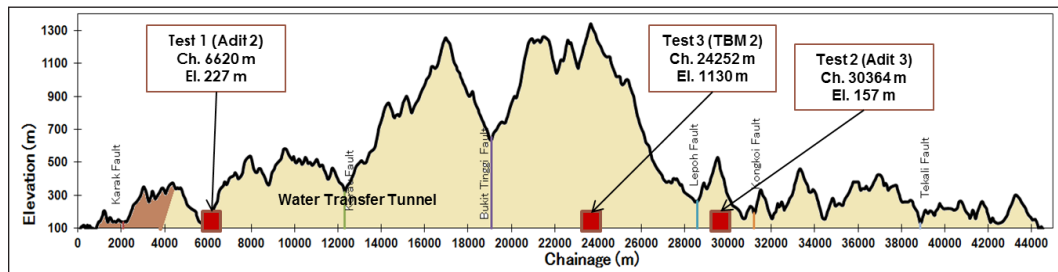


Figure 6. In-situ stress test locations

The gravitational vertical stress at a depth ( $z$ ) is the product of the depth and the unit weight ( $\gamma$ ) of the overlying rock mass. The vertical stress tends to be on average equal to the weight of the overburden. Thus, the vertical gravitational stress ( $\sigma_v$ ) was estimated from the simple relationship of  $\gamma z$  indicating that the overburden stress should increase linearly with depth. The horizontal stresses, which receive considerable attention from civil engineers, are influenced by global factors (e.g., plate tectonics) and local topographic features. Therefore, the ratio of horizontal stress to vertical stress ( $k = \sigma_H / \sigma_v$ ) was used for indicating the local tectonic stress settings.

## Analysis on Rock Burst

The radial stress, tangential stress and displacement around the tunnel were calculated using the Kirsch equation, referring to Equation:

$$\sigma_r = \frac{p+q}{2} \left( 1 - \frac{a^2}{r^2} \right) + \frac{p-q}{2} \left( 1 + \frac{3a^4}{r^4} \right) \frac{4a^2}{r^2} \cos 2\theta \quad (1)$$

$$\sigma_\theta = \frac{p+q}{2} \left( 1 + \frac{a^2}{r^2} \right) + \frac{p-q}{2} \left( 1 + \frac{3a^4}{r^4} \right) \cos 2\theta \quad (2)$$

$$\tau_{\theta r} = \frac{p-q}{2} \left( 1 - \frac{3a^4}{r^4} + \frac{2a^2}{r^2} \right) \sin 2\theta \quad (3)$$

where  $a$  and  $r$  are the tunnel radius and distance from the centre of tunnel,  $\theta$  is counter clockwise angle from the spring line of right side wall, and  $p, q, \sigma_v$ , and  $\sigma_h$  are the vertical and horizontal stress respectively.

Along the face of tunnel wall,  $r$  is equal to  $a$ , stress for radius direction  $\sigma_r$  and shear stress  $\tau_{\theta r}$  along the tunnel wall are both zero. The positions of maximum stress along the wall are right and left side wall as 0 and 180 degrees by means of  $\theta$ . Maximum stress on the side wall ( $\theta$  as 0 and 180 degrees) is simplified and calculated by:

$$\sigma_\theta = 3\sigma_v - \sigma_{hmin} \quad (4)$$

where  $\sigma_\theta$  is a tangential stress,  $\sigma_v$  is a vertical stress, and  $\sigma_{min}$  is a minimum horizontal stress.

## RESULT AND DISCUSSION

### In-situ Stress Test Results

Test results in Adit 2, Adit 3 and TBM 2 are shown in Table 1 and Schmidt Net Projection of each principle stress is shown in Figure 4. Maximum stress values are 7.45 MPa, 28.76 MPa and 10.85 MPa in Adit 2, TBM 2 and Adit 3 respectively. General trend of the maximum stress conditions in Adit 2 and Adit 3 are rather horizontal trend of north-south to northeast-southwest, whereas in TBM 2 is almost vertical as 28.22 MPa. This vertical stress value is similar to the calculated overburden pressure ( $\rho gh$ ) as 29.4 MPa bellow overburden of 1130 m by assumed density of 2.655 g/cm<sup>3</sup>. Maximum stress on the side wall ( $\theta$  as 0 and 180 degrees) is simplified and calculated by stress value from TBM 2 as vertical stress as 28.22 and minimum horizontal stress as 5.17.

The principal stress directions are plotted on the lower hemispherical stereographic projection displayed in Figure 7. In Adit 2, the maximum principal stress inclined from the south side (outlet of the tunnel) to the north. In this section, the maximum principal stress was about three times of the minimum principal stress, and the differential stress among the principal stresses was relatively large. The stress state measured at Adit 2 and Adit 3, which maximum principal stress axis is conformable to the axis of the tunnel, is beneficial to the stability of tunnel excavation.

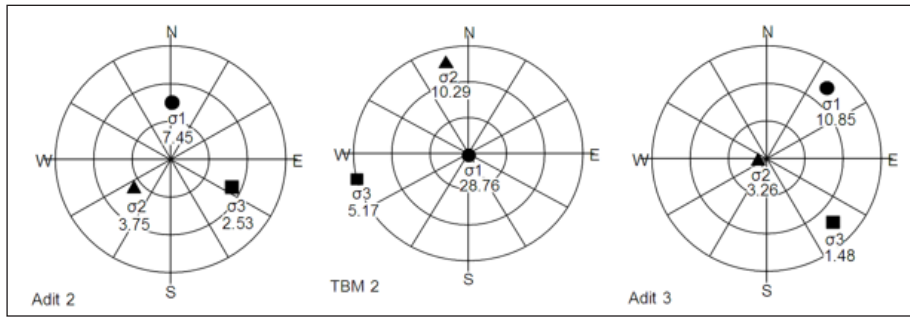


Figure 7. Projection of Major Stress (Lower hemisphere projection)

Only the result from TBM 2 was selected for this analysis. The in-situ measurement of TBM 2 indicates that the direction of the maximum principal stress was nearly vertical with a value of 28.76 MPa, while the minimum principal stress was observed as 5.17 MPa. The measured value is close to the expected vertical stress of 29.6 MPa ( $1130 \text{ m} \times 2.67 \text{ g/cm}^3 \times 9.81 \text{ m/s}^2 = 29.6 \text{ MPa}$ ). The K value (ratio of horizontal and vertical stress) was 0.38, which is very low for an area supposedly unaffected by active tectonic movement.

### Analysis of Rock Burst

According to Kirsch theory of elasticity for circular openings, the maximum tangential stress has been calculated using Eq. (4). Based on the maximum principal stress of the in-situ stress measurement, the maximum tangential compressive stress ( $\sigma_{\theta_{max}}$ ) is 81 MPa, while the mean value of the UCS ( $\sigma_c$ ) of the rock ranges from 78 MPa to 120 MPa. Thus, the problem of rock burst is estimated to be highly likely. A rock burst occurs in a brittle and isotropic rock mass when the strength ( $\sigma_c$ ) of this mass is less than the value of the maximum tangential compressive stress. However, considering all possible variations of rock strengths and rock stresses, only a minor rock burst or spalling is likely to occur. Table 3 shows the overstressing characterization from Hoek & Marinos (2009), minor to moderate spalling has been estimated at the PSRWTP.

The ratio of the maximum boundary stress to the uniaxial compressive strength ( $\sigma_{\theta_{max}}/\sigma_c$ ) is suggested as the key parameter in identifying the severity of rock burst. Figure 8 presents a plot of the tangential stresses versus the uniaxial compressive strength ( $\sigma_{\theta}/\sigma_c$ ) and elevation versus chainages based on the horizontal stress ratios of 0.38. Sections with high overburden (more than 1,000 m) exhibit the possibility of medium rock burst. Based on site observations, the overstress situation around the excavation site is seemingly favorable in the circle area highlighted in Figure 8.

Table 3. Overstressing Classification (Hoek & Marinos, 2009)

$\sigma_{\theta_{max}}/\sigma_c$	Overstressing Classification
0.45	minor spalling
0.6	moderate spalling
0.9	severe spalling
1.2	extreme spalling
1.6	rock bursts

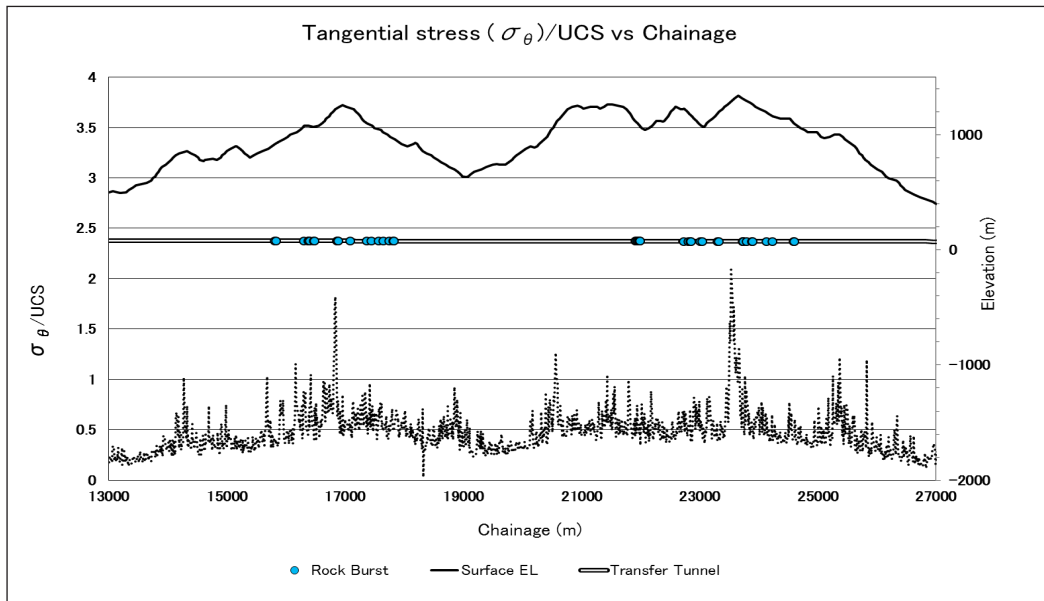


Figure 8. The tangential stress to the uniaxial compressive strength and observed rock burst

## CONCLUSION

As a result of In-situ stress test, the vertical stress and maximum horizontal stress are 28.22 MPa and 10.83 MPa respectively, lateral stress ratio  $k$  is 0.38. Vertical stress dominates in deeper part of the Main Range Granite in Malaysia, and it is match to the 1130 m overburden pressure of rock by approximate density of  $2.6 \text{ g/cm}^3$ . The maximum tangential stress at the circular tunnel wall is approximately 80 MPa at left and right wall. Considering above analyzed values, mechanical stability of tunnel under the high overburden, it is estimated that the rock burst is very unlikely to occur. However, due to the variation of rock strength and rock stress, there were some minor and medium rock burst phenomena. The rock burst occurred where certain criteria were fulfilled, such as overburden exceeding 800 m; the rock was brittle, massive with wide joint spacing, dry, had stress-strength ratio of tangential stress to compressive stress ( $\sigma_\theta/\sigma_c$ ) from 0.4 to 0.9.

The phenomena were occurred locally on the side wall in higher overburden zones in TBM 1 and TBM 2 section from Ch. 24612 to upstream within hard and massive rock conditions, no special additional countermeasures have been required in these breakout zones. The excavation successfully had been completed without major accident. Thus, with the tunnelling industry in Malaysia is developing rapidly, we believe this project will be a useful benchmark for future tunnel projects in Malaysia and elsewhere.

## ACKNOWLEDGEMENT

This research was supported by the Fundamental Research Grant Scheme of the Ministry of Education of Malaysia: Analysis of Rock Burst Behaviour under Overstressed Rock in Deep Tunnel Excavation across the Titiwangsa Range, Malaysia. Grant No.: 203/PAWAM/6071259.

## REFERENCES

- Aydin, A. (2009). ISRM Suggested method for determination of the Schmidt hammer rebound hardness: Revised version. *International Journal of Rock Mechanics and Mining Sciences*, 46(3), 627–634.
- Bhasin, R., & Grimstad, E. (1996). The Use of Stress-Strength Relationships in the Assessment of Tunnel Stability, *International Journal of Rock Mechanics and Mining Sciences*. 11(1), 93–98.
- Brox, D. (2013). Evaluation of overstressing of deep hard rock tunnels Examples of overstressing in deep tunnels, *World Tunnel Congress 2013 Geneva Underground – 731–737*.
- Castro, L. A. M., Carter, T. G., & Lightfoot, N. (2009). Investigating Factors Influencing Fault-Slip in Seismically Active Structures, *Proceedings of the 3rd CANUS Rock Mechanics Symposium, Toronto, 2009(May)*, 1–12.
- Dalgöç, È. (2002). A comparison of prediction and actual tunnel behaviour in the Istanbul Metro, Turkey. *Engineering Geology*, 63.
- Edelbro, C. (2003). Rock mass strength: a review. *Department of Civil Engineering Division of Rock Mechanics*, 1402–1536.
- Hadjigeorgiou, J. (2012). Where do the data come from. *Australian Centre for Geomechanics*, 259–278.
- E. Hoek, E. & Marinos, P. (2009). Tunnelling in overstressed rock. *Keynote address presented at EUROCK2009, Dubrovnik, Croatia, 29-31 October 2009*. 49–60
- Jiang, Q., Feng, X.-T., Xiang, T.-B., & Su, G.-S. (2010). Rock burst characteristics and numerical simulation based on a new energy index: a case study of a tunnel at 2,500 m depth. *Bulletin of Engineering Geology and the Environment*, 69(3), 381–388.
- Jin-shan, S. U. N., Qi-hu, Z. H. U., & Wen-bo, L. U. (2007). Numerical Simulation of Rock burst in Circular Tunnels Under Unloading Conditions, *Journal of China University of Mining & Technology*, 17(4), 2–6.
- Kang, S. S., Ishiguro, Y., & Obara, Y. (2006). Evaluation of core disk rock stress and tensile strength via the compact conical-ended borehole overcoring technique, *International Journal of Rock Mechanics and Mining Sciences*. 43, 1226–1240.
- Kawata, T., Nakano, Y., Matsumoto, T., Mito, A., Pittard, F., & Azman, A. A. S. (2014). The Relationship between TBM Data and Rock burst in Long-Distance Tunnel Pahang-Selangor Raw Water Transfer Tunnel Malaysia. *8th Asian Rock Mechanics Symposium*, 256-271.
- Khanlari, G. R., & Ali, B. (2011). Analysis of rock burst in critical section of second part of Karaj- Tehran Water Supply Tunnel, *ISGSR 2011 - Vogt, Schuppener, Straub & Bräu (eds)*, 661–667.
- Kumar, P. (2003). Development of empirical and numerical design techniques inburst prone groundat the Red Lake Mine.
- Lehtonen, a., Cosgrove, J. W., Hudson, J. a., & Johansson, E. (2012). An examination of in situ rock stress estimation using the Kaiser effect. *Engineering Geology*, 124, 24–37. doi:10.1016/j.enggeo.2011.09.012
- Li, S., Feng, X.-T., Li, Z., Chen, B., Zhang, C., & Zhou, H. (2012). In situ monitoring of rock burst nucleation and evolution in the deeply buried tunnels of Jinping II hydropower station. *Engineering Geology*, 137-138, 85–96.
- Liu, C. (2011). *Procedia Engineering First International Symposium on Mine Safety Science*

- and Engineering Distribution laws of in-situ stress in deep underground coal mines, 1–9.
- Li, T., Xiao, X., & Shi, Y. (2006). Comprehensive integrated methods of rock burst prediction in underground engineering, *Engineering Geology*, (594), 1–10.
- Manchao, H., Xuena, J., Peixoto, A., Sousa, L. R., Sousa, R. L., & Miranda, T. (2011). Prediction of Rock burst Based on Experimental Systems and Artificial Intelligence Techniques, 4.
- Obara, Y., & Sugawara, K. (2003). Updating the use of the CCBO cell in Japan : overcoring case studies *International Journal of Rock Mechanics and Mining Sciences*, 40, 1189–1203.
- Ortlepp, W. D. (2001). The behaviour of tunnels at great depth under large static and dynamic pressures. *Tunnelling and Underground Space Technology*, 16, 41–48.
- Panthi, K. K. (2012). Evaluation of rock bursting phenomena in a tunnel in the Himalayas. *Bulletin of Engineering Geology and the Environment*, 71(4), 761–769.
- Sharan, S. K. (2007). A finite element perturbation method for the prediction of rock burst, 85, 1304–1309.
- Sirait, B., Kresna, R., & Priagung, N. (2013). Rock burst Prediction of a Cut and Fill Mine by Using Energy Balance and Induced Stress, 6, 426–434.
- Torabi, S. R. (2008). An Empirical Approach in Prediction of the Roof Rock Strength in Underground Coal Mines, 132–136.
- Wang, J. -a., & Park, H. D. (2001). Comprehensive prediction of rock burst based on analysis of strain energy in rocks. *Tunnelling and Underground Space Technology*, 16(1), 49–57.
- Xiaohong Li, Xinfei Wang, Yong Kang, and Z. H. (2005). Artificial Neural Network for Prediction of Rock burst 2 Application of Artificial Neural Network, (50334060), 983–986.
- Xuan, Z., & Xuhui, B. (2009). The Forecasting of Rock burst in Deep-buried Tunnel with Adaptive Neural Network. *2009 International Conference on Industrial and Information Systems*, 3–6.
- You, Z., & Chen, J. (2012). In-situ Stress Features and Prediction Analysis for Rock Burst in Deep and Over-Length Highway Tunnel, (388), 2647–2657.
- Zhang, C., Feng, X., & Zhou, H. (2012). Estimation of in situ stress along deep tunnels buried in complex geological conditions. *International Journal of Rock Mechanics and Mining Sciences*, 52, 139–162.
- Zhu, W. C., Li, Z. H., Zhu, L., & Tang, C. A. (2010). Numerical simulation on rock burst of underground opening triggered by dynamic disturbance. *Tunnelling and Underground Space Technology incorporating Trenchless Technology Research*, 25(5), 587–599.



# PRE-CRACKED RC CONTINUOUS BEAMS STRENGTHENED IN SHEAR USING CFRP STRIPS ORIENTED AT 45°/135°

Noorwirdawati Ali<sup>1</sup>, Abdul Aziz Abdul Samad<sup>1</sup>, J. Jayaprakash<sup>2</sup>, Noridah Mohamad<sup>1</sup> and Shahiron Shahidan<sup>1</sup>

<sup>1</sup> Faculty of Civil and Environmental Engineering, Universiti Tun Hussein Onn Malaysia, 86400 Parit Raja, Batu Pahat, Johor, Malaysia

<sup>2</sup> The University of Nottingham University Malaysia Campus, Jalan Broga, 43500 Semenyih, Selangor, Malaysia

## Abstract

This study presents an experimental work on six full-scale reinforced concrete continuous beams with a size of 150x350x5800mm strengthened in shear using CFRP strips. Modes of failure and crack patterns of the beams were explained in detail. The strengthening scheme only focused on CFRP strips oriented at 45°/135°. The variables involved wrapping schemes which are four sides and three sides and shear span to effective depth ratio,  $a_v/d$  which are 2.5 and 3.5. The type of FRP used was bi-directional CFRP strips. Two beams were un-strengthened and treated as the control specimens whilst the other four beams were wrapped with CFRP strips with 45°/135° orientation. From the experimental results, all beams experienced shear failure. Beams wrapped with CFRP strips recorded shear capacity enhancement of around 19.05% to 43.74% compared to the control specimens. Beams wrapped on four sides showed the highest shear capacity enhancement which was 43.74% compared to the control specimen while beams wrapped on three sides showed the lowest shear enhancement which was 19.05%. The mode of failure of beams wrapped on four sides was shear with rupture of the CFRP strips. For beams wrapped on three sides, shear failure with CFRP rupture and debonding of CFRP strips from the concrete surface were observed.

**Keywords:** CFRP strips, Continuous beam, Shear strengthening, Repair, Pre-cracked

## INTRODUCTION

The use of Fibre Reinforced Polymer (FRP) laminates as a strengthening material has become a well-known method in the field of civil engineering. However, prior to civil engineering, in the early days back to the 1930s, FRP laminates have been widely used in many areas such as aerospace, transportation, maritime and electrical engineering (ACI 440, 2006). In civil engineering, old buildings such as historical building that need to be preserved are among the reasons why FRP has been widely used. FRP laminates are chosen because of their good characteristics such as high resistance to corrosion, high strength to weight ratio, ease of installation, non-magnetic properties, resistance to chemicals and high tensile strength. These advantages are among the reasons FRP composites materials are an alternative solution to strengthen existing structures (Chajes *et. al.*, 1995; Norris *et. al.*, 1997; Grace *et. al.*, 1998; Khalifa & Nanni 2000; Taljsten 2003; Adhikary & Mutsuyoshi 2004). Old buildings and existing structures have motivated many researchers and organizations to find alternative materials and techniques to restore deteriorating and deficient structures (Taljsten, 2003). In Malaysia, FRP laminates were used to strengthen and repair the structure of the Middle Ring Road 2 (MRR2) in Kepong when the flyover was seriously damaged and cracks were clearly seen at the piers and girders. Past researches have shown great interest in shear and flexural strengthening on reinforced concrete structures. Unlike flexural behaviour of cracked reinforced concrete beams which can be well predicted, the prediction of shear behaviour of reinforced concrete beams is a tough task due to the complexity of shear transfer

mechanism (El-Ariss, 2007).

Structures that fail in shear are more dangerous than flexural failure because shear failure occurs suddenly and without any warning (Khalifa & Nanni, 2000, Zhang and Hsu, 2005; Jayaprakash *et. al.*, 2008). Shear failure is a diagonal tension failure that is brittle in nature and should be avoided (Wang *et. al.*, 2007). The behaviour of reinforced concrete in shear is very complex as the current code and design procedures are based on analysis of experimental results and model assumption rather than an exact universally acceptable theory. The complexity is due to the non-homogeneity of material, nonlinearity of material, cracks, presence of reinforcement, load effects and the environment (Pillai *et. al.*, 1999). Generally, most of investigations carried out experimentally by previous researchers focused on shear strengthening of reinforced concrete beams that are simply supported. In reality, the existing model has not been confirmed for shear strengthening in areas subjected to combine high flexural and shear stresses or in regions of negative moment (ACI Committee, 2008), whereas most of existing beams are in the form of continuous condition. Furthermore, there are restraints to add shear reinforcement to existing reinforced concrete beams when beams are a part of a floor-beam system. For those reasons, FRP has been seen as the solution to overcome the problems observed. Therefore, the application of composite material has been emphasized to extend the service life of existing concrete structures. In this research, six continuous beams repaired using CFRP strips have been cast and tested where the results were then analysed and presented here. This study applied three and four-side wrapping schemes. Beams with the three-side wrapping scheme were not anchored using any technique or material. Several studies have been conducted on techniques to prevent debonding of FRP layers such as Near Surface Mounted (NSM), Externally Bonded Reinforcement on Grooves (EBROG) and Externally Bonded Reinforcement in Grooves (EBRIG) (Mostofinejad, 2016). However, most of the studies focused on flexural strengthening. Therefore, further research should be conducted in shear strengthening using these different techniques.

## **METHODOLOGY**

### **Specimens Design**

This study involved the fabrication and testing of six reinforced concrete two-span continuous beams measuring 150mm in width, 350mm in depth and 2630mm in effective length of each span. Beams were designed to fail in shear where it was provided with minimum links of R6-200 ( $A_{sv} = 56.55 \text{ mm}^2$ ) with the capacity of 79.72 kN whereas the shear force for  $a_v/d=2.5$  and 3.5 are 243.40 kN and 234.48 kN respectively. It means that the R6-200 was not enough to cater to the shear force applied. The size and length of the beam was selected and designed based on the limitation of testing frames available at the laboratory. The specimens were grouped based on two different values of shear span to effective depth ratio,  $a_v/d$ , which were 2.5, and 3.5 respectively as shown in Table 1. The value of shear span ( $a_v$ ) can be calculated with the determined  $a_v/d$  (2.5 and 3.5) and size of the beam (to get the value of effective depth,  $d$ ). For beams with  $a_v/d=2.5$  and 3.5, the shear span length was 780mm and 1080mm respectively.

**Table 1.** Summary of specimens

Specimen	$a_v/d$	CFRP Strips Orientation (°)	Wrapping Scheme
Beam 1-0	2.5	-	-
Beam 2-3	2.5	45/135	4 sides
Beam 2-4	2.5	45/135	3 sides
Beam 3-0	3.5	-	-
Beam 3-3	3.5	45/135	4 sides
Beam 3-4	3.5	45/135	3 sides

Beam 1-0 and 3-0 were the control specimens (without CFRP). For beams with  $a_v/d=2.5$ , Beam 2-3 was pre-cracked and wrapped on four sides with CFRP strips. For Beam 2-4, this beam was also pre-cracked but wrapped on three-sides of the beam. On the other hand, Beam 3-3 and Beam 3-4, having the same characteristics as Beam 2-3 and Beam 2-4 except for the shear span to effective depth ratio, had an  $a_v/d$  of 3.5. Except for control specimens, the other beams were pre-loaded prior to strengthening using CFRP strips. The pre-crack load was based on the ultimate load of the control beam. After the beams were pre-loaded, CFRP strips were applied and allowed to cure the epoxy for one week. During the one week curing period, pre-cracked beams were loaded with a sustained load of 10kN. After one week, the beam was loaded to failure. During the application of load, the behaviours of the beams were observed with respect to the first crack, ultimate load, formation of critical shear and flexural crack, crack pattern, load history and modes of failure. Figures 1 and 2 show the reinforcement details and cross-section of the beam. All specimens were designed with the same reinforcement details. Figures 3 and 4 show the wrapping scheme and arrangement of loading for beams with  $a_v/d$  values of 2.5 and 3.5 respectively.

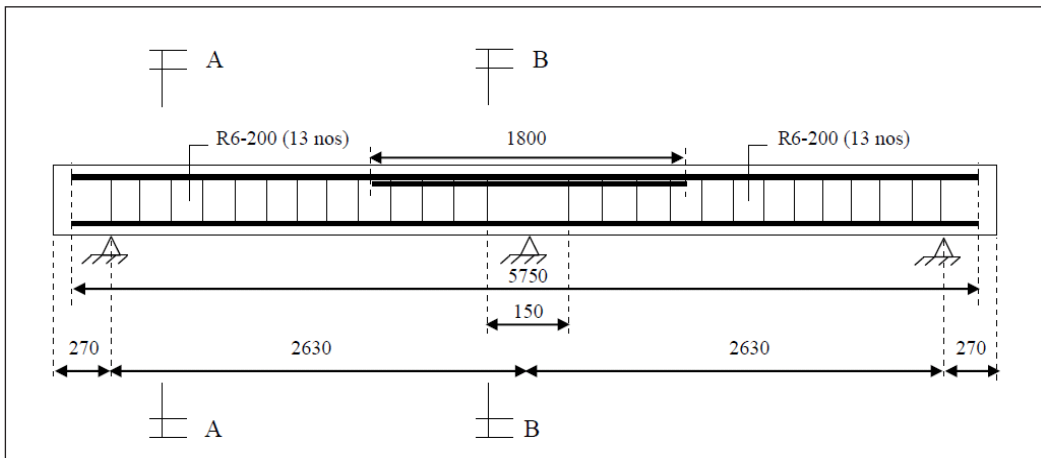


**Figure1.** Reinforcement details (unit in mm)

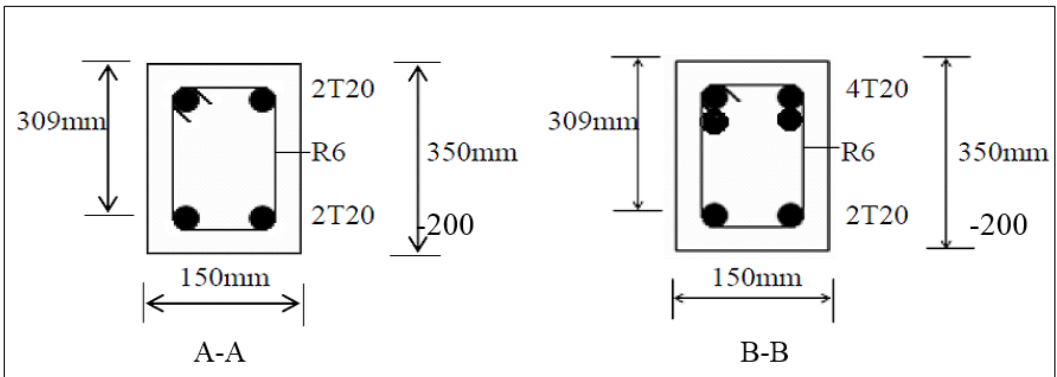


Figure 2. Typical cross section of the beams

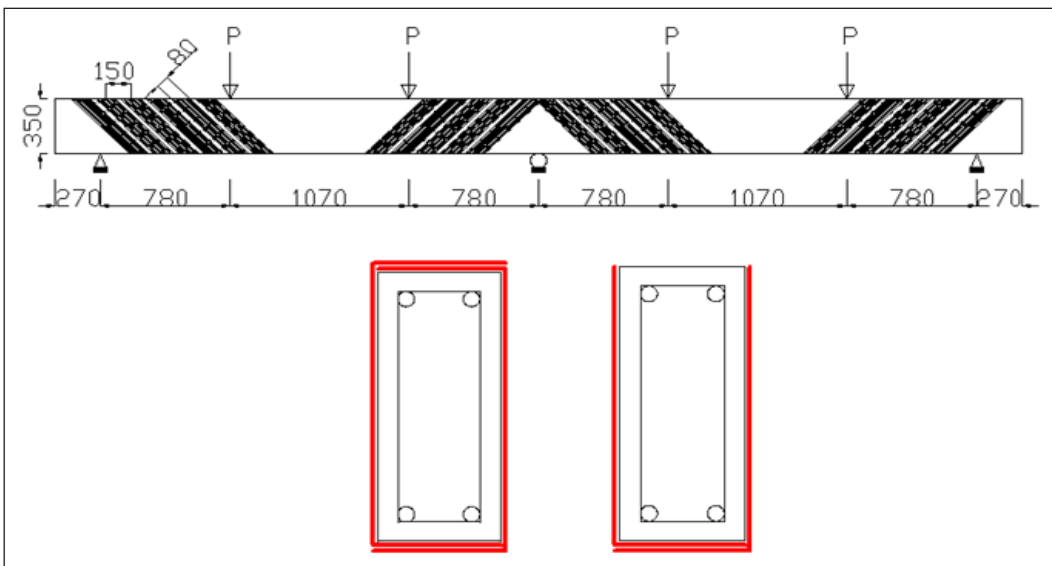


Figure 3. Wrapping scheme for beams with  $a_v/d=2.5$  (unit in mm)

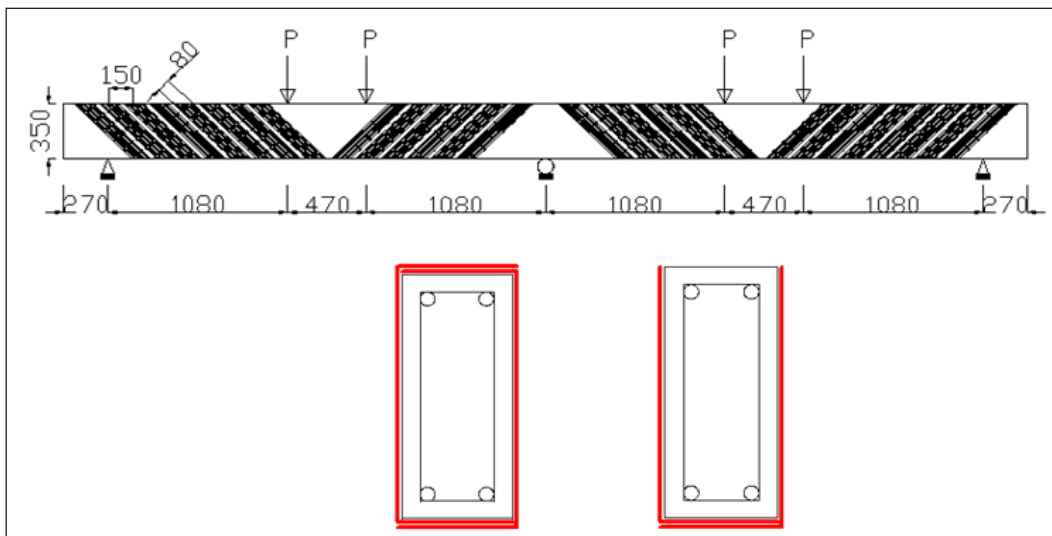


Figure 4. Wrapping scheme for beams with  $a_v/d=3.5$  (unit in mm)

## Material Properties

All specimens were cast using ready mix concrete with a compressive strength of 30N/mm<sup>2</sup> at 28 days. The main reinforcement used was high yield steel reinforcement with a diameter of 20mm whilst for links, the type of reinforcement used was mild yield steel reinforcement with a diameter of 6mm. In this research, SikaWrap-160 BI C/15 (bi-directional fibres), a woven carbon fibre fabric for structural strengthening was used as an external reinforcement of the specimen. The sheets are available in one roll of 50m length and 600mm width and the thickness of the fibre is 0.046mm in each direction. The test for this product was conducted by the Road and Bridges Research Institute Poland: IBDiM No AT/2003-04-336. Table 2 shows the material properties of the CFRP sheets based on the manufacturer's manual.

**Table 2.** Properties of SikaWrap-160 BI C/15

Fibre Orientation	Fabric Thickness (mm)	Tensile Strength (N/mm <sup>2</sup> )	Tensile E-Modulus (N/mm <sup>2</sup> )
0/90 (bi-directional)	0.046 / direction	3800	230000

The Sikadur-330 epoxy system was used as an adhesive in the strengthening system. The properties of Sikadur-330 are shown in Table 3 based on the manufacturer's manual.

**Table 3.** Properties of Sikadur-330

Density (kg/litre)	Tensile Strength (N/mm <sup>2</sup> )	Tensile E-Modulus (N/mm <sup>2</sup> )	Elongation At Break (%)
1.30±0.1	30	4,500	0.9

## EXPERIMENTAL RESULTS

### Ultimate Load

All beams failed in shear as expected because the beams were designed to fail in shear. For the strengthened beams, Beam 2-3 recorded the highest ultimate load at 411.25 kN whereas Beam 3-4 recorded the lowest ultimate load at 301.98 kN as shown in Table 4. For beams with  $a_v/d$  3.5, the experimental results recorded similar patterns for beams with  $a_v/d$  2.5 where beams wrapped on four sides recorded a higher ultimate load compared to the beams wrapped on three sides. It was also discovered that beams with  $a_v/d=3.5$  recorded a lower ultimate load compared to beams with  $a_v/d=2.5$ . It shows that as shear span to effective depth ratio ( $a_v/d$ ) increases, ultimate load decreases.

**Table 4.** Experimental results

Specimen	Wrapping Condition	Experimental Results						
		First Crack Load (kN)	Ultimate Load (kN)	Shear Force (kN)	Contribution of CFRP (kN)	Enhancement of Shear (%)	Modes of Failure	Shear Crack Angle (°)
Beam 1-0	-	96	286.10	93.70	-	-	Shear	24.3
Beam 2-3	4 sides	112	411.25	134.68	125.15	43.74	Shear & CFRP rupture	41.9°
Beam 2-4	3 sides	80	380.74	124.69	94.64	33.07	Shear, CFRP rupture & debonding	35.1°
Beam 3-0	-	72	253.65	86.24	-	-	Shear	44.2°
Beam 3-3	4 sides	64	325.39	110.63	71.74	28.28	Shear & CFRP rupture	30.4°
Beam 3-4	3 sides	76	301.98	102.67	48.33	19.05	Shear, CFRP rupture & debonding	55.2°

\* First crack load = for vertical crack load

Ultimate load = the total load from the four point load (4P)

Shear force =  $1.31 \times P$  (for  $a/d=2.5$ , 1.31P is the value of shear force in the shear force diagram)

Shear force =  $1.31 \times P$  (for  $a/d=3.5$ , 1.31P is the value of shear force in the shear force diagram) Contribution of

CFRP = (Ultimate load of wrapped beam) - (Ultimate load of control beam) Enhancement of shear =

$[(\text{Shear force of wrapped beam}) - (\text{Shear force of control beam})] / \text{Shear force of control beam} \times 100$

Shear crack angle = measured from the horizontal line to the diagonal crack

## Modes of Failure and Crack Pattern

The specimens tested in the experimental work were two-span continuous beams. The discussion on the results presented in this section refers to the weaker span. Beams were loaded equally (four point load of equal force) from the start to failure of the beam. However, at the point of failure only one span failed with an obvious diagonal crack compared to the other span. In order to better explain this section, there are some descriptions regarding flexural zone, shear span, flexural crack, shear crack, tension zone, and compression zone. Outer shear span is the shear span located near the outer support while inner support is located near the middle support. Flexural zone of the beam was located at the mid-span area near the maximum bending moment. The compression zone of the beam is located at the upper side of the beam while the tension zone is located towards the bottom side of the beam. Outer shear span, flexural zone, inner shear span, compression zone and tension zone are applied for both spans.

Flexural cracks refer to vertical cracks while shear cracks refer to diagonal cracks. Shear crack angle was observed because it has an effect on the theoretical model (Khalifa & Nanni, 2000; *fib*, 2001; Lee *et. al.*, 2012). The theoretical model by Khalifa & Nanni (2000) and *fib* (2001) assumed the value of diagonal or shear crack angle to be 45°. Based on the well-known Truss model, the angle of the cracks in concrete is assumed to be equal to the angle of the principal compressive stress of concrete while the tensile force in the stirrups cater the vertical component of the diagonal compressive strut under the equilibrium condition (Lee *et. al.*, 2010).

The control beam Beam 1-0 which was not strengthened with CFRP strips was tested and loaded till failure. It was observed that flexural cracks appeared initially at the bottom part

of the mid-span at a load of 96kN which was about 34% of the ultimate load of the beam. Shear cracks occurred later at a load of 204kN (at about 71% of the ultimate load). Then, new cracks developed at the tension zone of the mid-span area during the occurrence of the shear crack. The flexural (or vertical) cracks widened and propagated to the compression zone of the beam as the load was increased.

The first shear crack (or diagonal crack) appeared initially at the bottom part of the middle support area. The crack widened and propagated to the point load in a diagonal direction as the load increased. Other shear cracks were also observed propagating in the same direction as the first diagonal crack. As the load increased, the shear cracks widened and propagated until the beam failed due to shear at a load of 286.10kN. Figure 5 shows that Beam 1-0 failed in shear with a shear crack angle of 24.3° (see Figure 6). Several vertical cracks were also observed at the negative moment region (middle support area). The crack propagation for both vertical and diagonal cracks were similar to previous research done by others such as Khalifa *et. al.* (2000), Li *et. al.* (2002), and Jayaprakash *et. al.* (2008). From the observation of the beam test, vertical cracks in the flexural zone stopped propagating much earlier than the cracks in the shear span. As expected, the beam eventually failed in shear rather than in flexure as the specimen was designed to have insufficient stirrups in comparison to the longitudinal reinforcements. The shear failure resulted from a diagonal shear crack where the principal tensile stress has exceeded the tensile strength of concrete with insufficient stirrups provided onto the beam.

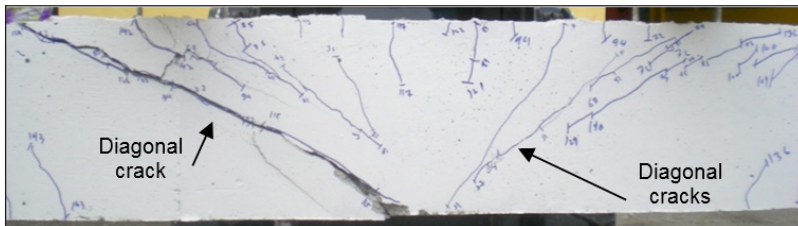


Figure 5. Shear failure of Beam 1-0 at a load of 286.10kN (shear force 93.70kN)

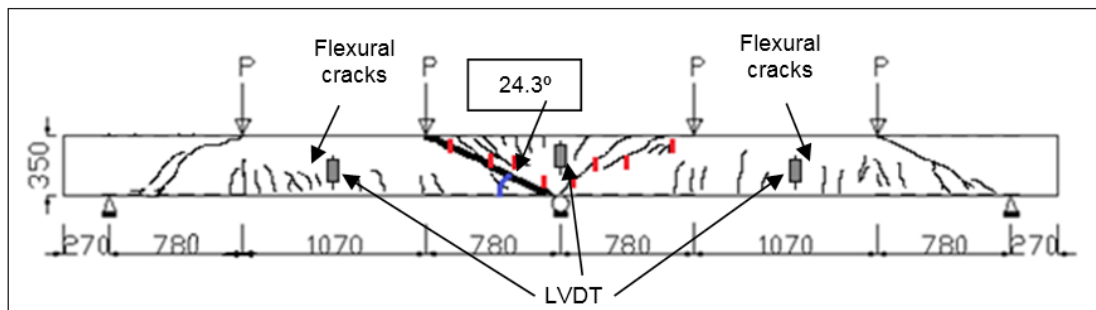


Figure 6. Crack pattern of Beam 1-0 (unit in mm)

For pre-cracked beams, the beam was pre-loaded to 224kN (for  $a_v/d=2.5$ ) and 200 kN (for  $a_v/d=3.5$ ) to develop shear cracks prior to CFRP wrapping. After pre-loading, the beam was unloaded to zero. The beam was then strengthened and it was later sustained with 10kN load for one week for the curing process of the epoxy (second phase). After one week, the beam was loaded again up to failure.

For Beam 2-3, from the observation during the pre-cracked phase, no crack was detected at the beam until at a load of 112kN or 27.2% of the ultimate load was applied. Diagonal cracks, on the other hand, initially appeared near the middle of the inner shear span at a load of

212kN or 51.6% of the ultimate load of the beam. After being repaired with CFRP strips, the beam was then loaded to failure until a load of 411.25kN where it fails with shear and CFRP rupture failure occurs as shown in Figure 7. The crack angle for the diagonal crack was  $41.9^\circ$  and Figure 8 shows the crack pattern of the beam. For this beam, there was an increase of 43.74% of shear capacity over the control beam (Beam 1-0).



Figure 7. Shear failure of Beam 2-3 at a load of 411.25kN (shear force 134.68kN)

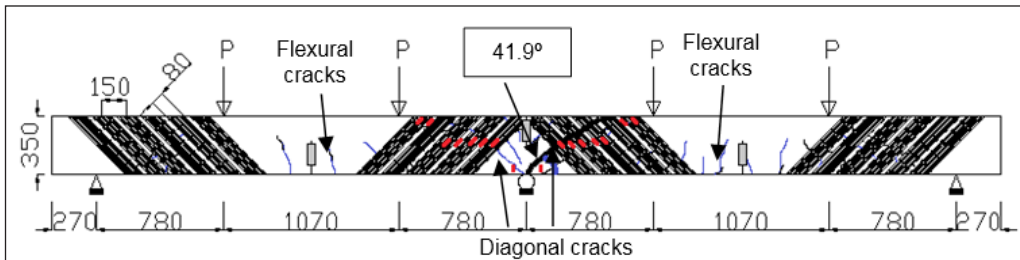


Figure 8. Crack pattern of Beam 2-3

For beam 2-4, the loading history was similar to the other pre-cracked beams. At the pre-cracked phase, flexural cracks initially appeared at a load of 80kN or 21% of the ultimate load of the beam. The first diagonal crack, on the other hand, was observed at a load of 180kN or 47.3% of the ultimate load of the beam. The ultimate load achieved for this beam was 380.74kN with the mode of failure by shear with CFRP rupture and debonding of CFRP strips from the concrete surface as shown in Figure 9. The increment of the shear capacity was about 33.07% from the shear capacity of the control beam (Beam 1-0). It decreased about 10.67% compared to Beam 2-3 (same orientation but wrapped on four sides of the beam). On the other hand, the crack angle for the diagonal crack of this beam was  $35.1^\circ$  as shown in Figure 10.

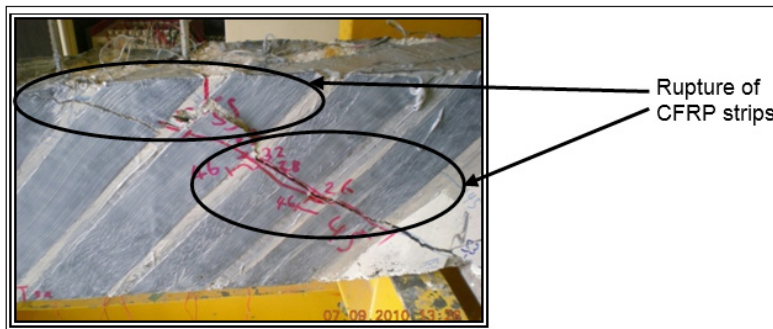


Figure 9. Shear failure of Beam 2-4 at a load of 380.74kN (shear force 124.69kN)

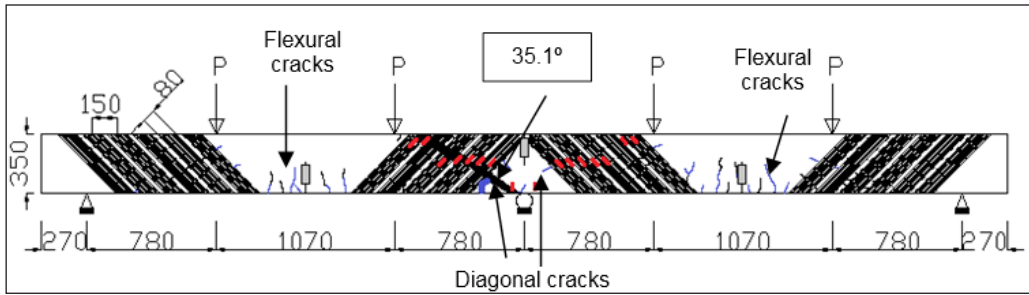


Figure 10. Crack pattern of Beam 2-4

Beam 3-0 was a control beam for  $a_v/d=3.5$ . Similar to Beam 1-0, this beam was also loaded to failure. The beam failed in shear at the ultimate load of 253.65kN. Flexural cracks initially appeared at a load of 72kN or 28.4% of the ultimate load of the beam. On the other hand, diagonal cracks were initially observed at a load of 144kN or 56.8% of the ultimate load of the beam. For beams with  $a_v/d=3.5$ , the shear span length was longer than beams with  $a_v/d=2.5$ . Therefore, the flexural cracks were not as many as beams with  $a_v/d=2.5$  as the area between the two point loads was smaller for beams with  $a_v/d=3.5$ . However, new diagonal cracks had appeared at the upper part or two thirds of the height of the beam at the inner shear span. The cracks moved towards the point load. It was also observed that new diagonal cracks appeared at the bottom part or one third of the height of the beam at a load of around 204kN. The cracks moved towards the point load location. Further observations also discovered that the main diagonal cracks had caused a crack along the cover of the beam which led to the crushing of concrete as shown in Figure 11.



Figure 11. Crushing of concrete of Beam 3-0

At failure, this beam failed with shear mode failure as shown in Figure 12 with a crack angle of 44.2° as shown in Figure 13. For this beam, more diagonal cracks were observed at the top zone near the applied load. The ultimate load was lower than the control beam with  $a_v/d=2.5$  (Beam 1-0). It had decreased about 11.3% compared to Beam 1-0 while the crack angle was higher than Beam 1-0 with an increase of about 19.9°. From the comparison between the two control beams, it shows that as the shear span to effective depth ratio increases, the shear capacity decreases.



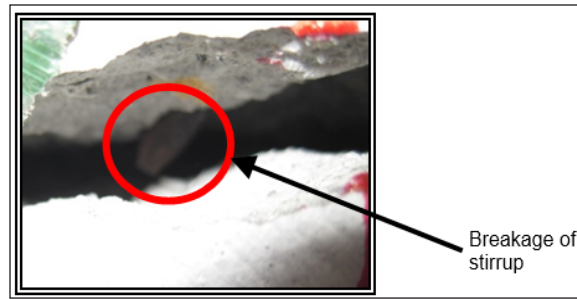


Figure 15. Stirrup failure of Beam 3-3

Immediately before failure at a load level of about 92% of ultimate load of the beam, rupture was detected in two CFRP strips closer to the mid support where the sound of rupture could be heard clearly. At the point of failure, a sudden fail with diagonal cracks occurred which involved a rupture of another three CFRP strips. The beam failed with a diagonal crack angle of 30.4° as shown in Figure 16. This crack angle was smaller at 11.5° than the crack angle of Beam 3-3 that had the same CFRP parameter.

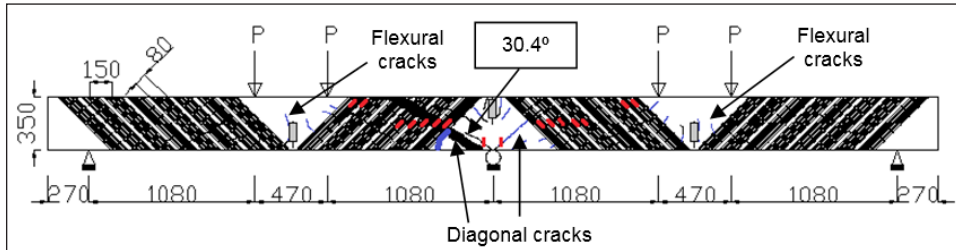


Figure 16. Crack pattern of Beam 3-3

On the other hand, for Beam 3-4, a flexural crack initially appeared at a load of 76kN, or 25.2% of the ultimate load of the beam during the pre-cracked phase. The first diagonal crack appeared at a load level of 116kN, or 38.4% of the ultimate load of the beam. After being wrapped with CFRP strips and allowing it to be cured for one week, the beam was loaded to failure. The ultimate load recorded was 301.98kN which showed an increment of about 19.05% of the shear capacity compared to the control beam (Beam 3-0). The mode of failure was shear with CFRP rupture and debonding of CFRP strips from the concrete surface as shown in Figure 17 below.

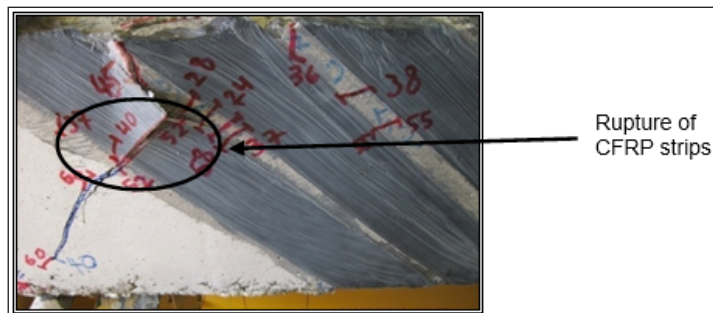


Figure 17. Shear failure of Beam 3-4 at a load of 301.98kN (shear force 102.67kN)

Figure 18 shows the cracks on the topside of the beam which occurred along the concrete cover of the beam. These cracks started to appear at a load of around 180kN and became wider as the load increased, especially when the first closest CFRP strip to the middle support

had ruptured at a load of 208kN. After the first CFRP strip had ruptured, the beam could still hold the applied load until it reached the ultimate load at 301.98kN. It was also observed that the splitting of concrete caused cracks to form on the concrete cover as shown in Figure 18.



**Figure 18.** Splitting of concrete of Beam 3-4

The main diagonal crack angle was 55.2° as shown in Figure 19. It was the highest angle recorded compared to the other beams. The shear enhancement achieved by this beam was 19.05%.

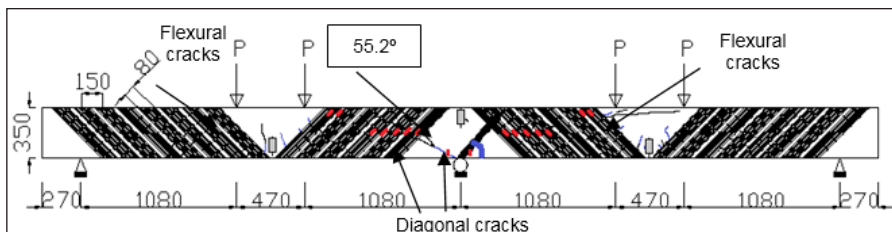


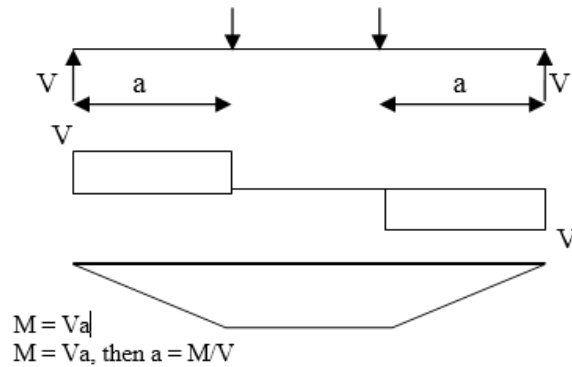
**Figure 19.** Crack pattern of Beam 3-4

For Beam 3-0 and Beam 3-4, it can be observed that at failure the concrete cover was extensively damaged which led to splitting or crushing of concrete. Beam 3-4 was wrapped at three sides with CFRP strips. The study by Khalifa *et. al.* (2000) mentioned that the damage of the concrete cover was probably due to over strengthening of the beam for shear and flexure in conjunction with relatively high longitudinal compressive stress development at the top of the beam which created transverse tension.

All beams with  $a_v/d=3.5$  showed lower shear capacity enhancement compared to beams with  $a_v/d=2.5$ . It shows that as the shear span to effective depth ratio ( $a_v/d$ ) increases, the shear capacity enhancement decreases. This is in line with the theory where the value of  $a_v/d$  provides the measure of the relative magnitude of flexural and shear stress and therefore enables the prediction of the modes of failure of the beam. The flexural and shear stress ( $f_x$  and  $\tau$ ) is then proportional to  $M/bd^2$  and  $V/bd$  (Sinha, 2003):

$$\frac{f_x}{\tau} = \frac{M/bd^2}{V/bd} = \frac{M}{Vd}$$

For reinforced concrete beam loaded as below:



$$\therefore \frac{f_x}{\tau} = \frac{M}{Vd} = \frac{a}{d}$$

From this theoretical equation, it shows that as the shear span to effective depth ratio ( $a/d$ ) increases, the shear capacity decreases.

## CONCLUSIONS

From the observations done on the behaviour of the beams during testing, loading history, ultimate load, crack patterns and modes of failure, there are some important points that can be deduced and summarized here:

- (i) The mode of failure of beams wrapped on four sides was shear with rupture of the CFRP strips. For beams wrapped on three sides, they failed in shear with CFRP rupture as well as debonding of CFRP strips from concrete surface.
- (ii) All beams recorded more than 30° crack angle and Beam 3-4 recorded the highest value at 55.2°.
- (iii) Beams wrapped on four-sides had shown higher shear capacity of about 9.23% to 10.67% compared to beams wrapped on three sides. Since it is not possible in practice to wrap four sides of the beam, the same results could be achieved by wrapping three sides of the beam with anchorage system to prevent debonding of the CFRP strips. In recent years, a technique called Near Surface Mounted (NSM) was applied to reduce the risk of debonding of the CFRP layer (Khalifa, 2016).
- (iv) During testing, both spans showed similar behaviours and it was difficult to predict which span would fail first. Only until the final stage of about 95% to 98% of loading, one of the spans showed wider diagonal cracks than the other and a sudden failure of the beam followed. In some beams, we could only actually see which span failed first during the failure stage. It shows that for continuous beams with similar dimension and properties, it is a tough task to predict which span will fail first because both spans behave similarly.

## REFERENCES

- ACI Committee 440 (2006). *Report on Fiber-Reinforced Polymer (FRP) Reinforcement for Concrete Structures*. Farmington Hills, USA: American Concrete Institute
- ACI Committee 440 (2008). *Guide for the Design and Construction of Externally Bonded FRP Systems for Strengthening Concrete Structures*. Farmington Hills, USA: American Concrete Institute
- Adhikary, B.B. & Mutsuyoshi, H. (2004) Behavior of Concrete Beams Strengthened in Shear

- with Carbon-Fiber Sheets. *Journal of Composites for Construction*. 8(3), pp. 258 - 264
- Chajes, M.J., Januszka, T.F., Mertz, D.R., Thomson, T.A.J. & Finch, W.W.J (1995). Shear Strengthening of Reinforced Concrete Beams using Externally Applied Composite Fabrics. *ACI Structural Journal*. 92(2), pp. 295 – 303
- El-Ariss, B (2007). Behaviour of Beams with Dowel Action. *Engineering Structures*. 29, pp. 899 - 903
- fib. (2001). *Externally Bonded FRP Reinforcement for RC Structures*. Switzerland: International Federation for Structural Concrete.
- Grace, N. F., Soliman, A.K. Abdel Sayed, G & Saleh K.R. (1998). Behaviour and Ductility of Simply and Continuous FRP Reinforced Beams. *Journal of Composites for Construction*. 2(4), pp. 186 - 194
- Jayaprakash J, Abdul Aziz AA, Ashrbov AA & Abang Abdullah AA. (2008). Shear Capacity of Pre-cracked and Non Pre-cracked Reinforced Concrete Shear Beams with Externally Bonded Bi-directional CFRP Strips. *Construction and Building Materials* 22, pp. 1148 - 1165
- Khalifa, A. M. (2016). Flexural performance of RC beams strengthened with near surface mounted CFRP strips. *Alexandria Engineering Journal*.
- Khalifa, A. & Nanni, A. (2000). Improving Shear Capacity of Existing RC T-Section Beams using CFRP Composites. *Cement and Concrete Composites*. 22, pp. 165-174
- Khalifa, A., Belarbi, A & Nanni, A. (2000). Shear Performance of RC Members Strengthened with Externally Bonded FRP Wraps. *Proceeding of 12<sup>th</sup> World Conference on Earthquake Engineering*. Auckland, New Zealand: American Concrete Institute. pp. 10 - 18
- Lee, J-Y, Hwang, H-B & Doh, J-H (2012). Effective Strain of RC Beams Strengthened in Shear with FRP. *Composites: Part B*. 43, pp. 754-765.
- Mostofinejad, D., Hosseini, S. A., & Razavi, S. B. (2016). Influence of different bonding and wrapping techniques on performance of beams strengthened in shear using CFRP reinforcement. *Construction and Building Materials*, 116, 310-320.
- Norris, T., Saadatmanesh, H. & Ehsani, M.R. (1997). Shear and Flexural Strengthening of R/C Beams with Carbon Fiber Sheets. *Journal of Structural Engineering*. 123(7), pp. 903 – 911
- Pillai, S.U., Kirk, D.W. & Erki, M.A. (1999). *Reinforced Concrete Design*. Canada: McGraw-Hill Ryerson Ltd.
- Sika Kimia Sdn. Bhd. (2007). *Sika Wrap®- 160 BI-C/15. Woven Carbon Fiber Fabric for Structural Strengthening*. Switzerland: Sika Manufacturer's Product Data Sheet.
- Sika Kimia Sdn. Bhd. (2007). *Sika Wrap®-330. 2-Party Epoxy Impregnation Resin*. Switzerland: Sika Manufacturer's Product Data Sheet.
- Sinha, S.N. (2003). *Reinforced Concrete Design*. 2<sup>nd</sup> ed. Tata McGraw-Hill.
- Taljsten, B. (2003). Strengthening Concrete Beams for Shear with CFRP Sheets. *Construction and Building Materials* 17, pp. 15-26
- Wang, C.K., Salmon, C.G. & Pincheira, J.A. (2007). *Reinforced Concrete Design*. 7<sup>th</sup> ed. New Jersey, USA: John Wiley.
- Zhang, Zhicao & Hsu, C.T.T. (2005). Shear Strengthening of Reinforced Concrete Beams Using Carbon-Fiber-Reinforced Polymer Laminates. *Journal of Composites for Construction*. 9(2), pp. 158 - 169

# PERFORMANCE OF INNOVATIVE CELLULAR MAT (NEW LIGHTWEIGHT MATERIAL) USING MINI TRIAL EMBANKMENT

**Reventheran Ganasan, Alvin John Lim Meng Siang and Devapriya Chitral Wijeyesekera**  
*Faculty of Civil and Environmental Engineering, Universiti Tun Hussein Onn Malaysia,  
86400 Parit Raja, Batu Pahat, Johor, Malaysia*

## **Abstract**

Construction of infrastructures on soft ground gives rise to some difficulties in Malaysia especially both in short and long term soil settlement. The most critical geo-environment challenges are excessive settlement and differential settlement leading to hazardous and discomfort in road usage. The objective of this paper is to investigate a new lightweight material which would overcome in minimizing both differential and non-uniform settlement in soft ground/soils. The behaviour and performance of the porous lightweight geo-material (in block form) used as a fill in embankment on soft ground for physical modelling was critically investigated. The mini trial embankment test was built with the innovative cellular mats placed underneath to identify the stiffness of the three different thicknesses. The innovative cellular mats thus can be proposed in laying it under the embankment surface in the future (real site/field testing). In the end of the test, less settlement was found along the mini trial embankment where the innovative cellular mat was placed. This has been proven by recording and plotting the settlement readings for all 15 sections along the mini trial embankment into a graph. The innovative approach has shown to also improve the stiffness of soils as well as helping in allowing water/moisture to flow through in or out without condition of floating due to the porosity characteristics of the cellular structure.

**Keywords:** *Physical modelling (mini trial embankment test), Construction materials, Innovative cellular mat*

## **INTRODUCTION**

In modern Civil Engineering, emerging problems in construction on soils are solved using both physical and software modelling (Ganasan *et. al.*, 2015). Modelling is defined as a process of solving physical problems by appropriate simplification of reality. The skill in modelling is to spot the appropriate level of simplification, distinguish important features from those that are unimportant in a particular application and use engineering judgment. The advancements in computational techniques and material science are incorporated into a software modelling based on the analysis of physical phenomena and constitutive laws applied majorly in roadway/highway engineering.

Soft soil areas are rapidly being used for infrastructure construction and other related development due to the limited availability of 'suitable' ground for infrastructure construction. These challenges arise towards engineers facing in all sorts of problem to design and construct foundation of building, road and highway embankment. It is because structures constructed on peat soil are often affected by stability due to high compressibility, low shear strength and high permeability. They are subjected to massive primary and long-term consolidation settlement even when subjected to a moderate load.

The most critical geo-environment challenges are excessive settlement and differential settlement leading to hazardous and discomfort in road usage (Ganasan *et. al.*, 2015). Many conventional methods (pile, vertical drain, soil replacement, soil stabilisation etc.) have been used to reduce these problems. However due to self-weight from the conventional methods used could not maintain the soil structure, allowing it to become as secondary subject towards excessive soil settlement. Field traffic loading test was carried out on a simulated embankment to investigate the appropriateness of the minimum cover depth ( $d_{min}$ ) obtained

for the structural integrity of the innovative cellular mat with traffic loading (motorcycle and rider). In the end of this simulated experiment, it would initiate in developing and proposing a design methodology guideline for the performance of a cellular mat using laboratory and field scale testing with appropriate instrumentation.

### **CASE STUDY: CONSTRUCTION OF PARIT YAANI BRIDGE**

A case study was done on a bridge construction at Parit Yaani which was first constructed on June 1<sup>st</sup>, 2010. Initially the old structure was just a small bridge and the construction area was covered with palm oil plantation. Then the Public Work Department of Batu Pahat took charge in funding the demolition of the old bridge and rebuilding it with a fully reinforced concrete bridge built on the marine clay soil. During the whole period of construction, the marine clay soil deposited along the river was covered with geotextile (Figure 1) in order to prevent the collapse of the preliminary structures. According to the engineer in-charge for highway department from Public Work Department (JKR) of Batu Pahat, before the piling works began, the sand and laterite soil was fill and compacted (Figure 2) on the surface of the marine clay. The fill work took place about three months to obtain an appropriate smooth surface layer.



**Figure 1.** The marine clay deposited along Parit Yaani's river covered with geotextile in 2010



**Figure 2.** The fill and compaction process were done on the surface of marine clay soil

According to the Public Work Department of Batu Pahat, the condition of soil surrounding in Batu Pahat have high intolerance level of acidity which may cause effect to the reinforced concrete structure. Thus, most of cement used in Batu Pahat area were mixed readily with the chemical substances due to fulfil the needs in become at least partially compatible with the



issue raised from this proposal was the cost for the material and the installation of permanent sheet pile which are expensive than the soil treatment and reconstruction works.



**Figure 4.** The current situation of site observation (taken on October 22, 2015) with the increment angle of the slant/edge of the embankment approaching to the Parit Yaani's bridge

## LIGHTWEIGHT MATERIALS IN FOUNDATION

The purpose of cellular mat studies in the foundations is to resist vertical, lateral and uplift load and to transmit a foundation load to a solid ground (Tuan Ismail *et. al.*, 2014). Suitable for loose soil or soils that tends to settle unevenly such as back filled inactive mining site. The thickness of the constructed foundation may exceed 1 m.

In civil engineering, the lightweight construction materials is used to describe particular methods for increasing economic efficiency which can reduce the weight of building structural constructions together with costs and work time by the use of special construction materials. Many attempts have been made to create highway and building that are both economical and environmentally friendly through the application of the lightweight material.

Expanded polystyrene (EPS) basically can be produced in four common grades based on its density such as Standard Duty (SD), Heavy Duty (HD), Extra High Duty (EHD) and Ultra High Duty (UHD) according to the BS 3837 Part 1 (1986) as they could be applied into construction material for foundation. Geof foam has been utilized in a number of countries (Norway, Netherlands, United States as shown in Figure 5, Japan, Germany and Malaysia).

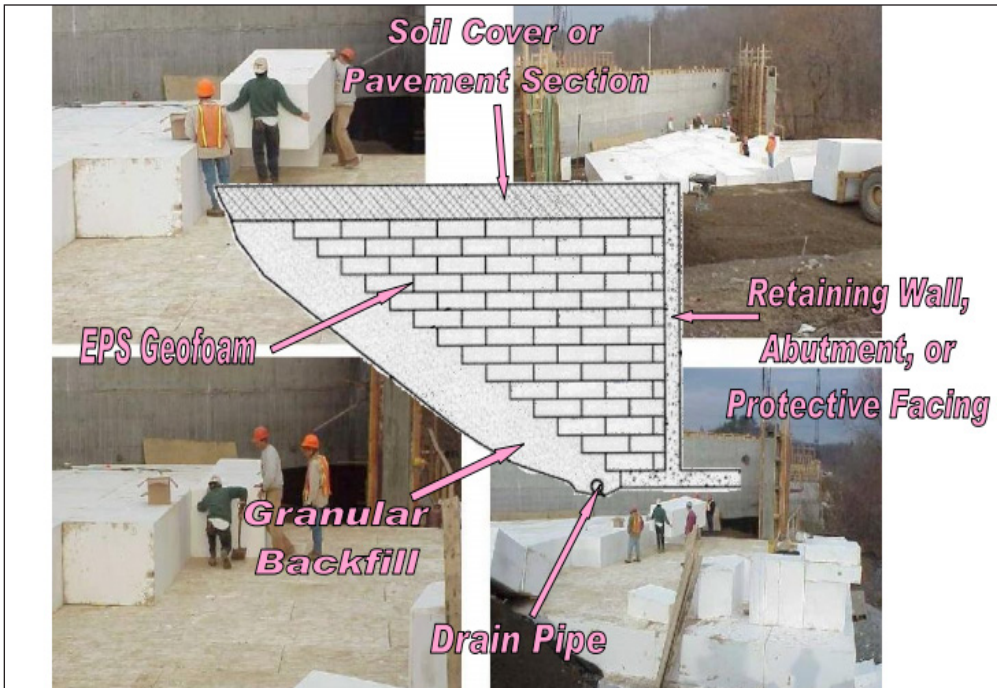


**Figure 5.** Design and construction of expanded polystyrene fill as a lightweight soil replacement (State of New York Department of Transportation Geotechnical Engineering Bureau, 2008)

According to Abdullah *et. al.* (2007), studies on various materials' filler have proved that EPS has its potential advantage in the application to remedy settlement of bridge abutment in Malaysia since 1992. Abdullah *et. al.* (2007) also mentioned that the EPS using the weight compensation technique is a viable option for lightweight structures. The output of this lightweight material can reduce the cost of lightweight structures since the cost of polystyrene are cheaper than the conventional materials. Apart from that, this lightweight can be reused and transportable but in contrary has defect towards chemical affect and also does not allow water to flow smoothly through closed porous of EPS.

Light-weight concrete generally has low density and low strength compared with normal concrete thus the application of lightweight concrete in construction for piling is very rare due to high porosity and underestimates the strength. According to Sulaeman *et. al.* (2010), foam concrete pile had the most resistance (30 % bigger than normal concrete pile) due to decreasing its own density. The PDA evaluation of the foam concrete also proves that the compression and tension during driving are within tolerable limit. The weaknesses of high porosity can be solved by coating the reinforcement by bitumen or epoxy resin whereas to increase the grade of lightweight concrete (foam concrete) including some additives (Neville and Brooks, 2001).

Air-foam treated lightweight soil is a ground material prepared by adding and mixing in a cement-type stabilizing agent and air foam made by a surfactant foaming agent to a source soil such as dredged soil and surplus construction soil. The purpose of this lightweight soil is to reducing earth pressure and containing land subsidence particularly at harbour and airport construction area. Kataoka *et. al.* 2014 stated that the air-foam treated lightweight soft clay used for the backfill of the quay wall or reclamation of the manmade island which in this case hydraulic conductivity and water absorption characteristics are important characteristics for the durability of this material. The permeability and absorption properties of this lightweight

soil are affected by air volume. The common disadvantage of air-foam treated lightweight soil affect when the air volume is higher, the air foam makes bleeding channels and the coefficient of permeability dramatically increases Kikuchi *et. al.* (2013). Table 1 shows the comparison of lightweight material applied in construction area.

**Table 1.** Properties of lightweight materials applied in construction field

Properties	Expanded Polystyrene (EPS) Footing	Lightweight Concrete Piles	Air-foam Treated Lightweight Soil (Foam clay)
Refs.	Abdullah <i>et. al.</i> (2007)	Sulaeman <i>et. al.</i> (2010)	Kikuchi <i>et. al.</i> (2013)
Unit weight (kN/m <sup>3</sup> )	0.15	15.00	10.00
Compressive stress (kN/m <sup>2</sup> )	60.00-110.00	3750.00	-
Shear strength (kN/m <sup>2</sup> )	80.00-130.00	-	-
Tensile strength (kN/m <sup>2</sup> )	110.00-290.00	800.00	-
Modulus of elasticity, <i>E</i> (kN/m <sup>2</sup> )	1600.00-5200.00	8000.00 x 10 <sup>3</sup>	-
Poisson' ratio, <i>u</i>	0.10	0.10-0.20	0.10-0.30
Dimension (m <sup>3</sup> )	0.65x0.65x0.25	0.15x0.15x6.00	(300mm cubic block from site) cut into a column of 0.05m in dia. and 0.10m in height tested in laboratory.

Other types of the lightweight foundation may not economical for this type of loose soil. Before the suggested new innovative cellular mat structure is implemented in rigid foundation, it is recommended for the following purposes:

- Bearing capacity of soil is low,
- Walls of the structure are so close that individual footings would overlap,
- It is used for large loads,
- Individual footings would cover more than about half of the construction area.

The advantages of the cellular mat foundation are as follows:

- ✓ It is capable in reduce the pressure exert in soil.
- ✓ It has higher stiffness compared to solid mat.
- ✓ It has high density and approachably lightest lightweight fill material compare to other lightweight materials (EPS and geofoam).
- ✓ It has open porous which help in buoyancy capability of allowing water or moisture from soft yielding soils to pass through it.
- ✓ It is rigid thus could prevent or reduce the differential settlement.
- ✓ Mat foundation is economic due to combination of foundation and floor slab.
- ✓ It requires little excavation.
- ✓ It can cope with mixed or poor ground condition.

## TRIAL EMBANKMENT TEST USING INNOVATIVE CELLULAR MATS AND RED LATERITE WITH MOTORCYCLE LOADING

The trial embankment was carried out as a mock test using red laterite soil to find out the strength of innovative cellular mats. The aim of this testing was to determine the effectiveness and deformation found in the cover depth values of 250mm, 300mm and 350mm measured from the surfaces of three different thickness of innovative cellular mats. Thus from this testing, the loading from motorcycle imposed on the laterite soil surface for three round would be fairly exhibit the occurrence physical damage towards the mats. The procedure of this testing was mentioned as per below:

- i. For the initial test, three innovative cellular mats with different thickness covered with fabrics on surfaces was used to carry out in the mini trial embankment.
- ii. The innovative cellular mats were placed inside the formwork/mould on the pavement surface as shown in Figure 6 (after site clearance) located in RECESS 1.
- iii. The red laterite soil was hauled, transported (in formwork/mould), place on the innovative cellular mats and fully compacted using plate compactor including the surrounding of it at the initial height/depth of 0.40m from road pavement.



**Figure 6.** The innovative cellular mats were placed inside the formwork/mould with the dimension of 2.0m (L) x 0.8m (W) x 0.4m (H) at the RECESS

- iv. The formwork was removed which result a fine moulded as it becomes a real imitation shape of a mini embankment.
- v. 15 steel rods attached with the dexion frame structure was made as an instrumentation for measuring the deflection/settlement formed on the surface of the laterite soil after the first run testing is conducted. This theory of instrumentation was adapted based on road deflectometer equipment owned by the 'Selia Selenggara' company in Melaka where this company specialise in road construction and maintenance in Malaysia. According to Smith (1973) from Transport and Road Research Laboratory (TRRL Report LR 525), the most widely used method of the surface deflection of the pavement done in Malaysia under a standard wheel load using a deflection beam. The deflection beam is simple to use, maintain and has strong attractions in many developing countries where more automated equipment such as the deflectograph can involve high operating and maintenance costs. The main disadvantages of the

deflection beam for the evaluation of long lengths of road is the slow and laborious procedure that is required to obtain the same density of measurement as can be easily acquired with a deflectograph. In carrying out a deflection survey with hand deflection beams a compromise has to be struck between the number of measurements that are required to obtain a knowledge of the variation in the strength of the pavement from point to point and the number of measurements it is practicable to take. Based from this statement by Smith (1973), a mini dexion frame structure was built to represent as an early movable instrumentation to investigate and determine the settlement and deformation occur on the surface of laterite soil.

- vi. The dexion frame structure as shown in Figure 7 was placed at the mini embankment to measure the initial reading before the moving load being imposed



**Figure 7.** 15 rod steels in dexion structure was pointed respectively on the surface of the mini embankment to determine the initial reading before the moving load being imposed

- vii. Next, the moving loading (Figure 8) with respective weightage of value was used across the embankment for the first run and then measurement was recorded of the settlement which take place on the 15 points along the surface of mini embankment. The test was repeated again on the second and the third as the final run of the testing.



**Figure 8.** The platform was set at the two edges of mini embankment respectively and the motorcycle (moving load) was imposed through the mini embankment

- viii. After the test has been run for all three times, the core cutter was used to take three samples of laterite soil in three different points to determine the possible constant density of soil.
- ix. At the end of the testing, the mini embankment was demolished to investigate the physical damage occurred on three innovative cellular mats with different thickness. The conditions of the innovative cellular mats were still kept in intact even after the three runs of the motorcycle loading.
- x. The raw data for the total of three runs then was tabulated and analysed further to determine the effectiveness of the cover depth values implemented in three innovative cellular mats.

### ANALYSIS OF MINI TRIAL EMBANKMENT USING INNOVATIVE CELLULAR MATS

The analysis was done by applying the cover depth values of 250mm, 300mm and 350mm measured from the surfaces of three different thicknesses (50mm, 100mm and 150mm) of innovative cellular mats. The testing was done using motorcycle (including the weight of the rider) as moving loading for total three runs/turns over the fixed height of mini trial embankment (0.40m from the pavement surface). Table 2 shows the settlement data occur at 15 different positions (steel rods) with the total of three turns across the mini trial embankment.

**Table 2.** The settlement data for three turns using moving loading in mini trial embankment

<b>D</b>	<b>0.00</b>	<b>142.86</b>	<b>285.71</b>	<b>428.57</b>	<b>571.43</b>	<b>714.29</b>	<b>857.14</b>	<b>1000.00</b>	<b>1142.86</b>	<b>1285.71</b>	<b>1428.57</b>	<b>1571.43</b>	<b>1714.29</b>	<b>1857.14</b>	<b>2000.00</b>
<b>H</b>	400.00	400.00	400.00	400.00	400.00	400.00	400.00	400.00	400.00	400.00	400.00	400.00	400.00	400.00	400.00
<b>1</b>	391.79	397.17	395.67	399.41	391.63	396.69	396.76	398.87	395.18	396.26	399.91	396.97	399.22	396.69	399.50
<b>2</b>	385.59	382.17	381.45	388.66	387.66	387.91	394.03	396.71	391.77	387.85	384.31	396.74	391.54	387.91	390.51
<b>3</b>	382.49	377.62	376.38	384.29	385.68	383.52	390.47	394.63	390.08	383.66	381.51	394.63	387.72	383.52	383.51

\* D: Distance between rods (mm)  
 \* H: Initial height of laterite soil  
 \* 1: 1st run of settlement (mm)  
 \* 2: 2nd run of settlement (mm)  
 \* 3: 3rd run of settlement (mm)

The tabulated data was plotted in graphical mode for the further analysis. Figure 9 exhibit the settlement occur with the respective thicknesses of innovative cellular mats while in the

Figure 10 focused particularly the rate settlement occurs after three turns over the mini trial embankment.

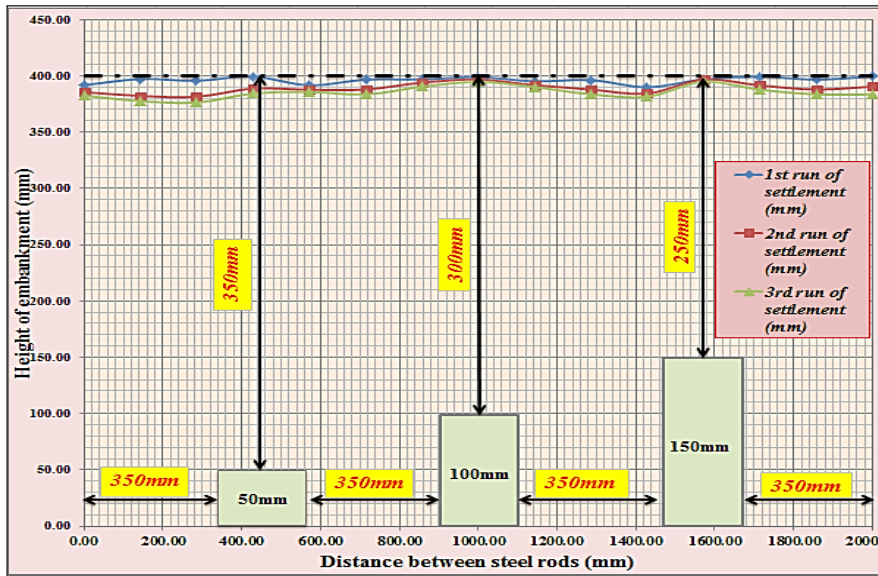


Figure 9. The settlement analysis occurs within three different thicknesses of innovative cellular mats

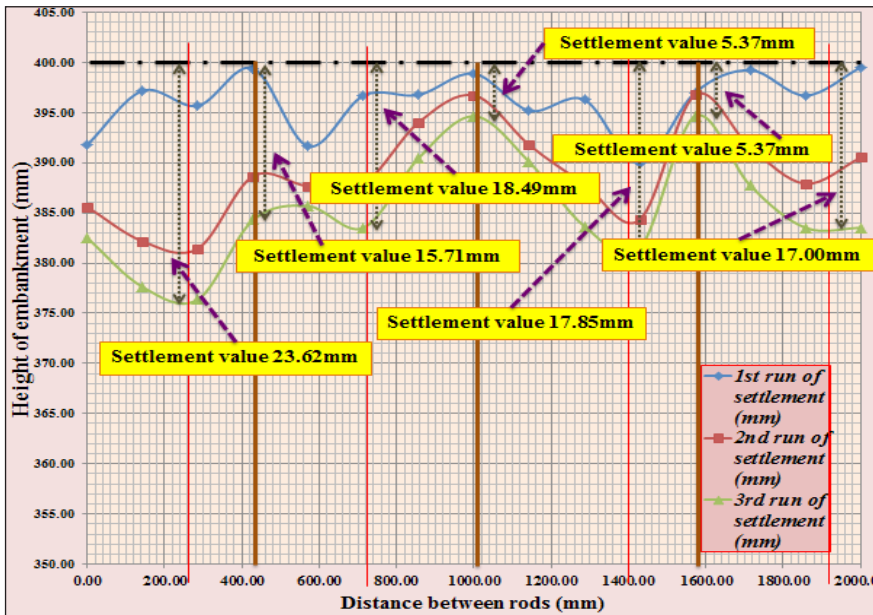


Figure 10. The detail settlement analysis occurs in the real mini trial embankment

Based on the detailed graph from Figure 10, it shows that the total settlement rate at the both 100mm and 150mm thicknesses of innovative cellular mats occur merely 5.37mm less than and compared to the three times of total rate settlement (15.71mm) occur in 50mm thickness of innovative cellular mats. The rate of settlement at the spacing between each innovative cellular mat has significantly occurred up to the maximum of 23.62mm particularly at the close area thickness of 50mm innovative cellular mat. The high settlement rate produced within the area of smallest thickness mat subjected due to low strength in bonding of soil with the height/cover depth of 350mm from the surface of the 50mm thickness of innovative

cellular mat. For every completion of testing in every turn, the properties of laterite soil were determined with the total of three samples using the core cutter testing equipment. The samples indeed show as in Table 3 where the density was controlled with the approximation of 4000kg/m<sup>3</sup> throughout in every turn.

**Table 3.** The properties of laterite soil using core cutter testing equipment for the real mini trial embankment

Sample	1	2	3
Mass of soil sample + core cutter (kg)	4.98	4.98	4.95
Mass of core cutter (kg)		0.94	
Volume of soil sample (m <sup>3</sup> )		1.021 x 10 <sup>-3</sup>	
Density, $\rho$ (kg/m <sup>3</sup> )	3956.90	3956.90	3927.52
Moisture Content, $w$ (%)		Average: 14.55	
Dry Density, $\rho_d$ (kg/m <sup>3</sup> )	3454.30	3454.30	3428.65
Specific Gravity, $G_s$		2.69 (Latifi <i>et. al.</i> 2013)	
Void Ratio, $e$	0.78	0.78	0.78
Porosity, $n$	0.44	0.44	0.44

The condition of the mini trial embankment had shown the aftermath final turns as the completion of the overall test. Eventually the height of the mini trial embankment had decreased approximately 12.5% where else the length of the mini trial embankment had increased up to 7.5 – 9.5% respectively. These percentage values were influenced directly from the total moving load approximately 230kg (2kN) came from both mass of motorcycle and the person who had riding on it through the mini trial embankment.

Prior to the approach in selected cover depth/height from the innovative cellular mat, the condition of the three different in thicknesses of innovative cellular mats were analysed in terms of the intact between tubes, the shape of mats, the dimension effect after the testing and finally the strength of the mats under the maximum compacted soil (using plate compacter) including the moving loading after three runs consecutively referring to Table 4.

**Table 4.** The condition of the innovative cellular mat after three runs (moving loading) in real mini trial embankment

No	Size of mat (mm <sup>2</sup> )	Thickness (mm)	Condition of mat (Before)	Condition of mat (After)	Remarks
1	297x210	50			The innovative mat structure was in good condition (with negligible physical appearance of the fabric) after the test was conducted. No changes occur in the dimension of the innovative cellular mat

No	Size of mat (mm <sup>2</sup> )	Thickness (mm)	Condition of mat (Before)	Condition of mat (After)	Remarks
2	297x210	100			The innovative mat structure was in good condition (with negligible physical appearance of the fabric) after the test was conducted. No changes occur in the dimension of the innovative cellular mat
3	297x210	150			The innovative mat structure was in good condition after the test was conducted. No changes occur in the dimension of the innovative cellular mat

## CONCLUSION

This paper has identified that the infrastructure built on soft ground/soils will cause a major problem that needs to be solved. An investigation was made to find the efficacy of the performance of a porous lightweight product that will minimize the differential and non-uniform settlement on soft yielding soils. During the mini field test that was conducted in RECESS in an open view place, an instrument was built using dexion frame steel to record the settlement that occurs over the mini trial embankment with a total of three passes (motorcycle/moving loading). The indicated result showed that the porous lightweight innovative cellular mat with different thicknesses had displayed remarkable increase in strength respectively. Apparently, a design guideline was established with a suitable and appropriate cover depth for the purpose in placing the innovative cellular mats at the embankment area in the future (real site testing).

## RECOMMENDATION FOR FUTURE WORK

The performance of this new lightweight construction material should be carried out at the real site for the full-scale modelling including the correlation that can be obtained from the software modelling since the ratio between small scale against the full scale are too small to guarantee the correct physical response of the real place/site. If this experiment conducted in the real site, we can deduce and acknowledge these new innovative cellular mats as a lightweight material capable highly in reducing the settlement. This real site testing would be indicated the settlement design behaviour for a long period in field area as simulation take place in the bridge built at Parit Yaani as shown in Figure 11.



**Figure 11.** The field settlement design/mode (propose) shown in embankment area jointed with concrete bridge located at Parit Yaani, Batu Pahat, Johor.

## REFERENCES

- Abdullah, M., Huat, B.K.K., Kamaruddin, R., Ali, A.K., & Duraisamy, Y. (2007). Design and Performance of EPS Footing for Lightweight Farm Structure on Peat Soil. *American Journal of Applied Sciences*, Volume 4, Issue 7, pp 484-490.
- Ganasan, R., Lim, A.J.M.S., & Wijeyesekera, D.C. (2015). Physical and Software Modelling for Challenging Soil Structure Interaction. *ARPJ Journal of Engineering and Applied Sciences, Malaysian Technical Universities Conference on Engineering and Technology*, KSL Hotel, Johor Bahru, Johor.
- Ganasan, R., Lim, A.J.M.S., & Wijeyesekera, D.C. (2015). Use of Lightweight Cellular Mats to Reduce The Settlement of Structure on Soft Soil. *Soft Soil International Conference 2015 (SEIC'15)*, Resort World Langkawi, Vol. 11, No. 6, March 2016, pp 3668 - 3676.
- Geotechnical Engineering Bureau, (2008). *Geotechnical Engineering Manual: Guidelines for design and construction of expanded polystyrene fill as a lightweight soil replacement GEM-24*, State of New York Department of Transportation.
- Kataoka, S., Horita, T., Tanaka, M., Tomita, R. & Nakajima, M. (2014). Effect of Dredge Soil on The Strength Development of Air-Foam Treated Lightweight Soil. *Proceedings of the 18th International Conference on Soil Mechanics and Geotechnical Engineering*, Paris, pp 3227 – 3230.
- Kikuchi, Y. & Nagatome, T. (2013). Durability of Cement Treated Clay with Air Foam Used in Water Front Structures. *Soft Soil International Conference 2013 (SEIC'13)*, Kuching, Sarawak.
- Latifi, N., Marto, A. & Eisazadeh, A. (2013). Structural Characteristics of Laterite Soil Treated by SH-85 and TX-85 (Non-Traditional) Stabilizers. *EJGE*, Vol. 18, Bund. H, pp 1707 – 1718.
- Neville, A.M. & Brooks, J.J. (2001). *Concrete Technology*, Harlow, Essex: Pearson Education Limited.
- Smith, H. R. (1973). A Deflection Survey Technique for Pavement Evaluation in Developing Countries. *Transport and Road Research Laboratory (TRRL Report LR 525)*, Department of the Environment, Crowthorne, Berkshire.

Sulaeman, A., Haji Bakar, I. & S., Amirkhan (2010). *The Performance Evaluation of Lightweight Concrete Piles on UTHM's Soft Soil under Static and Dynamic Loading Tests*, 2(2), pp. 53 – 65.

Tuan Ismail, T.N.H., Hassanur, R., Ganasan, R., Wijeyesekera, D.C., Bakar, I. & Sulaeman, A. (2014). Physical and Software Modelling of Performance of Mat Foundations on Soft Soil. *International Conference at Bandung*.

# EXPERIMENT AND COMPUTATIONAL FLUID DYNAMICS (CFD) SIMULATION OF FLOW CHARACTERISTICS IN DISSOLVED AIR FLOTATION TANK

Nor Azalina Rosli, Mohamad Fared Murshed and Mohd Nordin Adlan

School of Civil Engineering, Universiti Sains Malaysia, Engineering Campus, 14300 Nibong Tebal, Penang, Malaysia

## Abstract

This research presents numerical and experimental investigations on the effects of number of nozzles and inlet velocity on the flow characteristics in a dissolved air flotation (DAF) tank pilot plant. The flow characteristics was modelled using a Eulerian multiphase and k- $\epsilon$  turbulence (RNG) model by using GAMBIT 2.3.16 and simulated using FLUENT 6.3.26 (Fluent Inc., Canonsburg, PA, USA) software. The velocity distribution, air injection location and internal baffle inclination were investigated for 4 different experimental setups; Case 1 (using 2 nozzles with inlet velocity 0.3m/s), Case 2 (using 2 nozzles with inlet velocity 0.15m/s), Case 3 (using 2 nozzles with inlet velocity 0.6m/s) and Case 4 (using 3 nozzles with inlet velocity 0.3m/s). The number of nozzles and inlet velocity (raw water influent) were investigated owing to the dispersion of saturated water in the flotation tank. The experiments were carried out on a typical DAF pilot plant with a total of 138 flow measurement per case at different location. It was indicated that the number of nozzles and inlet velocity were contributed to flow distribution and dispersion inside the tank and thus, influence the efficiency of the solid-liquid separation process in flotation tank. Current research gives insight into the determination of the optimal operating condition of inlet velocity and the number of nozzles.

**Keywords:** Dissolved air flotation; computational fluid dynamics; flow characteristics; inlet velocity

## INTRODUCTION

Dissolved air flotation (DAF) water treatment process has proved to be a reliable and effective measure for the treatment of algae-laden and highly coloured water with low turbidity, commonly found in impounded reservoirs. It is believed that DAF is the best technology for the removal of algae and organic matter from surface water (Henderson *et. al.* 2008; Teixeira *et. al.* 2010; Edzwald, 2010; Shutova *et. al.* 2016). It has a removal efficiency of turbidity and bacteria for 97 and 100 percent compared to sedimentation which was only 70 and 65 percent (Pei *et. al.*, 2007). Moreover, the capital cost of DAF units is less than the equivalent settling tank, and they require shallower and smaller tanks, which is important in coping with preparing foundations in difficult sites (Melo & Laskowski, 2006; Shutova *et. al.*, 2016). DAF tank is divided into three main zones (Edzwald, 2010) namely, inlet zone (where the influent is entering before it flows into the reaction zone), reaction zone (the location for the aggregation of bubbles and flocs) and separation zone (where the particle-bubble will agglomerate and rising to the surface of water).

In the open literature, many researches both experimental and numerical were reported on various issues of DAF. An investigation on the effect of the size of bubbles and particles on the efficiency of DAF was performed by Leppinen *et. al.* (2000) and Lakghomi *et. al.* (2015). The rise speed of bubble/particle agglomerates was modelled as a function of bubble and particle size, while the kinematics of the bubble attachment process was modelled using the population balance approach. It was found that flotation, in general, was enhanced by the use of larger particles and larger bubbles (Liu *et. al.*, 2010).

Substantial contribution to the experiments on DAF was reported by Lundh and co-

workers, who investigated the flow structure in separation zone (Lundh *et. al.*, 2000, 2001) and contact zone (Lundh *et. al.*, 2002) of a DAF pilot plant using an Acoustic Doppler Velocimeter (ADV). In their continued effort (Lundh *et. al.*, 2005), a numerical and analytical study was performed by using the residence time distribution (RTD) of the conservative dye rhodamine measured with a fluorometer. The experiments were numerically analysed with regard to the total volume of the DAF tank separation zone in order to detect differences between observed separation zone flow structures in the previous studies. The result showed a significant difference in RTD depending on the expected flow structure.

Later on, few researchers attempted to use computational fluid dynamics (CFD) modelling for handling DAF problems. Kwon *et. al.* (2006) investigated the effect of L/W (L; length, W; width) on the hydrodynamic behaviour in a DAF system. Emmanouil *et. al.* (2007) examined the flow patterns of the contaminated water and the air bubbles inside a large-scale off-nominally operating tank. Subsequently (Emmanouil *et. al.*, 2008), they performed two and three phase simulations of III- Functioning tank. A CFD Model for the design of large scale flotation tanks has been presented by Kostoglou *et. al.* (2007). Recently, Amato and Wicks (2009) and Bondelind *et. al.* (2010) also performed CFD analysis to improve the DAF plant design.

As most of the previous works were of only laboratory level, the need of on-site investigation under the real operating conditions is quite obvious. The current study focuses on the effect of number of nozzles and liquid inlet velocity on the flow characteristics in flotation tank using finite volume based commercial CFD code, FLUENT. The experiments are conducted on a typical DAF plant in Malaysia. As far as the authors are aware, a detailed CFD analysis and experiment of its kind has not been reported so far, from Malaysia.

## **NUMERICAL SIMULATION**

### **Description of the process**

Figure 1 shows the schematic of the flotation tank for the pilot plant study at Jalan Baru Treatment Plant. This rectangular tank is developed by using Perspex with 1.4 m long, 0.7m width and 0.8 m height. Flotation tank is the most important part in DAF where particles floating in water will be removed by using super saturated bubbles. These particles and bubbles will attach each other and become less dense than water and float on the surface, and eventually removed as sludge or scum.

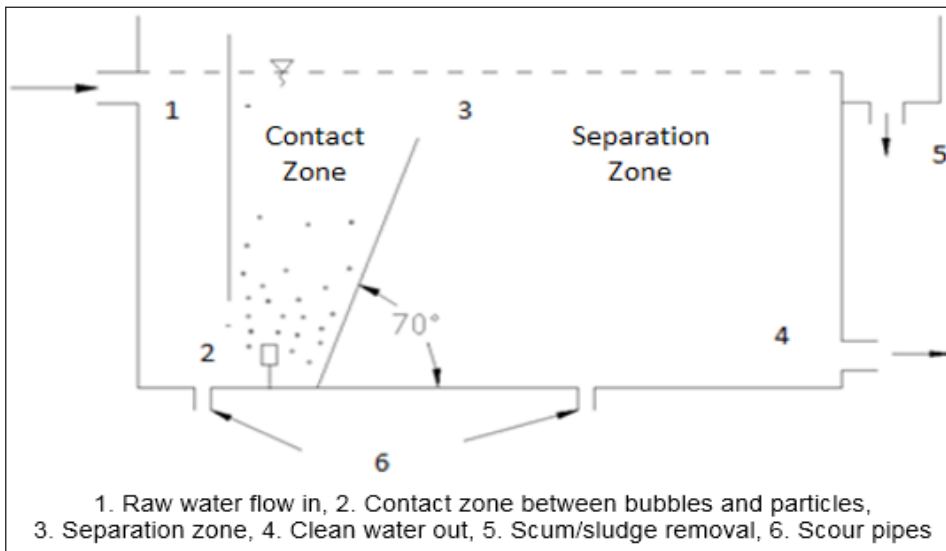


Figure 1. Schematic of the flotation tank

### Geometric modelling and meshing

The flotation model with the nozzle, used in this simulation has been modelled in GAMBIT pre-processor. The size of the grid element is set at interval size where the smaller size will give finer mesh and better solution. The grid dependency test was conducted using three different numbers of meshed, namely coarse mesh (10718), intermediate mesh (25362) and fine mesh (42110) at 0.15, 0.3, and 0.6 m/s inlet velocity (raw water influent) and with two nozzles as illustrated in Figure 2. The fine mesh indicated a higher flow distribution at 0.30 m/s compared to other inlet velocity. However, there is no significant difference between these three numbers of meshed even at low or high inlet velocity. In addition, the fine mesh produces first cell spacing normal to the nacelle ( $y^+$ ) of less than 8, which is lower than the maximum limit recommended by FLUENT. Therefore, the fine mesh was chosen for all computational models in this study.

In the model, the actual three-dimensional geometry of the experimental setup is simplified to a two-dimensional one as shown in Figure 3. The two-dimensional computational model considers the vertical mid-plane through the experimental test section. The size of the computational domain is the same as those used in the experiments (139 cm × 80 cm). Four cases have been designed for this study; Case 1 (using 2 nozzles with inlet velocity 0.3 m/s), Case 2 (using 2 nozzles with inlet velocity 0.15 m/s), Case 3 (using 2 nozzles with inlet velocity 0.6 m/s) and Case 4 (using 3 nozzles with inlet velocity 0.3 m/s). In addition, the tank is also designed for different internal baffle inclination, location of air injection nozzles and the number of nozzles from 2 to 3. The flotation tank was designed to maximize interaction between bubbles and particles in the contact zone. Therefore, a single nozzle is not enough to produce fine bubbles as reported by Murshed *et. al.* (2007).

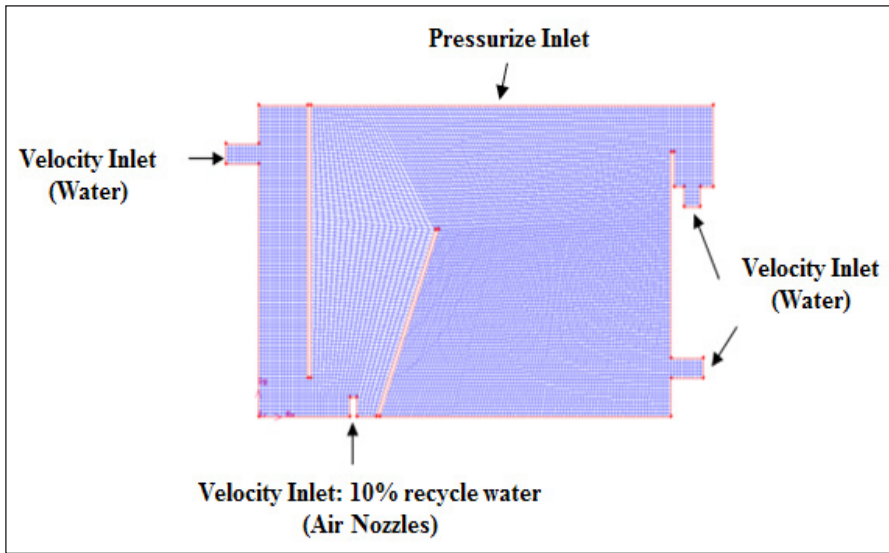


Figure 2. Meshing and boundary condition of flotation tank

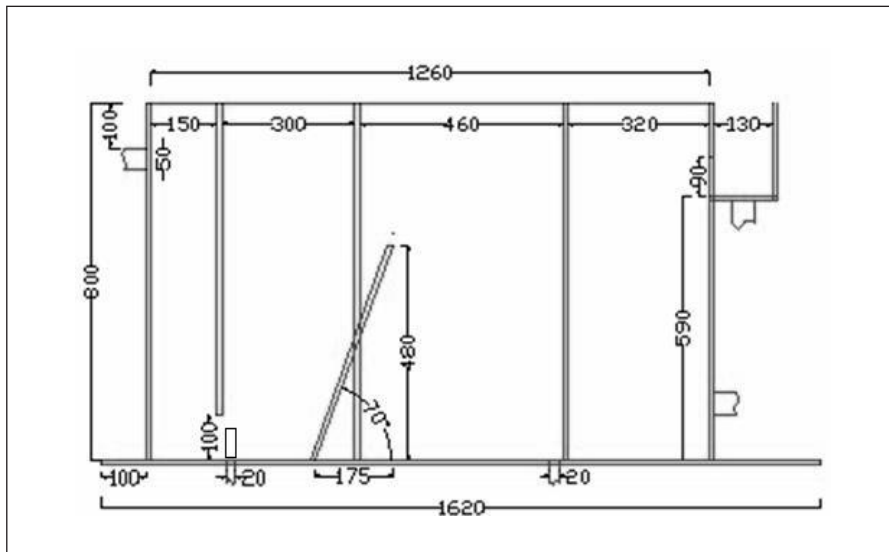


Figure 3. Flotation tank dimensions

### The mathematical model

The governing equations describing the fluid flow are conservations of mass and momentum. FLUENT normally solves the governing equations using Cartesian spatial coordinates and velocity components. The flow is assumed to be turbulent, incompressible and mixture model. Standard  $k-\epsilon$  model is used to describe the turbulence inside the tank. Turbulence model capable of resorting to a wall function formulation (automatic wall treatment) in the presence of coarse mesh resolutions near the wall without any further user input. Wall function models are also useful for calibrating our CFD models, due to the decreased simulation time. The conservation of mass or continuity equation is:

$$\frac{\partial p}{\partial t} + \frac{\partial pu}{\partial x} + \frac{\partial pv}{\partial y} = 0 \quad (1)$$

Equation 1 is the general form of the mass conservation equation and is valid for incompressible and compressible flows.

Conservation of momentum is described by:

$$\frac{\partial u}{\partial t} + u \frac{\partial u}{\partial x} + v \frac{\partial u}{\partial y} = -\frac{1}{P} \frac{\partial P}{\partial x} + \frac{\partial \tau_x}{\partial x} + F_x \quad (2)$$

$$\frac{\partial v}{\partial t} + u \frac{\partial v}{\partial x} + v \frac{\partial v}{\partial y} = -\frac{1}{P} \frac{\partial P}{\partial y} + \frac{\partial \tau_y}{\partial y} + g_y + F_y \quad (3)$$

Where, P is the static pressure,  $\tau$  is the viscous stress tensor and g and F are the gravitational acceleration and external body force in x and y direction, respectively.

First-order upwind discretization is used both for the momentum, and the SIMPLE scheme, for pressure-velocity coupling. The total duration of the simulation is selected such that the iteration has reached a convergence during this period. This took around 2,000 iteration, which corresponds to approximately half an hour of computation time per each case on a Pentium D processor (each 2.8 GHz) computer with 0.512 GB of memory.

## EXPERIMENTAL WORK

### DAF pilot plant testing

The pilot plant for DAF is constructed at the premises of Lembaga Air Perak (LAP) treatment plant, Malaysia. It has been developed based on the one employed by Packham and Richards (1975) for water reclamation studies in England. This Pilot plant is built up in a building in area of 88 m<sup>2</sup> and is discharged into a storage tank with capacity of 100 gallons. Figure 4 shows the schematic diagram and actual pilot plant of DAF pilot plant for water treatment process. The raw water is extracted during experimental works and normally run continuously at a flow rate of 20 litres per minute. The storage tank is provided with a ball-valve to control the water level and the raw water is delivered to the rapid mixing tank by means of unplasticized polyvinyl chloride (uPVC) pipe of 50 mm diameter. The mixing tank is made of Perspex with capacity of 0.048 m<sup>3</sup> and provided with motor rotating at 300 revolutions per minute (rpm). Alum is dosed at the rapid tank and the amount used is based on pin point size floc jar test. Two litres of liquid alum at different optimum dosage is prepared in the laboratory to feed into the chemical tank for 6 hours running to complete the experiment.

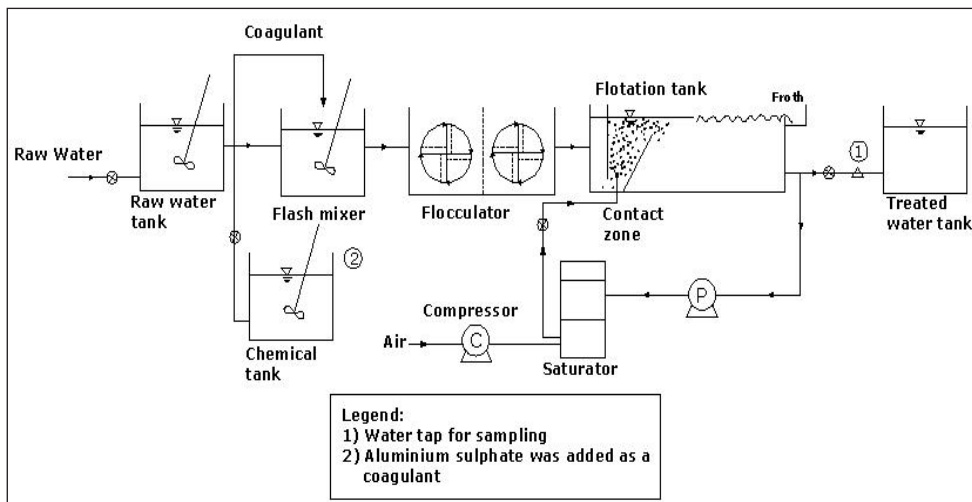


**Figure 4.** Schematic diagram of DAF pilot plant system for water treatment at LAP, Parit Buntar, Perak

This is followed by two stage flocculation at 60 rpm and 40 rpm for the formation of micro-bubbles prior to flotation. The paddle of mixer and flocculation tank is made by stainless steel and using gravitational flow through this experiment. The sample is then delivered to the flotation tank and a given amount of recycle is introduced by opening the nozzle to allow dissolved recycle into the flotation chamber. The dissolved water is compacted in the unpacked saturator and then injected into the contact zone to produce micro-bubbles. The water-bubble mixture is then diverted at 70° by a baffle into the separation zone of the flotation tank. The unpacked saturator is made up of stainless steel vessel efficiency of 81% (Adlan *et. al.*, 2005; Palaniandy *et. al.*, 2010). This saturator is equipped with sprayer nozzle, level sensor, pressure gauge and pressure release valve. This pilot plant also comprises air compressor of 1 kW and pressure mono-pump is used to dissolve the air into the water in the unpacked saturator. This unpacked saturator is capable to withstand a pressure of 12 bars and the system also consists of an electronic inverter that controls the water level in the unpacked saturator. The effluent then flows down to the treated water tank by uPVC pipe located at the lower part of the tank. Part of the effluent is recycled into the saturator.

Recycle flow rate to the flotation unit at contact zone is varied as 4 LPM (liters per minute), 5 LPM and 6 LPM. The unpacked saturator pressure is varied as 400 kPa, 500 kPa and 600 kPa and the combination set for each flow rate and pressure is made to obtain better removal. Supernatant water samples are drawn off and analyzed for duration of 180 minutes after steady state of flotation. Steady state is determined by leaving the pilot plant run freely about 2 hours after the water being flown through the flotation unit. This procedure is repeated for different recycle flows and coagulant dose for various samples are tested. The DAF plant allowed for careful control of recycle flow, unpacked saturator pressure and coagulant dose. The parameters such as rapid mix time, flocculation time and flotation time were fixed.

### Velocity measurement

Valeport Velocity Meter Model 801, (Serial No. 21198) was used to measure flow velocities in the DAF pilot plant. This small solid-state sensor has been designed for use in open channels, river, stream and hydrometric studies. It is ensured that Valeport Model 801 is a high precision instrument which can be relied upon to give accurate readings ( $\pm 0.5\%$  of reading plus zero stability) over a wide flow range ( $\pm 5$  m/s), (Valeport, 1999). The control

display unit provides a choice of averaging modes, standard deviation of the data, and an optional logging facility. Furthermore, it is unaffected by changes in conductivity and can be used in a ranges of fluids including fresh and waste water, salt water or foodstuff.

The velocity was measured at the center of each velocity node. There are 138 nodes of velocity measurement for a single run of experiment. Figure 5 shows the location where the velocity data were obtained from front view, plan view and side view. From this number of point, 12 points are at between the entrance and first baffle, 39 points are at contact zone, 84 points are at separation zone and 3 points at the outlet zone. There were some place where the velocity could not be obtained due to restricted space.

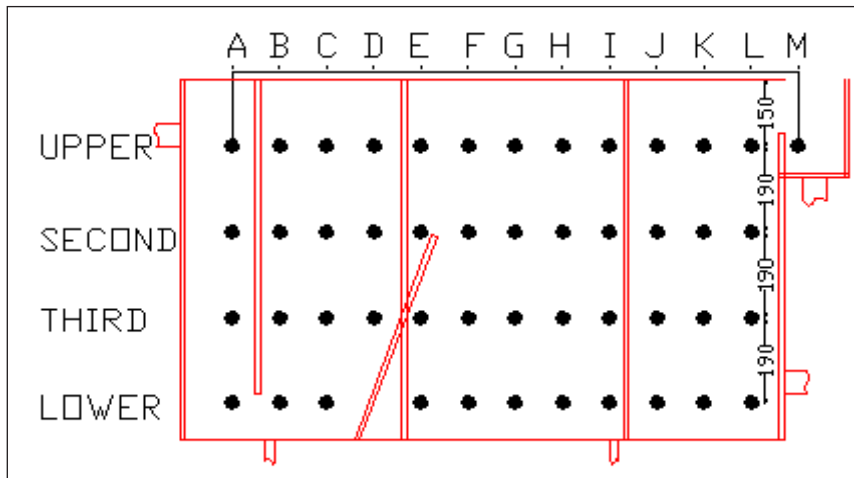


Figure 5. Side view for velocity measurement point

## RESULTS AND DISCUSSION

### Simulation results

#### *Comparison of Velocity Distribution*

#### *For Case 1 and Case 4*

Figure 6 shows the velocity contours for Cases 1 and 4; both the cases exhibit a similar flow pattern. However, there is difference in velocity magnitudes; case 4 gives the highest velocity, 0.84m/s (at reaction zone) compared to 0.42m/s for case 1, the difference being 48%. This is because, by using more nozzles, higher pressure will be released from the nozzles.

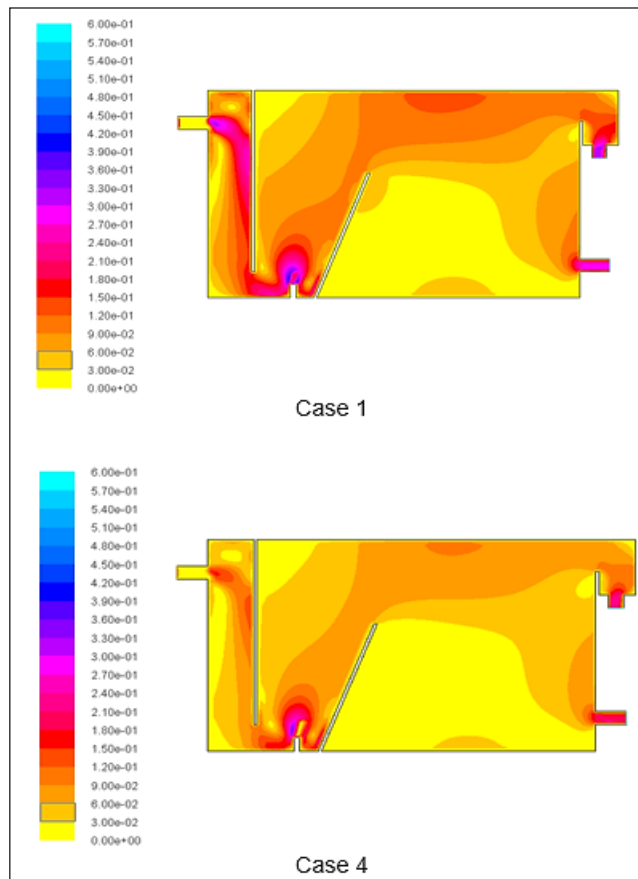


**Figure 6.** Velocity contours for Case 1 and case 4

**For Case 1, Case 2 and Case 3**

Figure 7 shows the velocity contours for Case 1, Case 2 and Case 3; the Cases 1 and 2 give a similar flow pattern. However, for Case 3, the contour is bit extreme where the velocity is quite high (0.594 m/s to 0.625 m/s); this is situation is risky, because it is worried that the floc will break-up due to high speed of flow. It is observed that the velocity distribution in Case 3 is the highest followed by Case 1 and Case 2 with approximately 33-50% velocity difference. Thus, the results show that the changes in inlet velocity will affect the velocity distribution inside the tank.

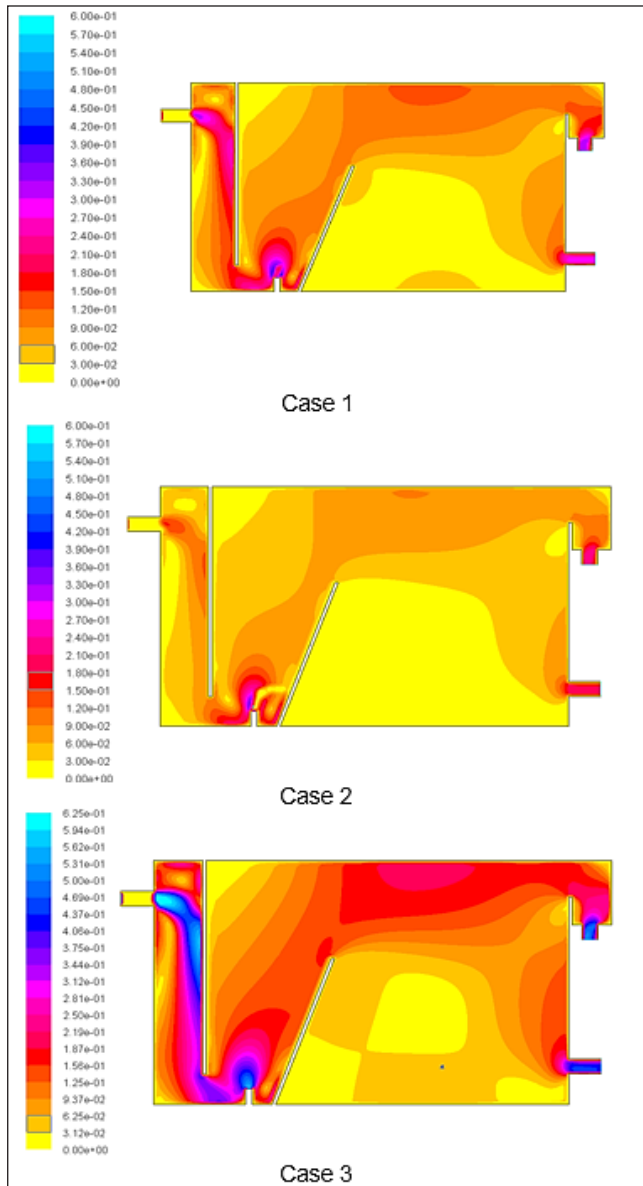


**Figure 7.** Velocity contour for Case 1, Case 2 and Case 3

### *Effect of the Internal Baffle Inclination*

The predicted velocity contours for different types of internal baffle inclination is shown in Figure 8. It is evident that when the baffle is inclined the velocity gradients are smoothed out and so a more uniform flow leaves the reaction zone. The velocities near the reaction zone are somehow lower with the inclined baffle (0.42m/s to 0.3m/s), indicating that bubbles/particles aggregates may deposit at the bottom of the tank. This is highly undesirable because it will require the tank to be drained and cleaned on a regular basis. Lower velocities are largely noticed at the surface of the tank with inclined baffle compared to vertical baffle and combined inclined and vertical baffle. This is due to the wider area for flow separation at the top of the inclined baffle as compared to the area available above the vertical baffle. Hence it is concluded that inclination baffle can give better performance in flotation process.

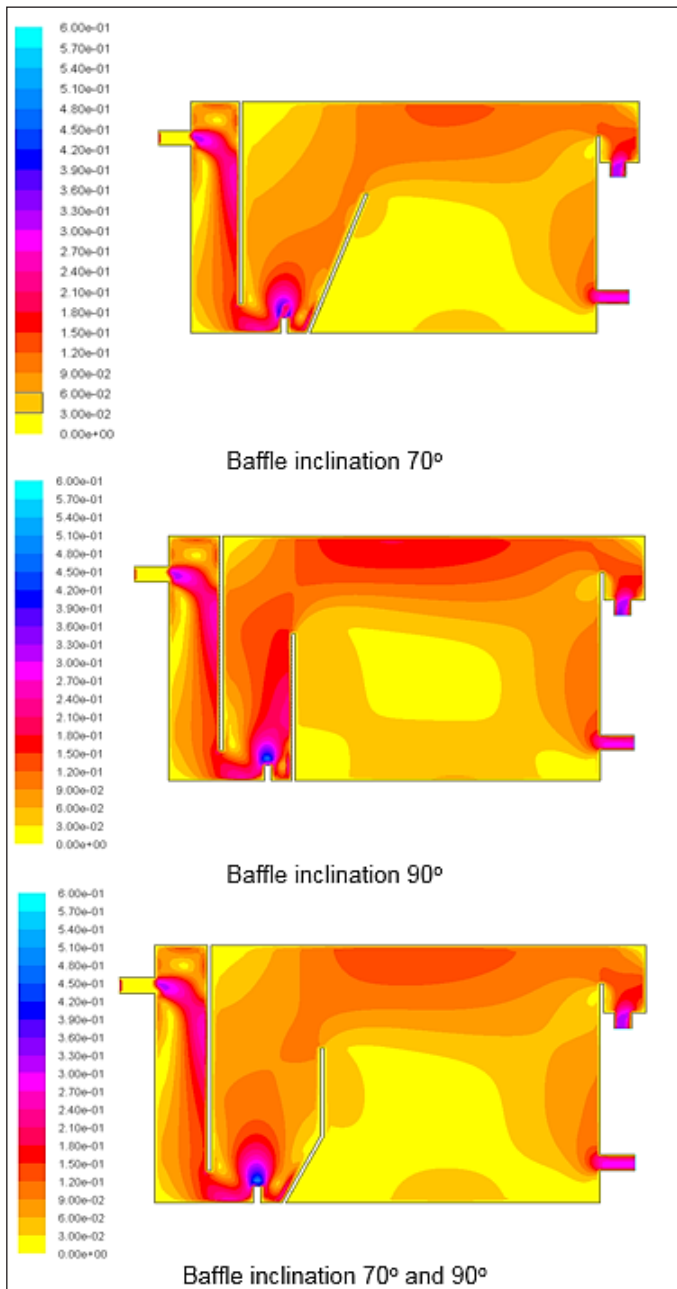
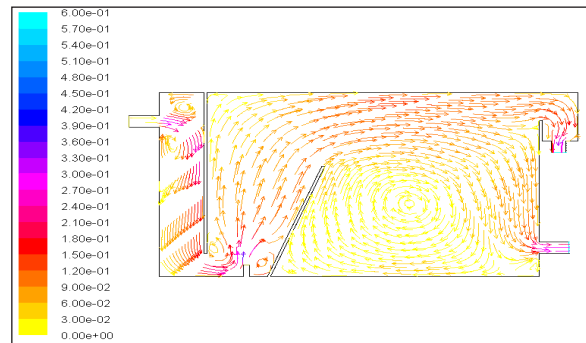


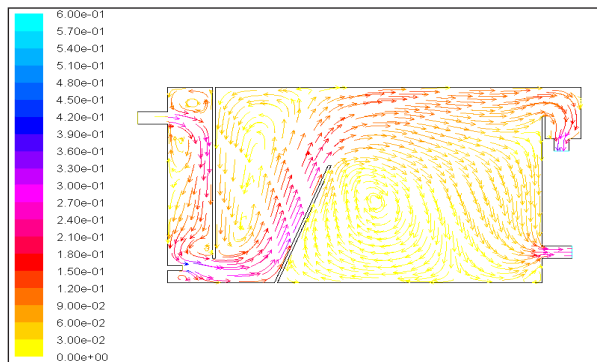
**Figure 8.** Velocity contour for different baffle inclination

**Effect of nozzle Location**

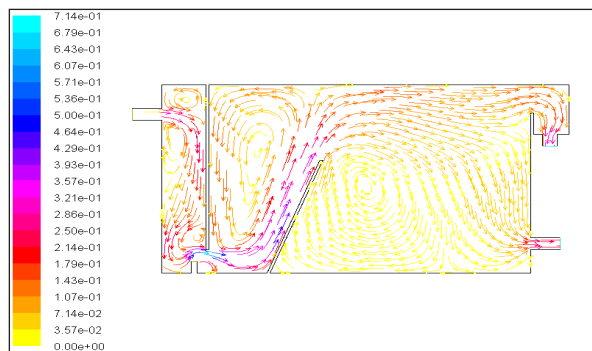
Three different injection locations are examined and the results are presented in Figure 9. The results indicate that, by applying injection at bottom vertical in reaction zone (Figure 8a) will give more uniform flow compared to applying injection at bottom horizontal in inlet zone (Figure 8b) and at bottom vertical in inlet zone (Figure 8c). The circulation loop flow is detected at reaction zone near the first baffle for Figure 8(b) and 8(c). This is undesirable because some of the floc-bubbles are not moving into separation zone.



a. Bottom vertical injection in reaction zone



b. Bottom horizontal injection in inlet zone



c. Bottom vertical injection in inlet zone

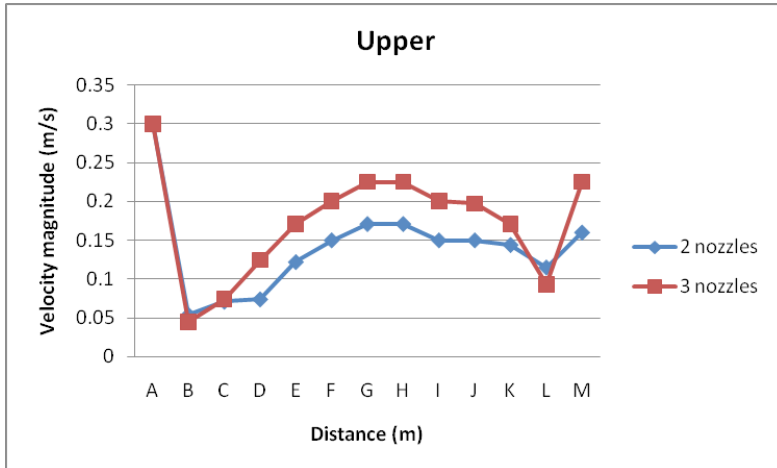
**Figure 9.** Velocity contour for different injection location

## Experimental results

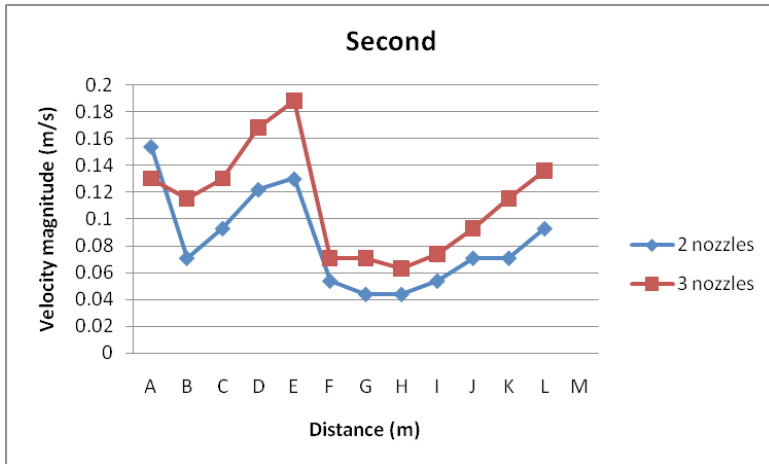
### Comparison of Velocity Distribution between Case 1 and Case 4

Figure 10 shows a comparison of velocity distributions in flotation tank between Case 1 and Case 4. The results show that the effect of number nozzles can be seen clearly at the contact zone (Column B to Column E) where the nozzles are placed. Using three nozzles gives the highest velocity, 0.35m/s (Column C at lower level) compared to 0.2m/s for two nozzles. This is because by using more nozzles, more water was injected to the tank and high saturated water is required to maintain high bubbles concentration in each nozzles.

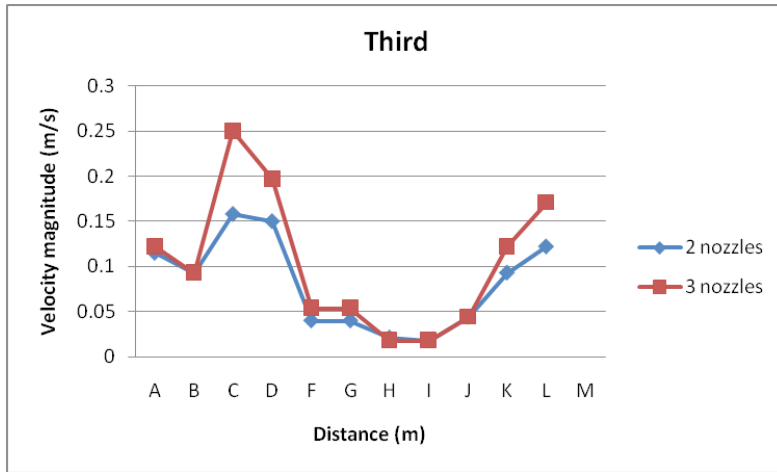
For the separation zone, the velocity is still higher for three nozzles at upper level (37% higher) and second level (40% higher) compared to two nozzles. The difference is due to the number of nozzles that are used inside the tank, which will release different pressure. In contrast, for third and lower levels, the velocity magnitude is almost similar for three and two nozzles.



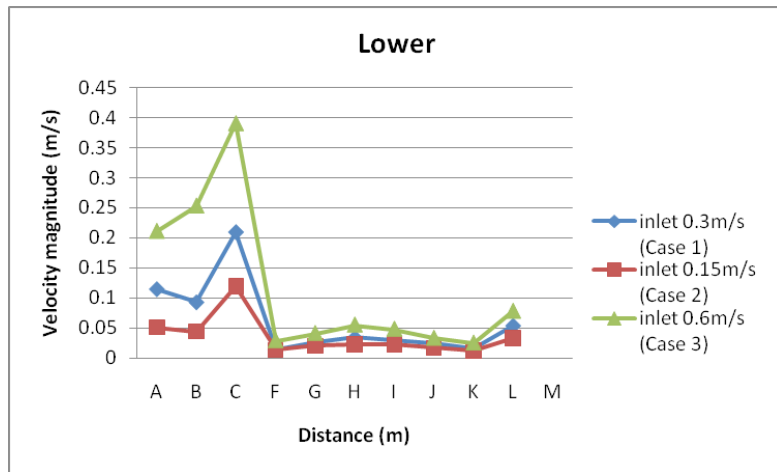
a: Upper level



b: Second level



c: Third level



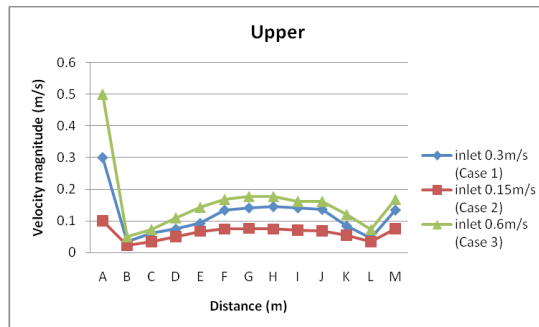
d: Lower level

Figure 10. Comparison of velocity distributions of Case 1 and Case 4

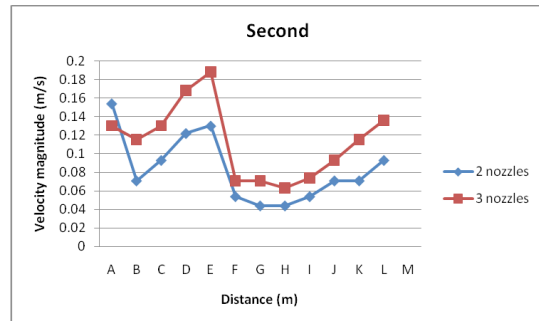
### Comparison of velocity distributions for cases 1, 2 and 3

Comparison of velocity distribution is made for Case 1, Case 2 and Case 3 to study the effect of inlet velocity on the velocity distribution inside the flotation tank. The cases are operated using the same number of nozzles (2 nozzles) but with different inlet velocities (influent of raw water), 0.3m/s (Case 1), 0.15m/s (Case 2) and 0.6m/s (Case 3). The results are shown in Figure 2. From the graph, at Column A the velocity magnitude is higher for Case 3 because when the inlet velocity is increased, the velocity of water coming into the tank from the inlet pipe is higher.

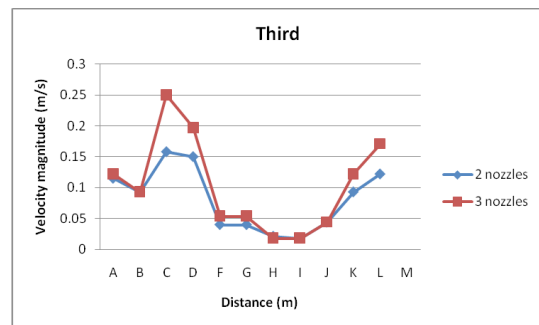
Although the number of nozzles used for these case is just the same (2 nozzles), there is a difference in velocity distribution at the contact zone. This shows that the changes in inlet velocity will affect the velocity distribution inside the tank. In the separation zone, there are differences in velocity distributions for all the levels but it is not as significant as in the contact zone.



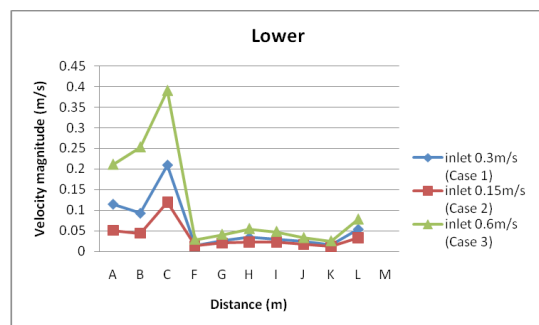
a: Upper level



b: Second level



c: Third level



d: Lower level

**Figure 11.** Comparison of velocity distributions for Case 1, Case 2 and Case 3.

### Comparison of water quality for Case 1 and Case 4

In order to see the effect of number of nozzles on the performance of the flotation process, the water turbidity in Case 1 and Case 4 are compared. Initial observation from the box-plot in Figure 12 suggests that Case 4 can reduce the turbidity of raw water more than Case 1.

The result of the ANOVA for the comparison of number of nozzles to turbidity is presented in Table 1. ANOVA is performed to check the effect of number of nozzles on the water turbidity. The p-value indicates that 100% of the time, the number of nozzles has significant impact on the water turbidity. This is because by using 3 nozzles, more bubbles can be produced. Thus, the probability for more particles to be attached to the bubbles is higher and concurrent with research findings by Lui *et. al.*, (2010) and Painamakul, *et. al.*, (2010). As a result, the water turbidity will decrease as more particles can be removed from the water.

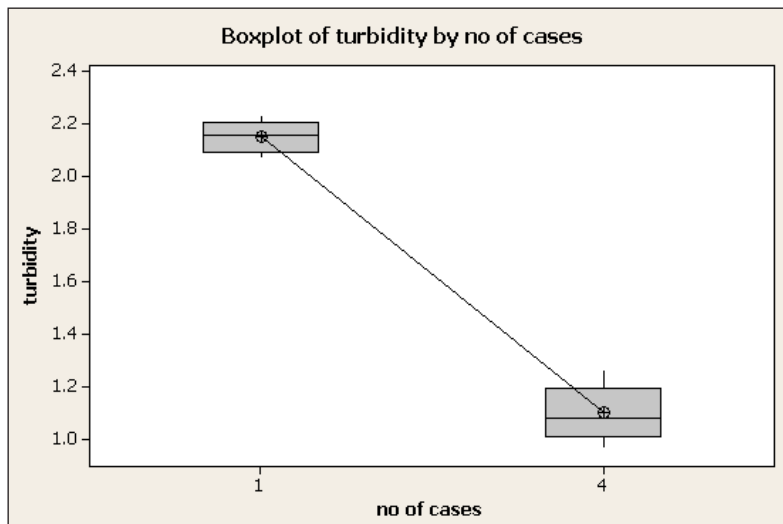


Figure 12. Box-plot of turbidity vs number of nozzles

Table 1. One way ANOVA of turbidity vs. number of nozzles

Source	DF	SS	MS	F	P
No. of cases	1	2.787	2.787	366.82	0.000
Error	8	0.061	38.072		
Total	9	2.848			

R-Sq = 97.60%

### Comparison of water quality for Case 1, Case 2 and Case 3

Water turbidity for cases 1, 2 and three are compared as shown in in Figure 13. The water samples for treated water were taken after 45 minutes of the run process. The box-plot shows that higher inlet velocity (Case 3) will produce water with lower turbidity. The result of the ANOVA for the comparison of inlet velocity to turbidity is presented in Table 2. It is evident that, the inlet velocity has significant effect on the water turbidity. This is because by increasing the liquid inlet velocity, it will speed up the movement of water inside the tank; so, the time required for the water purification is reduced. But, the inlet velocity should not

be too high because it can lead to the flocs break-up and some of the particles might not be able to attach themselves to the bubbles and carried away by the main flow to the outlet pipe.

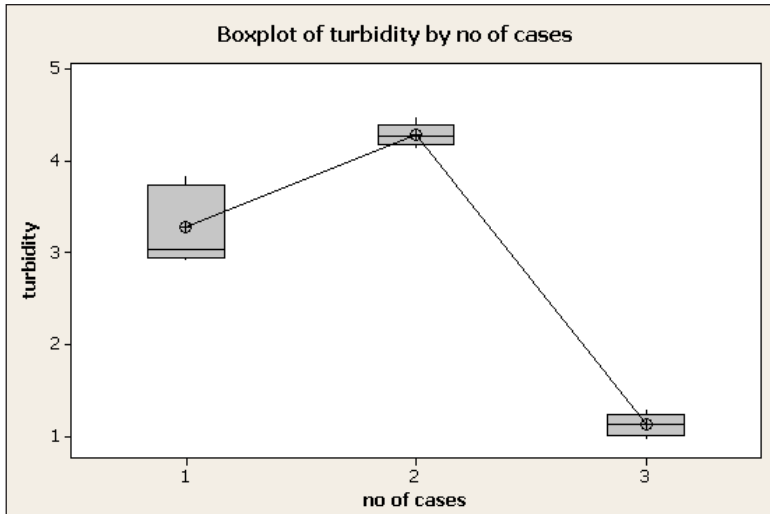


**Figure 13.** Box-plot of turbidity vs. inlet velocity

**Table 2.** One way ANOVA of turbidity vs. inlet velocity

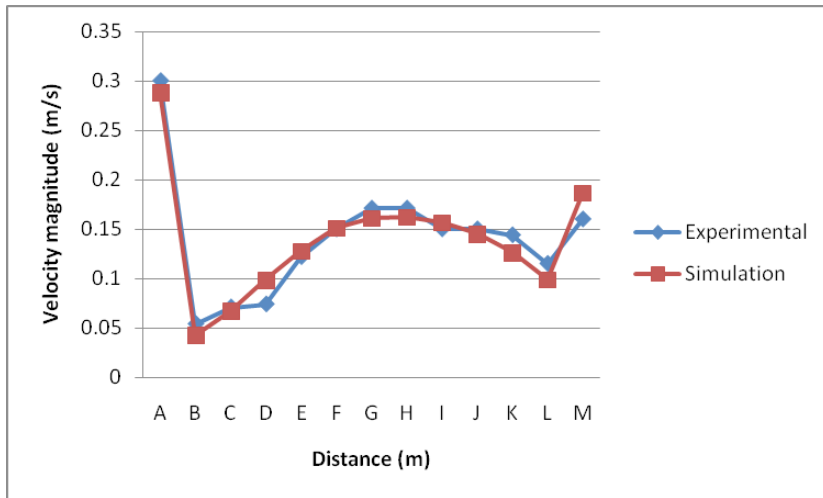
Source	DF	SS	MS	F	P
Pressure (kPa)	2	26.118	13.059	185.03	0.000
Error	12	0.847	0.0706		
Total	14	2			

R-Sq = 96.34%

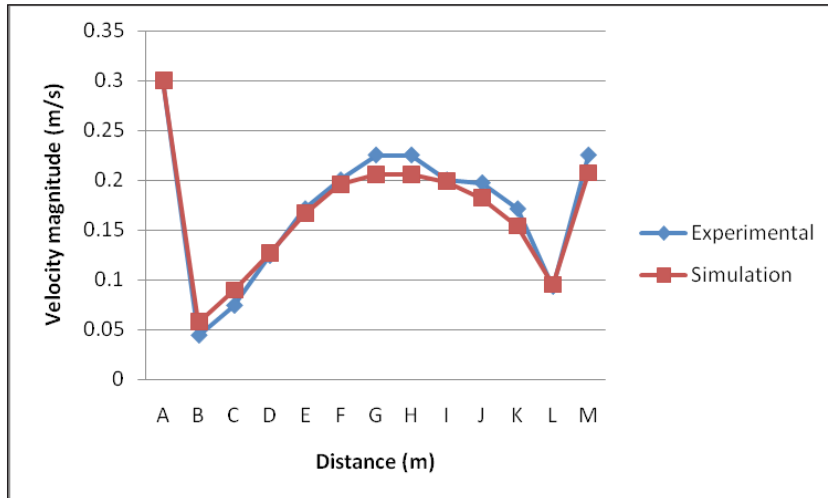
## Model verification

### *Comparison of velocity profile*

The comparison of predicted and experimental velocity profiles at Row 1 is shown in Figure 14 for Case 1 and Case 4. The discrepancy is 8.13% for Case 1 and 5.54% for Case 2 with regression coefficients ( $R^2$ ) 0.947 and 0.98 respectively. Thus, the simulation and experimental results are in good agreement, which proves that the present model and the FLUENT simulation are strong enough to handle DAF issues.



Case 1



Case 4

Figure 14. Comparison of experimental and predicted velocity profiles

## CONCLUSION

A two-dimensional CFD analysis and experimental validation on the effect of number of nozzles and inlet velocity on the performance of DAF plant was performed. Use of model of FLUENT 6.3.26 (Fluent Inc., Canonsburg, PA, USA) software (finite volume based study), focus on number of nozzles and baffle inclination, and on-site experiment are the significant features of the current study. As expected, the velocity distribution is influenced by the number of nozzles and the inlet velocity (raw water influent). The velocity is increasing as the number of nozzles increase. This is because, by using more nozzles, higher pressure will be produced from the nozzles. Besides, as the liquid inlet velocity is increasing, the velocity distribution is also increase. Using more nozzles could increase the removal efficiency, and higher liquid inlet velocity could reduce the time required for the water clarification. The good agreement between simulation and experimental results indicate the effectiveness of the proposed model and FLUENT simulation.

## ACKNOWLEDGEMENTS

This study was financial support by Lembaga Air Perak (LAP) and Universiti Sains Malaysia research grant (RUI) 814259. The authors would like to thank to my colleagues for their useful discussion and support to this work. Lastly, I would like to give my appreciation to my families for their prayers and support and those who are reviewed this manuscript.

## REFERENCES

- Adlan, M.N., Tan, E.W.J., Aziz, A.H (2005). Development and performance evaluation of an unpacked saturator for the dissolved air flotation process. In: *Asia water 2004 Conference. An international conference on water and wastewater*. The Mines, Kuala Lumpur.
- Amato, T. and Wicks, J. (2009). The Practical Application of Computational Fluid Dynamics to Dissolved Air Flotation, Water Treatment Plant Operation, Design and Development. *Journal of Water Supply: Research and Technology – AQUA*, Vol 58 No 1 pp 65–73
- Bondelind, M., Sasic, S., Kostoglou, M., Bergdahl, L and Petterson, T. J. R (2010): single and two phase numerical models of dissolved air flotation: comparison 2D and 3D simulations. *Colloids and surface A: Physicochemical and Engineering Aspects*, Vol. 365 (1-3): 137-144
- Edzwald, J. K (2010). Dissolved Air Flotation and me. *Water Research*. Vol. 44 (7): 2077-2106
- Emmanouil, V., Karapantsios, T. D. and Matis, K. A (2008). Two and Three Phase Simulations of an III- Functioning Dissolved Air Flotation Tank. *International Journal of Environment and Waste Management*, Vol. 9: 7-13.
- Emmanouil, V., Skaperdas, E. P. Karapantsios, T. D. and Matis, K. A. (2007). Two- Phase Simulations of an Off-Nominally Operating Dissolved Air Flotation Tank. *International Journal of Environment and Pollution*, Vol. 30 (2), 174-182
- Harwood, R. (2000). CFD and the Water Industry. *Journal Article by FLUENT Software Users*: 1-3.
- Henderson, R, Parsons, S. A., and Jefferson, B (2008). The Impact of Algal Properties and Pre-oxidation on Solid-Liquid Separation. *Water Research*. Vol. 42(8-9): 1827-1845
- Kostoglou, M., Karapantsios, T. D. and Matis, K. A. (2007). CFD Model for the Design of Large Scale Flotation Tanks for Water and Wastewater Treatment. *Industrial & Engineering Chemistry Research*, Vol. 46 (20): 6590–6599.
- Kwon, S.B., Park, N.S., Lee, S.J., Ahn, H.W., Wang, C.K. (2006). Examining the effect of length/width ratio on the hydro-dynamic behaviour in a DAF system using CFD and ADV techniques. *Water Science and Technology*, Vol. 53 (7): 141-149
- Lakghomi, B., Lawryshyn, Y. and Hofmann, R. A model of Particle Removal in a Dissolved Air Flotation tank: Importance of stratified flow and bubble size. *Water Research*, Vol. 68: 262-272
- Leppinen, D. M., Dalziel, S. B. Linden, P. F. (2000). Modelling the Global Efficiency of Dissolved Air Flotation. *Journal of Water Science Technology: Dissolved Air Flotation in Water and Wastewater Treatment*, Vol. 43: 159-166
- Lui, S., Wang, Q., Ma, H., Li, J., Kikuchi, T (2010). *Effect of micro-bubbles on coagulation flotation process of dyeing wastewater. Separation and Purification Technology*, Vol. 71(3): 337-346
- Lundh, M., Jönsson, M., Dahlquist, J. (2000). Experimental Studies of the Fluid Dynamics in the Separation Zone in Dissolved Air Flotation. *Water Research*, Vol. 34(1): 21-30
- Lundh, M., Jönsson, M., and Dahlquist, J. (2001). The Flow Structure in the Separation Zone of a DAF Pilot Plant and the Relation with Bubble Concentration. *Water Science and Technology*, 43 (8): 185-194

- Lundh, M., Jönsson, M., Dahlquist, J. (2002). The Influence of Contact Zone Configuration on the Flow Structure in a Dissolved Air Flotation Pilot Plant. *Water Research*, Vol. 36: No. 6: 1585-1595
- Lundh, M., Jönsson, M., and Dahlquist, J. (2005). Residence Time Distribution Characterization of the Flow Structure in Dissolved Air Flotation. *Journal of Environmental Engineering*, Vol. 131 (1): 93-101
- Melo, F., Laskowski, J.S (2006). Fundamental properties of flotation frothers and their effect on flotation. *Minerals Engineering*, Vol. 19: 766-773
- Murshed, M.F. (2007). *Removal of turbidity, suspended solid and aluminium using DAF pilot plant*. MSc thesis. Universiti Sains Malaysia, Penang, Malaysia.
- Packham, R. F. and Richards, W. N. (1975) Water clarification by flotation 3; treatment of Thames Water in a pilot-scale flotation plant. *WRC Tech. Report TR2*, Medmenham.
- Painmanakul, P., Sastaravet, P., Lersjintanakarn, S and Khaodhiar, S (2010). Effect of bubble hydrodynamic and chemical dosage on treatment of oil wastewater by induced air flotation (IAF) process. *Chemical Engineering Research and Design*, Vol. 88 (5-6): 693-702.
- Pei, L. S., Shan, W. Q., Jie, H. W., Da, H. H., Hong, F. X. and Jia, G. T. (2007). Comparison of Dissolved Air Flotation and Sedimentation in Treatment of Typical North China Source Water. *The Chinese Journal of Process Engineering*, Vol. 7(2): 283-287
- Palaniandy, P., Adlan, M. N., and Murshed, M. F. Application of dissolved air flotation (DAF) in seme-aerobic leachate treatment. *Chemical Engineering Journal*, Vol. 157 (157): 316-322
- Shutova, Y., Karna, B.L., Hambly, A.C., Lau, B., Henderson, R.K., Le-Clech, P. Enhancing organic matter removal in desalination pretreatment systems by application of dissolved air flotation. *Desalination*, Vol. 383: 12-21.
- Teixeira, M. R., Sousa, V., and Rosa, M. J (2010). Investigating Dissolved Air Flotation Performance With Cyanobacterial Cells and Filaments. *Water Research*, Vol. 44 (11): 3337-3344



# THE ADOPTION OF PASSIVE COOLING STRATEGY IN DESIGNING PUBLIC ASSEMBLY BUILDING – A DESIGN TYPOLOGY FOR THE TAOIST ACADEMIC CENTRE IN TROPICAL CLIMATE

Loo Kok Hoo<sup>1</sup>, Benson Lau<sup>2</sup> and Foo Chee Hung<sup>3</sup>

<sup>1</sup> KH Loo Architect, 2, Jalan Hujan Batu, Overseas Union Gdn, Jalan Klang Lama, 58200 Malaysia

<sup>2</sup> Department of Architecture & Built Environment, Nottingham University, Architect/Course Director. University Park, Nottingham NG7 2RD, UK

<sup>3</sup> Construction Research Institute of Malaysia (CREAM)

## Abstract

Passive cooling strategy is a key element of sustainable building. Its optimum performance and potential benefit can be realized with careful and meticulous design. As a design option for public assembly spaces, however, passive cooling strategy is seldom given a fair consideration as compared to the mechanical cooling approach, especially in the tropical climate where high humidity prevails. This paper presents an extensive study on the technological aspects of vernacular architecture in Malaysia, particularly on the efficiencies and limitations of the passive house design, thereby exploring the workable sustainable architecture prototype for public assembly spaces in the tropical climate. With the lessons learnt from the vernacular architecture, the design typology for a Taoist Academic Centre (TAC) was proposed. By adopting an integrated environmental design approach which involved performative analysis through computational studies, the design scheme was tested and modified to achieve the optimum spatial and environmental delight. Ultimately, the paper aims to demonstrate that modern tropical architecture prototype is possible to be developed from vernacular architecture, and the proposed prototype will not only respond well to the local climates, but also is able to accommodate different cultural contents.

**Keywords:** *Thermal comfort, tropical climate, Malay house, passive design*

## INTRODUCTION

All built developments, from the small to the large, make a long-term impact, either on the communities they house or on the surrounding neighbourhoods. Where they are, how well designed and built they are, and how well they knit into the fabric of existing or new communities, are factors that can colour the lives of people on a daily basis and for future generations. Public assembly spaces (i.e. churches, meeting halls, school classrooms etc.) in particular, have a considerable influence on the urban culture and city life. These spaces not only ensure a physical link between buildings and land uses in order to sustain the marketing, manufacturing, administrative, and transportation activities of the cities, but also facilitate a link among people, facilities, communication and interaction, thereby serving to bind together the social order of local community by creating a locus for randomized social interaction (Gencel and Velibeyoglu, 2006).

Following the increases of awareness on global warming and the dependence of built environment on energy for everyday life, building sustainability is increasingly being emphasized around the world. Occupants are now more conscious the importance of sustainability for a better quality of life (Jamaludin *et. al.*, 2014). Public assembly spaces are of no exception to fulfil their contribution to the society with respect to sustainability. At a building level, the social benefits of sustainability focus on ensuring occupants' health, comfort, and satisfaction. Studies show that building environment can have negative impacts on the occupants. These

impacts include illness (Brightman and Moss, 2001; Fisk, 2002), absenteeism (Milton *et. al.*, 2000), discomfort (Heerwagen *et. al.*, 1991; Wyon, 1996; Leaman and Bordass, 2001), stress (Heerwagen, 2000), and distractions (Leaman and Bordass, 2001), resulting from poor indoor air quality, thermal conditioning, lighting, and specific aspects of interior space design (i.e. materials selections, furnishings, and personnel densities). Reducing these problems through sustainable design can improve occupant's health and performance. Besides, buildings also contain features and attributes that can create positive psychological and social experiences. Emerging evidence shows that certain sustainable building features, such as access to daylight and views (Leather *et. al.*, 1998), and connection to nature (Ulrich, 1984; Clearwater and Coss, 1990), are likely to generate positive states of wellbeing and health.

Passive cooling strategies, such as thermal mass, external shading, building orientation, cross ventilation, and better insulation in buildings, are the key element of sustainable building. In addition to its less reliance on mechanical system in maintaining comfortable internal temperatures, passive design building has become synonymous with quality, comfort, and ultra-low energy buildings that require less energy for space heating and cooling (Wimmer *et. al.*, 2013). Extensive research on passive house design in temperate climates has been carried out in the last two decades and remarkable improvements have been achieved with regard to the energy performance of buildings. In contrast, there are far less documentation and examples available for the tropical climates. As pointed out by Groenhout and Partridge (2010), it is relatively easy to achieve energy efficient climate control through passive measures alone for most or even all of the year in temperate climates, but much more challenges associated with elevated external temperatures, such as higher humidity for much of the year, significantly more direct solar radiation throughout the year, and the lower diurnal temperature variation, are to be expected in the tropical climates. In the case of public assembly spaces, the challenges of achieving comfort conditions are even compounded by the high occupant density and intermittent or infrequent usage as they have very different occupancy and space loads to more conventional spaces. As a consequence, attempts to achieve building comfort in tropical climates, particularly for those public assembly spaces, are mainly through improved mechanical cooling.

However, it is believed that the optimum performance and potential benefit of passive cooling strategy can be achieved with careful and meticulous design. A good building design can decrease power consumption, saves money, and contribute to the reduction of greenhouse gas emissions. A bioclimatic design that based on local climate, aimed at providing thermal and visual comfort, as well as making use of solar energy and other environmental sources can even provide a comfortable environment by virtue of the passive features of design. Research suggests that bioclimatic buildings use 5 to 6 times less energy than conventional buildings over their lifetime through the use of the buildings' microclimate, form and fabric, rather than through the use of efficient mechanical equipment (Jones, 1998). In fact, using natural phenomena to reach indoor comfort has been well known since the early eras. The vernacular architecture of the Malay *kampung* house has responded with such phenomena as very good solution for tropical climate region. It realizes the optimum comfortable indoor temperature throughout the most days of the yearlong by equating the volume adopting and the space taming with the different natural elements forces of the sun, atmosphere, biosphere, and climate, which are common in these days as passive design strategies. Since the vernacular architecture has

been recognized as a climate responsive approach that accomplishes sustainability in human environment (Choi and Yu, 2013), building for sustainability may need to reconsider back these pre-industrial times design techniques and principles, so as to draw a stronger insight in encountering the human quality of life in built environment for the present day.

It is with this aim that the present study is conducted, by undertaking a case study of work to propose and optimize the design of a public assembly space – Taoist Academic Centre (TAC) – with the use of passive design strategy extracted from the vernacular architecture – a typical Malay *kampong* house. By further assessing the efficiency and limitation of the passive cooling strategies for hot and humid climates, the study aims to prove that modern tropical architecture prototype is possible to be developed from the vernacular architecture, and this prototype will not only respond well to the local climates, but also able to accommodate different cultural contents. Ultimately, the findings from this study will be functioning as an input to the real life project that takes place in Sri Kembangan, Kuala Lumpur.

## METHODOLOGY

The study started with the analysis of local climate, by using the Ecotect software, to identify the thermal comfort zone to be achieved in the later on architecture design. Then, the simulation was done to a typical traditional Malay *kampong* house, to identify the embedded environmental design strategies. Based on the preceding analysis, the prototype of TAC was developed to form the basic module for the design of the mentioned real life project.

## TROPICAL CLIMATE STUDY

Since the real life project will be taking place in Sri Kembangan – a town that located 20km from the centre of Kuala Lumpur, the zone setting and other thermal properties for local climate analysis were based on the one that applicable to Kuala Lumpur. Figure 1 shows the location of the real life project. The length and breadth of the site are 290m and 280m, respectively, with a small lake in the centre. Four sides of the site are connected with roads, with the North South Highway situated in the southern part of the site.



Figure 1. Site plan for the real life project

## Malay Kampong House Simulation

There are three approaches commonly adopted in the investigation of thermal performance for building envelopes: (i) by calculation with formula as in Grigoletti *et. al.* (2008); (ii) by field measurement as in Healthcote (2007); and (iii) computer simulations. As for the present study, the simulation of a typical Malay *kampong* house was carried out to identify the details of its climatic responses.

Through literature review, it was found that most of the traditional Malay *kampong* house shares the same strategies in attaining the optimal climatic control. Amongst are (i) allowing adequate ventilation for cooling and reduction of humidity; (ii) using of low thermal capacity building materials so that little heat is transmitted into the building; (iii) controlling direct solar radiation; (iv) controlling glare from the open skies and surroundings; (v) protecting against heavy rain; and (vi) assuring adequate natural vegetation in the surroundings to provide a cooler microclimate. As such, a simplified model of the typical Malay *kampong* house, with the following conditions, was constructed to capture the essence of its design strategies:

- The house is elevated 1500mm above ground.
- The interior spaces are divided into three rooms connected with doors. The height of the rooms is 3000mm from ground which is 1500mm above 1st floor.
- The high pitch roof has opening on both gable ends; this is common features for Malay house.
- There is no ceiling; the roof space and the room space as one high volume of space.
- There are two zones assigned, the room zone includes the roof space and the room space and the ground zone, which is the elevated space below the room.
- The materials are mainly timber for walls and roof using shingles
- The façade has large openings, using void instead of windows from the software.
- Overhangs are 1500mm all round.
- The longer elevation is facing north south orientation
- The date chosen is on 21st March, Equinox, where the Sun is directly above the equator and shortest distance to Earth.

Both the model zoning and views are shown in Figure 2 and Figure 3, respectively.



**Figure 2.** Malay house Ecotect model zoning

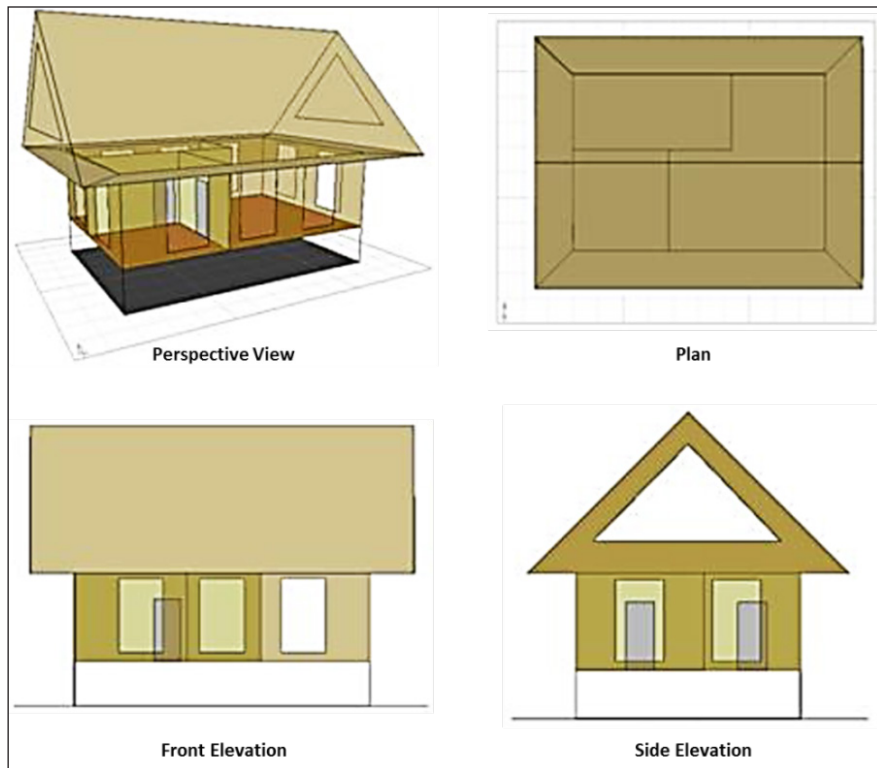


Figure 3. Malay house Ecotect model views

## Proposed Prototype Design – The Concept of Eco-Pavilion

Based on the results from the preceding analysis, the concept of Eco-pavilion was proposed as an initiator towards sustainable public assembly building in tropical climate. Conceptually, the Eco-pavilion is a reflection of the passive cooling strategies found in Malay *kampong* house that considers the issues of space, internal circulation, cross ventilation, and numbers of openings, but proposes for the reverse of space functions within the house. Three models of TAC were simulated and their thermal performance was compared.

## RESULTS AND DISCUSSION

### Local Climate Analysis

The results of local climate analysis are as shown in Figure 4, while the other important points are summarized as follow:

- The average temperature in Kuala Lumpur, Malaysia is 27.5 °C (82 °F).
- The range of average monthly temperatures is 1 °C.
- The warmest average max/ high temperature is 33 °C (91 °F) in February, March, April, May & June.
- The coolest average min/ low temperature are 22 °C (72 °F) in January, February, July, September & December.

- Kuala Lumpur receives on average 2409 mm (94.8 in) of precipitation annually or 201 mm (7.9 in) each month.
- On balance, there are 202 days annually on which greater than 0.1 mm (0.004 in) of precipitation (rain, sleet, snow or hail) occurs or 17 days on an average month.
- The month with the driest weather is July when on balance 102 mm (4.0 in) of rain, sleet, hail or snow falls across 11 days.
- The month with the wettest weather is April when on balance 279 mm (11.0 in) of rain, sleet, hail or snow falls across 21 days.
- Mean relative humidity for an average year is recorded as 62.6% and on a monthly basis it ranges from 58% in March to 66% in May & November.
- There is an average range of hours of sunshine in Kuala Lumpur of between 4.9 hours per day in November and 7.4 hours per day in February.
- On balance, there are 2228 sunshine hours annually and approximately 6.1 sunlight hours for each day.

To note, the belt with green colour, as shown in Figure 4, is the thermal comfort zone for Kuala Lumpur, which ranges from 20 – 25°C for environmental designers. It is, thus, important to achieve this range in the proposed prototype design.

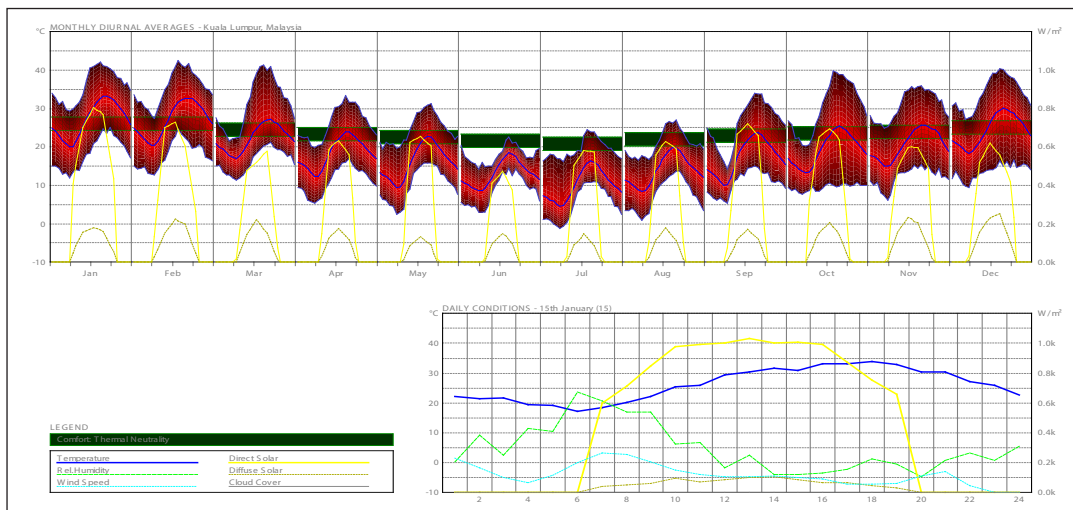


Figure 4. Monthly Diurnal Average – Kuala Lumpur

### Ecotect Analysis of Malay Kampong House

Amongst the analysis to be undertaken are solar exposure, daylight analysis, insolation analysis, and thermal comfort analysis.

#### Solar Exposure

Figure 5 shows the average daily solar exposure of the model. The direct solar exposure average daily from 0900hr – 1800hr is ranging from 400 – 640W/m<sup>2</sup> for the whole year. In January, the radiation reaches as high as 792.1W/m<sup>2</sup> at 1300hr, which is the highest throughout the year. This indicates that the room receives tremendous solar exposure in the day. The shading graph, as depicted in Figure 6, indicates that the shading of the Malay



**Table 1.** Summary of daylight analysis

Daylight analysis	Room zone (3000mm above ground)	Ground level zone (1500mm above ground)
Daylight factor	66.45%	48.95%
Daylighting level	5648.00 lux	4160.51 lux
Internal reflection	25.18%	10.89%
Sky component	41.24%	38.05%

### Insolation Analysis

This section looks at the insolation effect and radiation from the vegetation around the building. It includes sky factor and photo-synthetically active radiation (PAR), which is the total radiation, percentage visible sky, and plant radiation. The average daily PAR for the ground floor and room zone is almost similar, which is 3.60 MJ/m<sup>2</sup>/d and 3.79MJ/m<sup>2</sup>/d, respectively. The average daily total is 2368.45Wh (ground floor zone) and 2495.40Wh (room zone). Although the room zone is exposed to more radiation, the difference is only 129.95 Wh, due mainly to the effects of vegetation around the house on ground level.

**Table 2.** Summary of insolation analysis

Insolation analysis	Room zone (3000mm above ground)	Ground level zone (1500mm above ground)
PAR	3.79MJ/m <sup>2</sup> /d	3.60MJ/m <sup>2</sup> /d
Average daily total	2495.40Wh	2368.45Wh

### Thermal Comfort Analysis

The mean radiant temperature is high, with 32.50°C in the ground floor zone and 35.83°C in the room zone. The results are beyond the ideal range of thermal comfort (25.5°C – 28°C). This renders the house to a relatively high discomfort level in the day. The Predicted Mean Vote (PMV) index shows the mean response of a large group of people according to the ASHRAE thermal sensation scale. Based on this scale, both ground floor (2.6 PMV) and room zones (3.6 PMV) are considered warm and hot. Another indicator – Predicted Percentage Dissatisfied (PPD) – also indicates that over 95% of the occupants are dissatisfied staying in the house. Further study on the hourly temperature found that the temperature of the room zone increases beyond 30°C at 1130hr to 40°C at 1430hr, and decreases back to 30°C at 1600hr, in which the temperature in this period is totally above the thermal comfort level. The temperature of the room zone is much higher than the outdoor temperature as heat trapped within four walls, while the ground floor zone is generally within the thermal comfort zone, with the highest temperature in the same period is 28°C, due to vegetation on ground, no walls nor partition, and the air flow freely through the space. The main heat gain is from Direct Solar. The rate of hourly heat gain for the ground floor zone is faster. However, the values at ground zone is only 7200W, peak at 1200hr then decreases to 4800W at 1330hr and slightly rise to 5000W at 1500hr and then continue to decrease. The room zone, on the other hand, takes longer to increase, and the gain goes beyond 100,000W at 1700hr. This means a lot of heat is trapped in the room zone between 1300 – 1500 hrs. Heat gain is 14 time more in room zone.

As shown in Table 3, the ground floor zone losses heat through fabric (58%) and inter-zone (35.90%), while gains heat from solar (67.9%) and internal (15.0%). The room zone losses heat through fabric (86.5%) and gains from solar (87.00%). Room zone highest heat

gain value 18400W/m<sup>2</sup> and ground zone highest heat gain 2400W/m<sup>2</sup>, which is 7.6 times more in room zone.

**Table 3.** Results of passive gain breakdown

Category	Ground floor zone		Room zone	
	Losses	Gains	Losses	Gains
FABRIC	58.50%	6.40%	86.50%	4.90%
SOL-AIR	0.00%	0.00%	0.00%	5.00%
SOLAR	0.00%	67.90%	0.00%	87.00%
VENTILATION	6.20%	0.80%	6.70%	0.40%
INTERNAL	0.00%	15.00%	0.00%	1.60%
INTER-ZONAL	35.30%	10.00%	6.80%	1.10%

The result appears to coincide with the field measurement by Hassan and Ramli (2010), in which the thermal comfort of the room space is not satisfactory. The simulation shows that the ground floor zone open space of the Malay house performed better than the room zone due to:

- The ground space is open and allow cross ventilation while the room above is enclosed with walls. Even though the openings are able to facilitate cross ventilation, it is not as good compare to the ground. The room zone is not comfortable to stay in from 1100 – 1800hrs.
- The ground level has two layers of protection against the sun, the first layer is the roof and the second layer is the room directly above. The heat reaches the ground space is greatly reduced. Also since the ground space is open with vegetation, ventilation is possible, together with green, heat will be absorbed or flushed away.

### Development of Eco-Pavilion – An Ideal Model Formation

The simulation results show that space within the comfort zone is the elevated space below the room (ground floor level). As such, the house can be conceptually made climatically responsive by reversing its functions, which is making use of the ground level space as functional rooms while leaving the 1st floor as an open pavilion. The features of the Eco-pavilion are summarized as follow (Figure 7):

- An elevated space as ground level. The space is of multifunctional use. It can be used as an open space, similar to the Malay traditional house, or to be used for various functions. Rooms, office, canteen and so on can be at the ground level.
- Around the ground level, an interstitial space is developed on four sides to serve as a climatic buffer zone.
- Above the ground floor is the open deck or “pavilion deck”. This deck will be primarily used as open deck for human activities; no physical rooms will be built here.
- The eco-pavilion is in a basic form of a square or circle, the size and dimension can vary according to functions. This basic unit will be in modular construction and will be above to comply with the geometrical layout requirements of fengshui.
- The module is flexible and expandable according the site conditions. It follows the modular principles of the Malay house discussed earlier.
- The rooms are encouraged to open, although can be enclosed by windows and bi-fold doors.

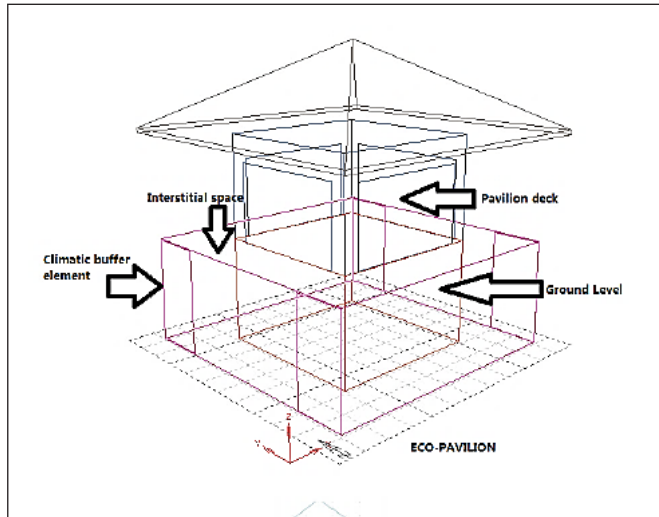


Figure 7. Eco-Pavilion model

Since the main heat gain is from solar (67.9%) at ground level, it is crucial to design a buffer element to reduce the external heat. The Eco-pavilion with the primary functions located at ground level has two major climatic buffer zones: (i) roof buffer zone; and (ii) wall buffer zone. The roof buffer consists of the open terrace above plus the roof with overhang. The roof will be installed with solar panels and gutter that collect rainwater. The absorption of solar energy reduces the impact of the sun to the space below. This means the room space at ground level has double layer protection (Figure 8). Wall buffer integrates the ideas of interstitial space and added an addition of 2m corridor on four sides around the ground level. The external envelope can be in the form of green walls, or water curtain as main features.

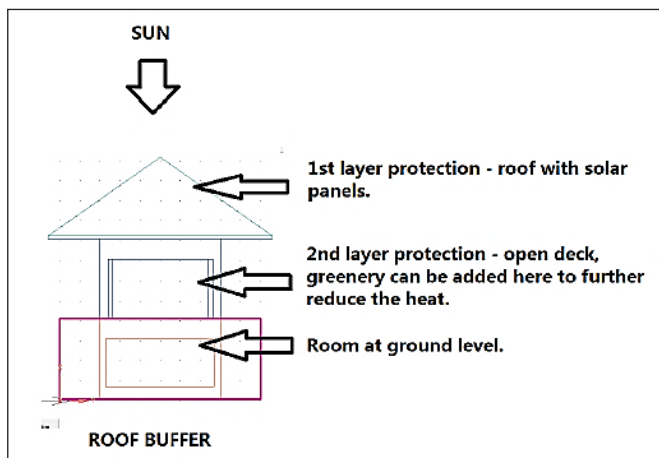


Figure 8. Eco-Pavilion roof buffer

An ideal model was developed based on the analysis of Malay *kampong* house. The computational studies found that the reversed functional arrangement, i.e. with the room at ground floor, terrace above, water curtain at the site, together with greenery around will form the most ideal scenario (Figure 9). Further analysis was conducted to investigate the performance of such ideal model. The hourly temperature graph was tabulated (Figure 10), which shows that the temperatures are within comfort band, in which the hottest hour is at 1600hr (26.80°C).

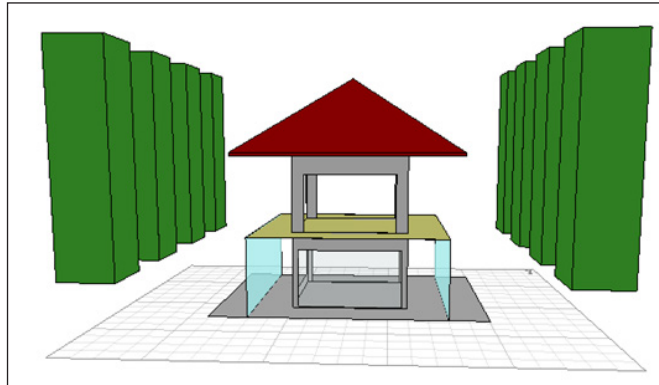


Figure 9. Ideal Model

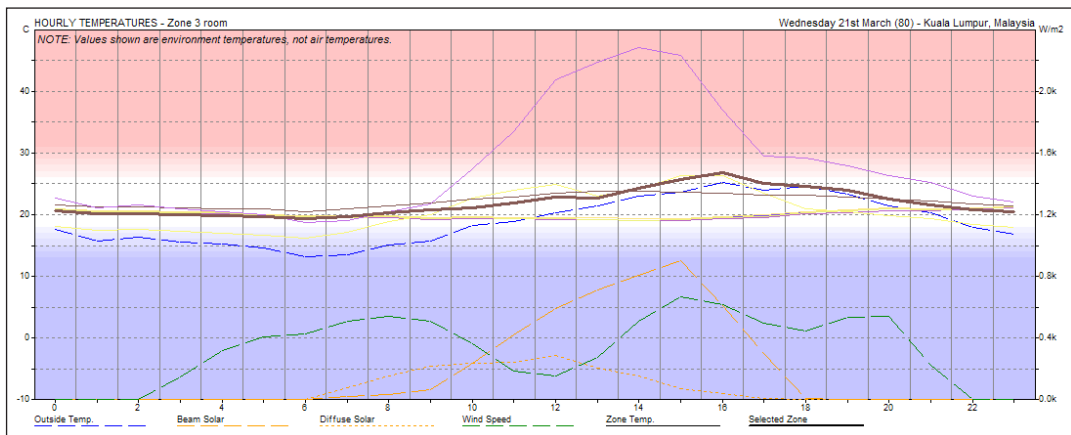


Figure 10. Hourly Temperatures, Zone 3 (Room) – Ideal Eco-Pavilion

The overall results are satisfactory. The model provides good thermal comfort conditions for a dual mode function. A few major characteristics of the eco-pavilion are such as:

- The ideal pavilion model with water curtain and plants offers the most suitable model for the tropics.
- The room space at the ground level performs better than the traditional Malay house;
- The deck space above open with full ventilation is suitable for other tropical activities in open air. Trees allow the open deck above for longer hours usage in afternoon.
- The double space usage is suitable for activities in the tropics, for those activities required enclosed space use the room on ground level, for those in open use the open deck above. This is in line with the tropical living. Hence the model offers a dual mode operation in different times of the day.
- The Eco-pavilion as a basic unit is flexible in spatial arrangement for site planning
- The structure of the pavilion can be designed for modular construction easily.
- This unit will be the basic unit for the design and site planning of the project. A permutation and combination of the basic unit will form the overall design of the project.

## Development of TAC

The basic building form of the TAC is derived from the preceding analysis, using the proposed Eco-pavilion concept as a base unit, forming clusters of pavilions in a structured manner. An open courtyard is in the centre, while on both sides of the courtyards nestled the eco-pavilions; the meditation pavilion is in the north, which is the enlarged version of the eco-pavilion; the main entrance hall is in the south (Figure 11). Landscaping is designed around the pavilions according to the climatic analysis, to provide the required thermal comfort environment. Earth mounds are built around the perimeter of the site with trees on top to shield away from the traffic as well as for visual screen.

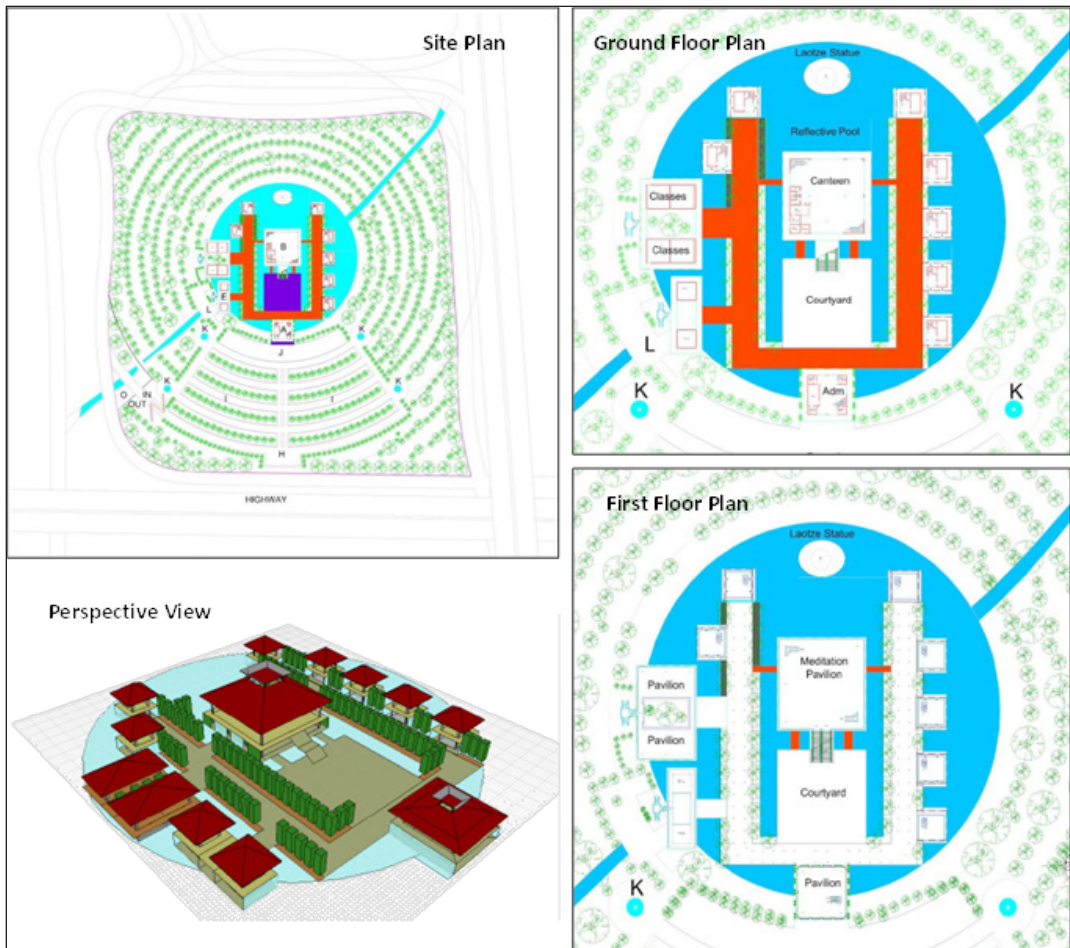


Figure 11. Different views of TAC project

Evolving from the ideal Eco-pavilion, some of the buildings need to increase in size to accommodate the architecture program. For example, the meditation hall and canteen need to accommodate 300 peoples; the classroom pavilion required fours classes; and the entrance pavilion needed a larger scale. Each of the building blocks is developed from the variants of the ideal Eco-pavilion, and tested using Ecotect. The meditation hall located at the first floor has temperature almost beyond the thermal comfort zone at 1500hr (Figure 12). However, no issue with regard to the thermal comfort of the occupants because the meditation activities are conducted only from 0500 – 1000hr and from 1800 – 2300hr, in which these are the period

where the first floor is having a comfortable temperature variant.

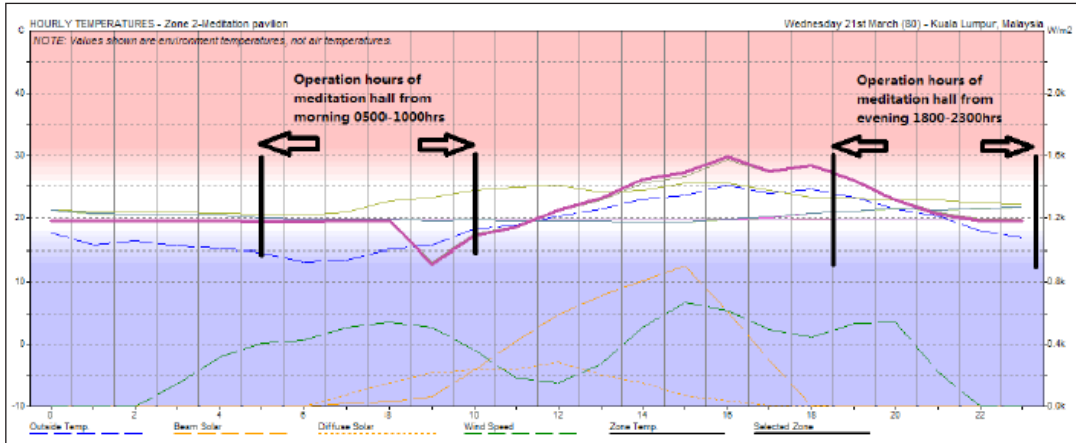


Figure 12. Hourly temperature – meditation pavilion

The canteen is located at the ground floor (Figure 13). Since the estimated daily usage of the canteen is about 20 people, it is possible to operate in natural ventilation mode. The Mean Radiant Temperature (MRP) for 20 people is 27.79°C, which is well within the comfort band. If there is enough air flow, the comfort requirement can be met, since 80 – 90% of the heat gain and loss is through ventilation (Table 4); hence, a demarcation of space near the perimeter of the building with maximum opening can be allocated for normal daily usage where air flow is enhanced (Figure 14).

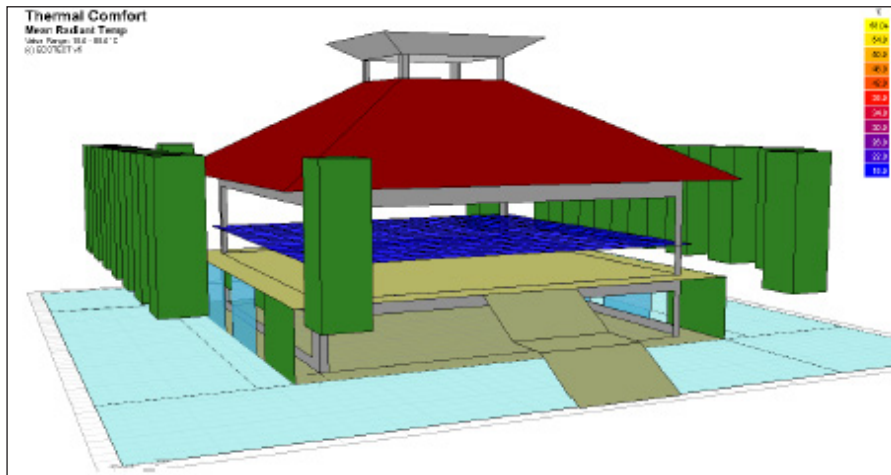
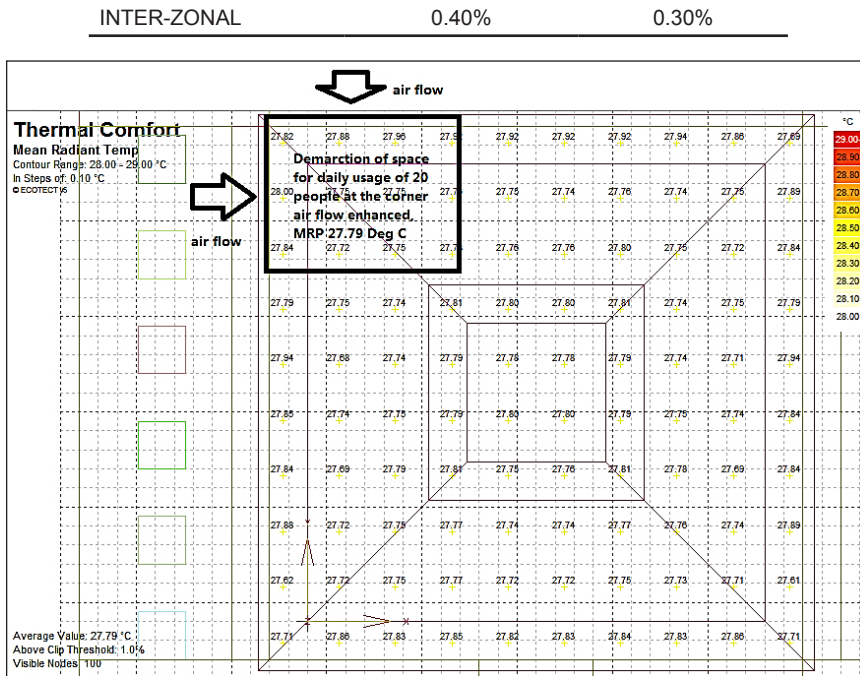


Figure 13. Location of the canteen and meditation pavilion

Table 4. Gains breakdown graph – Canteen

Category	Losses	Gains
FABRIC	2.70%	0.70%
SOL-AIR	0.00%	0.00%
SOLAR	0.00%	5.70%
VENTILATION	96.90%	85.60%
INTERNAL	0.00%	7.70%



**Figure 14.** Demarcation area for 20 people in the canteen daily usage

Ceiling fans will be installed and used when necessary, to generate a required air velocity of 2m/s. Air-conditions will be installed but will only be used during festival seasons. As the hourly temperature increases beyond 28°C around 1600hr, air conditioned is recommended, in festivals, operate from 1500 – 1800hrs. Other times of the day will be using mechanical fans. This mixed mode system will keep the overall temperature below 26°C throughout the day and is ideal for activities of 300 people (Figure 15).

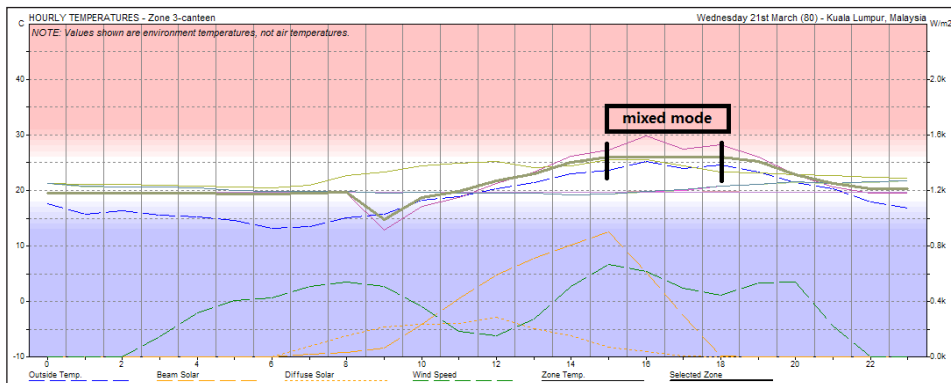


**Figure 15.** Hourly temperature – with mixed mode operation for canteen

The four classrooms are a combination of two eco-pavilions separated by landscaping (Figure 16 and Figure 17). The principle remains the same – the ground floor used as classrooms with open deck above for outdoor activities of the students in the morning, evening or at night. Each classroom is estimated to accommodate 20 students and designing for natural ventilation. The operation hours are from 0900 – 2200hrs. The main entrance is oriented to face north south. Trees planted on both sides of the classes help to provide shades to the classroom on ground floor, on the first floor, sunlight penetrates quite extensively.

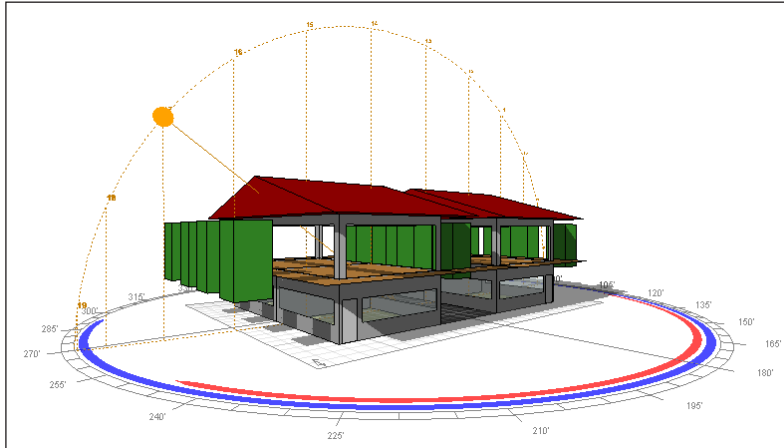


Figure 16. Classrooms shading

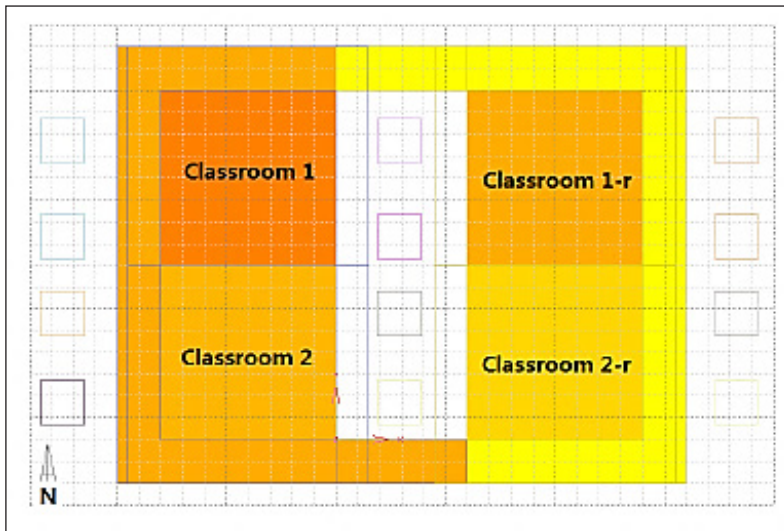


Figure 17. Classroom layout

The hourly temperature in the class room is within the comfort band, where the highest is 25.10°C at 1600hr (Figure 18, 19, 20 and 21). The solar gain can be further reduced by having a green roof pavilion on top of the classroom and more green walls to the external wall of the classrooms. More trees can be planted around the classrooms as trees are good buffer for solar heat and provide good environment for the children. With more trees and green to reduce solar heat gain, mechanical fans will be recommended to generate air flows; the rate recommended is 2m/s. Since the classrooms are not facing each other, the exposed wall can open fully open when classes are on. As heat, also losses through fabric, (over 30% for all classrooms), cavity walls between classrooms is recommended so that heat will escape instead of transferring from one zone to another. Time schedule of the classes is important. As heat also generated from internal activities and to avoid high outdoor temperature, it is better to arrange the classes in the morning or in the evening or at night, when the outdoor temperature is lower. The hourly temperature graph indicated that the good time schedule for classes is from 0700 – 1100hr and from 1800hr onwards. In general, it is believed that with the above recommendations, naturally ventilated classrooms are possible, however, air conditions will still be installed and standby in cases where classes need to be conducted outside the

recommended schedule.

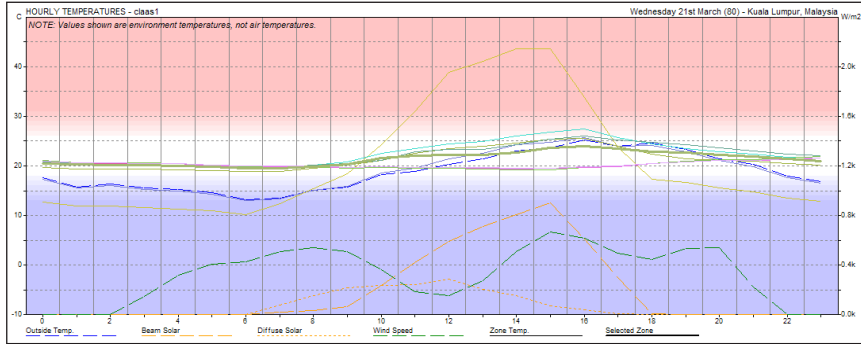


Figure 18. Hourly temperature – Classroom 1

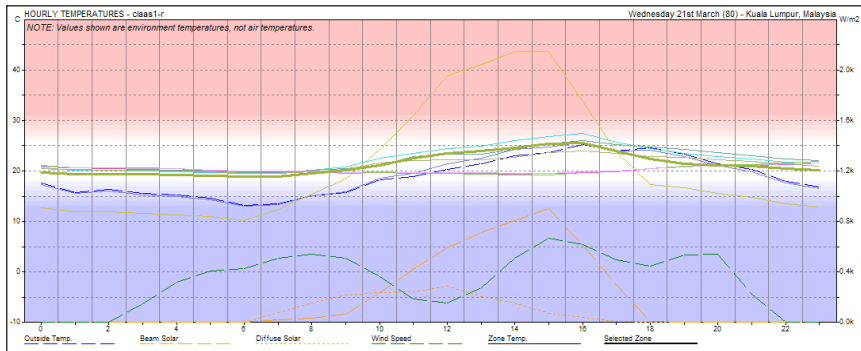


Figure 19. Hourly temperature – Classroom 1-r

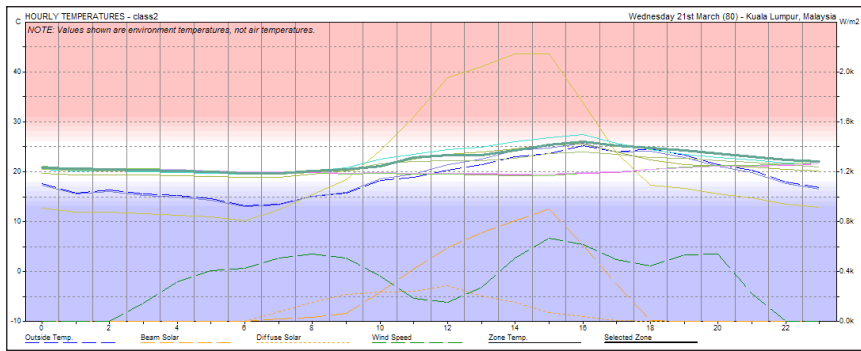


Figure 20. Hourly temperature – Classroom 2

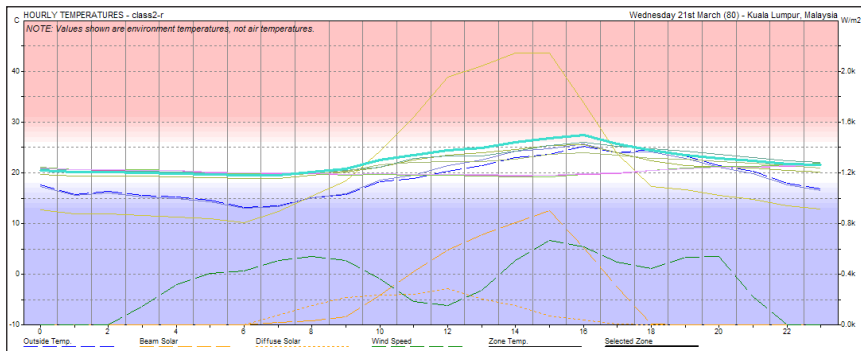


Figure 21. Hourly Temperature – Classroom 2-r

The office block is mainly for reception and general administration. The orientation is the same as the meditation hall – east west oriented, with the front and back facing the rising and setting sun. It is designed for 10 persons in natural ventilation mode. The principle is the same as the eco-pavilion where all functional activities are below, with water curtain and plants at both sides. Unlike other building blocks that have full openings on four sides, the office is open on two sides due to internal partitions of rooms (Figure 22). This helps to reduce daylight and insolation and maintain MRT at 24°C but the resulting PPD and PMV are not satisfactory due to the internal room blockage. Human activities are the main heat generator. When air is saturated, humidity increases and thus PPD and PMV values also increase, causing occupants feel uncomfortable. It is, thus, necessary to increase air flow in the office to flush out the heat and humidity generated from human activities (main heat gain). Mechanical fans recommended for air velocity above 2m/s. As the hourly temperature falls within good comfort temperature range throughout the day, air condition is not necessary (Figure 23). Localized air conditions zone is recommended for working areas with auto-sensors that turn on the air condition when indoor temperature increases beyond 28°C. Task lighting is also recommended for office.

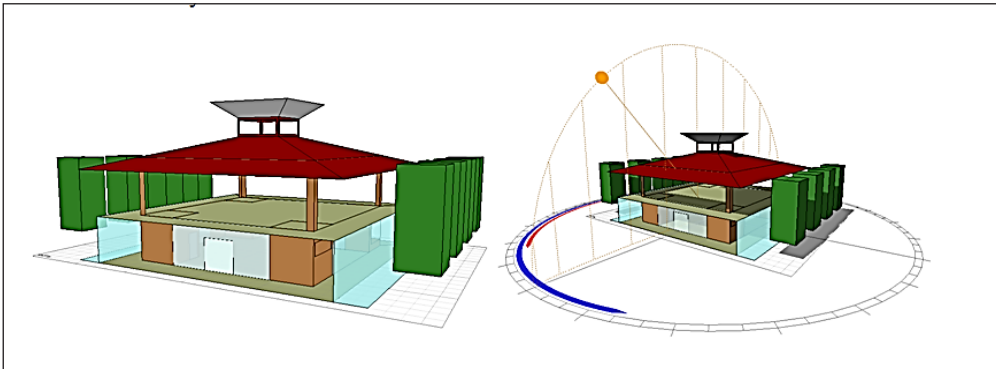


Figure 22. Administration office with sun path diagram

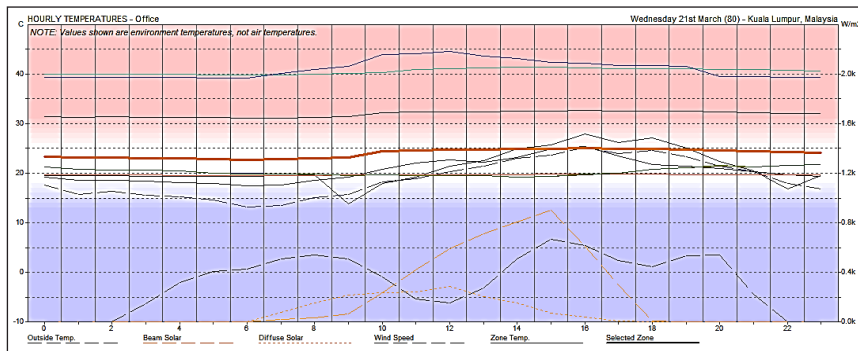


Figure 23. Hourly temperatures – Office

Table 5, 6, and 7 summarize the results of daylight factors, daily insolation, and thermal comfort of all the eco-pavilion building blocks, respectively. The daylight factor for the meditation hall pavilion is high (12.30%) due to the open deck that allows for daylighting penetration (Table 5). For other building blocks, the values range from 2% to 4%. The lux level is sufficient for normal designated activities except for administration office, and hence, task lighting is recommended. The internally reflected daylight is low (1.5 – 7%), while the externally reflected daylight is negligible. Sky component is highest in Ideal Eco-pavilion

(5.5%). Overall, the daylight works well in all building blocks.

**Table 5.** Summary of lighting analysis

Building Block	Daylight Factor (%)	Daylight Level (lux)	Internally Reflected (%)	Externally Reflected (%)	Sky Component (%)
Ideal eco-pavilion	11.50	1000.00	5.00	1.90	5.50
Meditation canteen	4.00	330.00	2.90	0.60	3.60
Meditation hall pavilion	12.30	1000.00	7.60	1.50	3.00
Classroom CR1	3.50	330.00	1.90	0.60	1.50
Classroom CR2	3.70	340.00	1.95	0.60	1.80
Classroom CR1-r	4.60	420.00	3.30	0.44	1.60
Classroom CR2-r	4.80	450.00	3.60	0.50	2.20
Administration office	2.00	60.00	1.50	0.90	0.70

The average daily insolation penetrating into the functional space is low, with total daily up below 400Wh (Table 6). The outdoor values sometimes went up to more than 4000 Wh, this means the proposed models able to reduce outdoor insolation up to 10 times. All building blocks are well shaded (over 90%) with minimum solar exposure.

**Table 6.** Summary of insolation analysis

Building Block	Average Daily PAR MJ/m <sup>2</sup> /d	Average Daily Total Wh	Diffuse Fraction (%)	Average % Exposure	Average % Shading
Ideal eco-pavilion	0.65	390.00	0.07	0.80	99.50
Meditation canteen	0.43	257.00	0.01	0.00	100.00
Meditation hall pavilion	0.50	310.00	0.03	3.30	97.40
Classroom CR1	0.46	263.00	0.01	0.00	99.00
Classroom CR2	0.46	279.00	0.01	0.00	99.00
Classroom CR1-r	0.47	300.00	0.01	0.00	100.00
Classroom CR2-r	0.48	310.00	0.01	0.00	100.00
Administration office	0.43	253.00	0.00	0.01	99.00

While the spatial comfort of the ideal eco-pavilion works well (MRT=23.6°C, PMV=-0.8, PPD=17) and thus no air flow is needed for thermal comfort, other building blocks such as canteen, classrooms CR1-r, and classroom CR2-r, are having MRT above the recommended temperature of 23.5 – 28.5°C, which is 29.32°C, 28.9°C, and 29.6°C, respectively (Table 7). This is due to the large space and indoor activities that generate heat. It is noted that these high temperatures all occurred at 1600hr of the day, which is the hottest hour of the day and is considered as the “critical design hour”. In other pavilions, the MRTs are within the recommended range.

**Table 7.** Summary of thermal comfort analysis

Building Block	MRT (°C)	PMV	PPD	Recommended Air Velocity (m/s)	Solar Gain (Watt)
Ideal eco-pavilion	23.60	-0.80	17.00	0.00	6.50
Meditation canteen	29.32	3.82	100.00	2.00	0.85
Meditation hall pavilion	22.15	2.67	96.50	2.00	7.5
Classroom CR1	25.50	3.25	99.74	2.00	0.15

Classroom CR2	26.40	3.40	99.92	2.00	0.16
Classroom CR1-r	28.90	3.82	100.00	2.00	0.17
Classroom CR2-r	29.60	3.99	100.00	2.00	0.17
Administration office	24.30	3.14	99.50	2.00	0.00

Two notable results for thermal comfort are the Predicted Mean Vote (PMV) and Predicted Percentage Dissatisfied (PPD). Except for the ideal eco-pavilion, all building blocks are having high PMV and PPD, indicating that there is a high level of dissatisfaction. However, such values cannot be interpreted literally because there are a few crucial factors to be considered in order to evaluate these values correctly.

First and foremost, the Ecotect worked on full operation hours. For example, in the case of meditation hall, in reality, activities normally happen in the morning from 0500-1000hrs and evening after 1800hrs, however, in Ecotect, it assumes operations from 0800 to 1800hrs, the software is not able to break into two periods. Interestingly, even when separate simulations were conducted, the results are the same. Therefore, Ecotect is simulating 300 people using the meditation hall from morning till night, with the heat of the Sun and activities throughout the day, the PPD and PMV naturally will be high. To evaluate if the thermal comfort works, the schedule of operation is important consideration. A more realistic solution to this is to study the hourly temperature graph, identify the temperature range and relate it to the schedule of activities. Taking the same meditation hall as example, morning activities (0500-1000hrs) is at temperatures 13-20°C and evening is at temperature reducing from 28.3 – 19.5 °C. In addition, as the simulation had identified that the main heat loss is through ventilation and recommended air velocity of 2 m/s, hence, mechanical fans are recommended to generate the required air flow to achieve the desired comfort.

In order to investigate further the thermal comfort conditions, the Olgyay's bioclimatic chart (Figure 24) was adopted. Using meditation hall, taking temperature at 1800hr, DBT 24.6°C (outdoor), radiation at centre of the hall is 0.480MJ/m<sup>2</sup>/d, converting it to Wh/m<sup>2</sup>, 0.48x277.78Wh/m<sup>2</sup>/d=133Wh/m<sup>2</sup> (1MJ=277.78Wh), if air velocity is increased to 2m/s, as recommended by Ecotect, the extend of thermal comfort zone will increase. Air flow rate is therefore an important design strategy for thermal comfort. However, the air flow needs to be generated by mechanical means with maximum open space shaded by trees. Since the prevailing winds in Kuala Lumpur is not that reliable as the site is blocked by buildings around, the prevailing wind analysis is not included in this study and it is taken as additional bonus on top of other design solutions.



- Plants as landscaping are used outside each of the building and to cover the remaining of the site;
- Making use of the existing pond and convert it into a reflective pool, locate the building block on the pool, surrounded by water elements;
- As ventilation is the main heat loss medium, beside façade openings, mechanical fans are recommended to generate air flow at minimum speed of 2m/s. This will increase the extend of the comfort zone; and
- In specific case, for example, activities required in critical hot hour (1600hrs), mixed mode system will be used. Air condition can operate for a few hours until the temperature drops, then revert back to mechanical fans or natural ventilation.

## CONCLUSION

Occupants comfort and health are important in sustainable building design. The indoor thermal environment should be designed to maintain maximum human productivity and performance. The present building design is said to have lost its build form identity in terms of rainforest and tropical landscape, due to planning patterns and construction systems, which by adopting planning laws, building codes, and regulations borrowed from the West. Besides, the practicing building construction method which is derived from systems used since the 1800s (the period of Industrial Revolution in Europe) is unlikely taking environmental concern as a primary consideration. Thus, it is important to reconsider the design approaches derived from the vernacular architecture that highly takes into account the fundamental nature of climate understanding.

The present study successfully explores the workable sustainable architecture prototype for public assembly spaces in the tropical climate. By conducting model simulation, the technological aspects of the Malay *kampong* house in climatic responses are identified, and the concept of Eco-pavilion – which is a reflection of the passive cooling strategy found in the Malay *kampong* house but proposes for the reverse of space functions within the house – is suggested. It is evidenced that with a perusal and detail research by involving various knowledge disciplines, vernacular architecture is potential to give a very mean contribution in the design of comfortable and sustainable building for modern society. On a much larger scale, the present study provides a data base for future explorations that emphasized on bioclimatic design. As the study focused on the thermal performance of the public assembly building, future research can investigate further on modular construction system, materials, and even the renewable energy systems of the basic unit, as well as how such unit, in modular system, can be expanded through permutation and combination of various design programs.

## REFERENCES

- Adenan, R.H. (2013). *Passive cooling for houses on water in Brunei Darussalam*. 29th Conference, Sustainable Architecture for a Renewable Future, Munich, Germany, 10th – 12th September 2013.
- Brightman HS and N Moss. 2001. “Sick building syndrome studies and the compilation of normative and comparative values.” In *Indoor Air Quality Handbook*. eds. JD Spengler, JM Samet, and JF McCarthy, McGraw-Hill, New York.
- Clearwater Y and RG Coss. 1990. “Functional aesthetics to enhance well-being in isolated and confined settings.” In *From Antarctica to Outer Space: Life in Isolation and Confinement*. eds. AA Harrison, YA Clearwater, and CP McKay. Springer-Verlag, New York.

- Fisk WJ. 2001. "Estimates of potential nationwide productivity and health benefits from better indoor environments: an update." In *Indoor Air Quality Handbook*. eds. JD Spengler, JM Samet, and JF McCarthy, McGraw-Hill, New York.
- Gencel, Z. and Velibeyoglu, K. (2006), Public Spaces in the Information Age, Reconsidering the Planning and Design of Urban Public Spaces in the Information Age: Opportunities & Challenge, 42nd ISoCaRP Congress, Istanbul.
- Grigoletti, G., Sattler, M. A. and Morello, A. (2008). Analysis of thermal behaviour of a low cost, single-family, more sustainable house in Porto Alegre, Brazil. *Energy and Buildings*, 40: 1961-1971
- Giane de Campos Grigoletti, M. A. S. (2008). Thermal performance evaluation method for low cost single family one-floor housing for Porto Alegre - Brazil. PLEA 2008 – 25th Conference on Passive and Low Energy Architecture, Dublin, 22nd to 24th October 2008.
- Groenhout, N. and Partridge, L. (2010). Optimisation of passive ventilation design for public assembly buildings in a tropical climate. *Ecolibrium*, February, 28 – 34.
- Hassan, A.S. and Ramli, M. (2010). Natural ventilation of indoor air temperature: a case study of the traditional Malay house in Penang. *American Journal of Engineering and Applied Science*, 3(3): 521 – 528.
- Heathcote, K. (2007). *Comparative Analysis of the Thermal Performance of Three Test Buildings*. Earth Building Research Forum, School of architecture, University of Technology Sydney <http://www.uts.edu.au>.
- Heerwagen, J. (2000). Do Green Buildings Enhance the Well Being of Workers? *Environmental Design+Construction* 3(4): 24 – 30.
- Heerwagen, J., Loveland, J. and Diamond, R. (1991). *Post Occupancy Evaluation of Energy Edge Buildings*. Center for Planning and Design, University of Washington, Seattle, Washington.
- Jamaludin, N., Khamidi, M.F., Wahab, S.N.A. and Klufallah, M.M.A. (2014). Indoor thermal environment in tropical climate residential building. *Emerging Technology for Sustainable Development Congress (ETSDC)*.
- Jones, D. (1998). *Architecture and the environment*, London, Laurence King Publishing. ISBN 978-0879518196
- Leaman, A. and Bordass, B. (2001). The Probe occupant surveys and their implications. *Building Research and Information*, 29(2): 129 – 143.
- Leather, P., Pyrgas, M., Beale, D., and Lawrence, C. (1998). Windows in the Workplace: Sunlight, View, and Occupational Stress. *Environment and Behavior*, 30(6): 739 – 762.
- Milton, D.K., Glencross, P.M. and Walters, M.D. (2000). Risk of Sick Leave Associated with Outdoor Air Supply Rate, Humidification, and Occupant Complaints. *Indoor Air*, 2000 10: 212 – 221.
- Olgay, V. (1963). *Design with Climate Bioclimatic Approach to Architectural Regionalism: Princeton University Press*, Princeton, New Jersey.
- Szokolay, A. (1997). *Thermal Comfort*. PLEA Note 3 PLEA International, University of Queensland.
- Ulrich, R. (1984). View through a window may influence recovery from surgery. *Science* 224:420 – 421.
- Wimmer, R., Eikemeier, S. and Reisinger, K. (2013). *Renewal material and energy, zero carbon potential in urban context*. Sustainable Building 2013, Oulo Finland.
- Wyon DP. 1996. "Indoor Environmental Effects on Productivity." In *Proceedings of IAQ '96, Paths to Better Building Environments*. American Society of Heating, Refrigerating, and Air Conditioning Engineers, Atlanta, Georgia.

# A REVIEW OF BUILDING INFORMATION MODELLING (BIM)–BASED BUILDING CONDITION ASSESSMENT CONCEPT

Adi Irfan Che-Ani<sup>1</sup>, Mohd Harris<sup>2</sup>, Muhammad Farihan Irfan Mohd-Nor<sup>1</sup>, Mohd Zulhanif Abd Razak<sup>1</sup> and Afifuddin Husairi Hussain<sup>2</sup>

<sup>1</sup> Department of Architecture, Universiti Kebangsaan Malaysia, 43600 UKM Bangi, Selangor

<sup>2</sup> CIDB Malaysia, Menara Dato' Onn, Pusat Dagangan Dunia Putra, Jalan Tun Ismail, 50480 Kuala Lumpur

## Abstract

Building Information Modelling (BIM) is a new technology growing rapidly worldwide. The use of BIM in the architectural, engineering, and construction (AEC) industries has increased substantially because its advantages have been recognized. Many researchers studied the potential of BIM in their fields of expertise. The purpose of this conceptual paper is to study the potential of BIM in building condition assessment practice. The method used for this study was literature review, and covers previous research, guidelines, reports, and other sources that were related to the subject. BIM has great potential for integration into building condition assessment (BCA) practices. BIM provides a “bridge” between virtual modelling and the physical building that provides accurate data for facility maintenance activities. However, most of the completed buildings do not have a BIM model as it still a new technology. In relation to this, this study was designed to produce a framework for building condition assessment via BIM for existing buildings. The objective of this framework is to demonstrate the implementation of BCA toward achieving sufficient facility management practices for preventive maintenance, repair, and upgrading work.

**Keywords:** *Building condition assessment, BIM, virtual model, integrated, building inspection.*

## INTRODUCTION

Traditional construction methods have raised various issues such as reworks, time delay, rising cost, lack of communication and coordination, and wastage (Mohd Nasrun *et. al.*, 2014), and is further supported by the studies of Khosrowashahi and Ariyaci (2012), who stated that organizations that implement construction projects through traditional methods are experiencing conflicts, complexities, uncertainties, and ambiguities. According to Jiao *et. al.* (2013), the fragmented nature among multiple collaborative enterprises in the construction industry has caused problems in data integration throughout the building lifecycle.

Recently, building information modelling (BIM) has become an emerging technology in the architectural, engineering, and construction (AEC) industries (Yen *et. al.*, 2014). BIM is an intelligent model-based process that provides insight to planning, design, construction, and management of buildings and infrastructure (Azhar *et. al.*, 2012; Kacprzyk and Kepa, 2014). The significant potential of virtual modelling in a construction project is that it can improve collaboration, integration, and communication between related parties (Akanmu *et. al.*, 2014). BIM implementation in AEC industries aims to shift the way of thinking and working process (Mohd Harris *et. al.*, 2014a). Process and team integration are key drivers of change necessary for successful projects (Mohd Nasrun *et. al.*, 2014). The effectiveness of BIM implementation significantly depends on the extent of integrated use and client/owner support (Cao *et. al.*, 2015).

Facilities management is regarded as the most expensive work within a building lifecycle (Hore *et. al.*, 2013). Therefore, minimizing the cost particularly for maintenance purposes, while maintaining the quality of the buildings at the best level, is important. Many research studies have been conducted and have proved that the use of BIM in AEC industries has had positive effects. Virtual models that link directly to the actual constructed building will enable the storage and retrieval of relevant information of the building required for maintenance work later during operation and maintenance phases (Akanmu *et. al.*, 2014).

This study aims to explore the potential of BIM in building condition assessment process by reviewing the ideas, theories and previous research studies that are related to the context of the study. The information gathered from this study are very important to develop the concept of building inspection reporting via BIM 3D models to replace traditional paper-based inspection methods in assessing the condition of a building. This concept will be developed and practiced to determine the effectiveness or disadvantages to improve the concept periodically. However, this paper only focused on the preliminary development of BIM-based BCA concept based on literature review.

## **RESEARCH METHODOLOGY**

Research is conducted by reviewing previous research studies to explore the potential of BIM in the building condition assessment field. Although the potential of BIM integration into the construction industry is widely discussed, there are still limited research studies that focus on building condition assessment via BIM. Given BIM is considered as a new technology in the construction industry, particularly in Malaysia, the literature review was conducted on research papers published between 2007 and 2015. Information obtained from previous research studies are collected and analysed subjectively to extract the relevant information needed.

### **Research Design**

According to Khosrowshahi and Arayici (2012), the beliefs of the authors in gathering, analysing, and using data about the phenomenon under investigation depend on research philosophy. They pointed that there are two branches of research philosophy, namely, ontology and epistemology (Khosrowshahi and Arayici, 2012). Chandrasekaran *et. al.* (1999) define ontology as "...content theories about the sorts of objects, properties of objects, and relations between objects that are possible in a specified domain of knowledge. They provide potential terms for describing our knowledge about the domain." Meanwhile, Lawson (2004) described ontology as the study of the nature of reality or existence in general and its categories, as well as their relations. While epistemology is concerned with the theory of knowledge and how to perceive reality and evaluate methods (Khosrowshahi and Arayici, 2012), it is required to obtain knowledge about the domain under investigation (Dawood and Underwood, 2010). Thus, Khosrowshahi and Arayici (2012) conclude, "epistemology is regarded as the philosophy of knowledge that helps the researchers to understand what knowledge is, describe the ways to acquire knowledge and subsequently answer the targeted research questions."

To develop a framework for BIM-based BCA, ontology and epistemology of both BIM

and BCA are required. Thus, an intensive literature review is conducted to collect and review all related theories, ideas, and findings from previous research. Figure 1 depicts the research design.

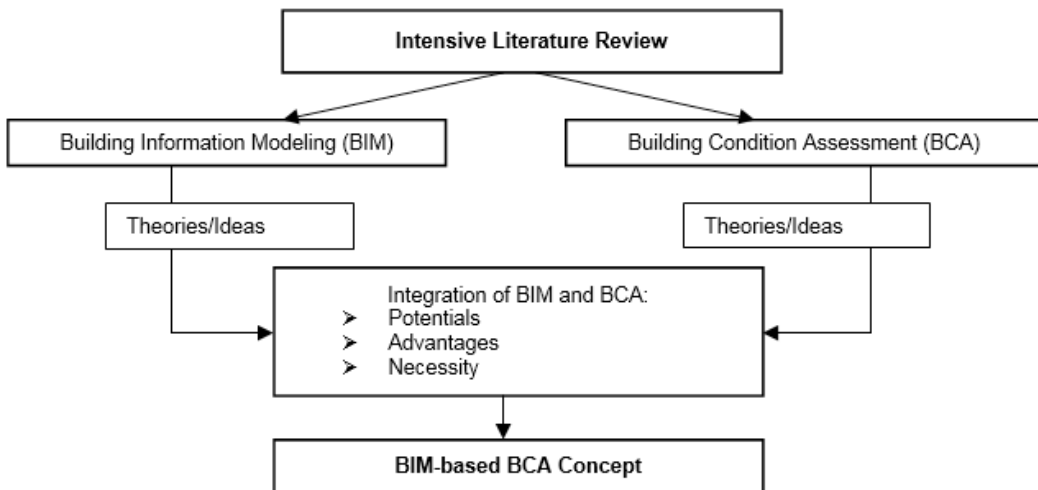


Figure 1. Research design

Based on Figure 1, the intensive literature review focused on two research subjects, namely, BIM and BCA, to study existing knowledge. Theories and ideas are gathered from previous research studies based on the ontology and epistemology of the subjects. The aim of this literature review is to collect all information to develop a BIM-based BCA concept. Thus, the potentials, advantages, and necessity of BIM and BCA integration need to be identified.

## LITERATURE REVIEW

Much research was conducted on BIM implementation in AEC industries. Bynum *et. al.* (2013) investigated the perceptions of the use of BIM for sustainable design and construction among designers and constructors. Cao *et. al.* (2015) investigated 106 projects involving the use of BIM in China, and found that BIM is principally employed as a visualization tool and how it is implemented is significantly associated with project characteristics. Chen and Luo (2014) explored and discussed the advantages of 4D BIM for a quality application tool based on construction code. Yen *et. al.* (2011) designed a module to execute the inspection task on site by using a mobile device, and the result can be uploaded to a remote server, wirelessly. Ho *et. al.* (2013) developed the BIMKSM system as a visual platform to improve construction knowledge sharing in building projects. Zhang *et. al.* (2013) developed a system that automatically analyses building models to detect safety hazards and suggest preventive measures to users. The system can analyse multiple and various types of cases involving fall related hazards. Zhang *et. al.* (2015) investigated how to identify and eliminate potential fall hazards that are unknowingly built into the construction schedule, early in the planning phase of a construction project. Qi *et. al.* (2014) developed a prevention through design (PTD) tool based on computer software as an automatic compliance-checking tool. Nguyen and Kim (2011) developed a framework for building code compliance checking using BIM technology.

BIM implementation in AEC industries aims to shift the way of thinking and the working process (Mohd Harris *et. al.*, 2014). BIM is now widely employed among design organizations because it has attracted the attentions of AEC industries (Son *et. al.*, 2015). Francom and El Asmar (2014) asserted that BIM is a process that has the potential to improve the performance of AEC projects. BIM is one of the virtual models that were specified by Akanmu *et. al.* (2014) proven highly beneficial and provided a great significant effect to AEC businesses. BIM also provides a “bridge” between virtual models and physical construction in bidirectional coordination consists of Cyber to Physical Bridge and Physical to Cyber Bridge (Akanmu *et. al.*, 2014). The Physical to Cyber Bridge is the sensing process involving sensors and data acquisition technologies to acquire information about building components or phenomena (Akanmu *et. al.*, 2014). Meanwhile, the Cyber to Physical Bridge represents the actuation that shows how the system is affected by sensed information (Akanmu *et. al.*, 2014).

Problems related to information delivery/sharing within consultants are the fundamental issues that need to be addressed with the effective implementation of BIM (Haron, 2013). According to Mohd Harris *et. al.* (2014b), the involvement of various parties in every construction project could result in poor information delivery, inaccurate information transferred, and worst, incorrect information. BIM is the answer to the fragmentation issue that exists among construction stakeholders; this is achieved by its ability to create and reuse consistent digital information models throughout the building lifecycle (Arayici *et. al.*, 2009). However, the collective adoption of BIM throughout the various construction disciplines and client support are essential for the success of BIM implementation (Mohd Harris *et. al.*, 2014b). The process component in BIM enables close collaboration and encourages the integration of the roles of all stakeholders in a project (Azhar *et. al.*, 2012).

In BIM, 3D CAD objects can be utilized to simulate the real world building elements with the ability to maintain life cycle information for a building (Yen *et. al.*, 2011). Virtual prototyping in construction will facilitate the coordination of the entire product design and production process (Kong and Li, 2009). Prior to project implementation, team members including owners, architects, engineers, contractors, subcontractors, and suppliers are constantly refining and adjusting their portions according to project specifications and design changes to ensure the model is accurate (Azhar *et. al.*, 2012).

In BIM, LOD may refer to *Level of Detail* or *Level of Development*. Level of Detail is essentially the amount of detail included in the model element while Level of Development by contrast is the degree to which the geometry and attached information of the element have been thought through (BIMForum, 2013). The development of BIM model comprises six levels of development (LOD), namely LOD 100, LOD 200, LOD 300, LOD 350, LOD 400, and LOD 500. The details of each LOD are described as follows (BIMForum, 2013).

- i. LOD 100 - The Model Element may be graphically represented in the Model with a symbol or other generic representation, but does not satisfy the requirements for LOD 200. Information related to the Model Element (i.e. cost per square foot, tonnage of HVAC) can be derived from other Model Elements.
- ii. LOD 200 - The Model Element is graphically represented within the Model as a generic system, object, or assembly with approximate quantities, size, shape, location, and

- orientation. Non-graphic information may also be attached to the Model Element.
- iii. LOD 300 - The Model Element is graphically represented within the Model as a specific system, object, or assembly in terms of quantity, size, shape, location, and orientation. Non-graphic information may also be attached to the Model Element.
  - iv. LOD 350 - The Model Element is graphically represented within the Model as a specific system, object, or assembly in terms of quantity, size, shape, orientation, and interfaces with other building systems. Non-graphic information may also be attached to the Model Element.
  - v. LOD 400 - The Model Element is graphically represented within the Model as a specific system, object, or assembly in terms of size, shape, location, quantity, and orientation with detailing, fabrication, assembly, and installation information. Non-graphic information may also be attached to the Model Element.
  - vi. LOD 500 - The Model Element is a field verified representation in terms of size, shape, location, quantity, and orientation. Non-graphic information may also be attached to the Model Elements.

However, this research focused on Level of Detail, which is composed of five LODs, such as LOD 100 – Conceptual, LOD 200 – Approximate geometry, LOD 300 – Precise geometry, LOD 400 – Fabrication, and LOD 500 – As built (Bedrick, 2008). According to Bedrick (2008) the content of each LOD model are as below:

- i. LOD 100 – Non-geometric data or line work, areas, and volumes zones.
- ii. LOD 200 – Generic elements shown in three dimensions (maximum size, purpose).
- iii. LOD 300 – Specific element, confirmed 3D, object geometry (dimensions, capacities, connections).
- iv. LOD 400 – Shop drawing or fabrication (purchase, manufacture, install, specified).
- v. LOD 500 – As built (actual).

Akanmu *et. al.* (2014) stated that there are many unutilized potentials of virtual models in the construction, operation, and maintenance phases. BIM purposes including visualization tools, clash detecting, building design, as built model, building assembly, construction sequencing, environmental analysis, model based estimation, facilities management, direct fabrication, and others (Mohd Faizal *et. al.*, 2014a). The combination of computer software with new working practices in BIM has improved the product delivery in construction projects, which includes quality, reliability, timeliness, and consistency of the process made (Mohd Harris, 2014).

Many researchers have recognized the benefits of BIM implementation in AEC industries (Akanmu *et. al.*, 2014; Mohd Faizal *et. al.*, 2014b; Mohd Harris *et. al.*, 2014a). BIM will provide a visual model and database throughout the building lifecycle (Wang *et. al.*, 2013). BIM models will allow the detection of discrepancies between as-built and as planned progress that provides the opportunity to initiate remedial actions and minimize overrun effects (Golparvar–Fard *et. al.*, 2009). This is supported by Akanmu *et. al.* (2014) as he stated that BIM will facilitate the detection of errors and conflicts prior to the construction process, thus reducing project schedule and cost.

Meanwhile, Arayici *et. al.* (2009) listed five benefits of BIM, such as efficient collaboration amongst the construction stakeholders; availability of the accurate documentation of the building development; common understanding of project costs, schedule and project progress; ability to assess the design alternatives and lifecycle effect; and reduced error, rework and waste – to improve sustainability of the design and construction. In terms of safety concerns, BIM is used to improve communications between construction players (Behringer and Azhar, 2012) to avoid potential hazards.

Even though there are many benefits recognized by previous researchers, Mohd Harris *et. al.* (2014a) found that some organizations have resisted change, or are still not ready to adopt BIM as a project delivery tool in their projects. Arayici *et. al.* (2009) listed six barriers based on their weighted ranks, such as firms unfamiliarity with BIM use; reluctance to initiate new workflows or train staff; firms do not have enough opportunities to implement BIM; benefits from BIM implementation do not outweigh the costs to implement it; benefits are not tangible enough to warrant its use; and BIM does not offer enough of a financial gain to warrant its use. A total of 24 criteria need to be addressed in the selection of BIM software, consisting of technical (15), managerial (8), and cost (1) issues (Mohd Faizal *et. al.*, 2014a).

Mohd Harris *et. al.* (2014a) have identified two critical issues as barriers to BIM implementation, that is, people and technology. The conversion from the traditional method to BIM models requires training, resources, content creation, teamwork, and new workflows, which all need to be managed simultaneously (Arayici *et. al.*, 2009). Selection of software for BIM implementation is also complicated because there are many programs that can be used for such purposes. Ruiz (2009) listed 33 different software packages developed by 11 software-developing companies that can be used as BIM. Lack of BIM standards for model integration and management by multidisciplinary teams is one technology-related risk (Azhar *et. al.*, 2012). Thus, different companies may use different software, and this may create a conflict among consultants in the same project.

Cost is regarded as the most concerning issue raised by contractors and consultants when it comes to investing in BIM tools (Mohd Harris *et. al.*, 2014a). In view of this, BIM should therefore be implemented efficiently by all parties involved in a project. Additional costs may arise if the BIM model is not managed properly, including difficulties in the implementation, supervision, and coordination (Suermann, 2009). By providing adequate information, the use of BIM for facility management can significantly help minimize this cost (Azhar *et. al.*, 2012). However, Azhar *et. al.*, (2012) raised questions on who should develop and operate the BIM among the stakeholders.

Cloud computing is essential in BIM as it helps in share information between the stakeholders to ensure a building project is successfully completed on time and within the budget (Blass, 2015). According to Chhibber and Batra (2013) cloud computing is an emerging information technology for storing, processing, and using data from remotely located computers that can be accessed over the Internet. By using cloud computing, all related parties could access information easily anywhere using portable devices, needing only 3G signals to get started (Blass, 2015). This technology is a convenient, cost-effective, and hassle-free method for connecting all stakeholders (Blass, 2015).

## **Building Condition Assessment via BIM**

Golparvar–Fard *et. al.* (2009) defined monitoring as *collecting, analysing, recording, and reporting* information. Manual monitoring is time consuming because the extraction of as-planned and as-built data is extensive (Navon and Sacks, 2007). The excessive amount of work required to be performed may cause human-errors and reduce the quality of manually collected data (Golparvar–Fard *et. al.*, 2009). Lin and Su (2013) pointed out that maintaining those facilities by relying on paper-based documents is inconvenient for maintenance staff. In addition, manual measurement and recording methods during on-site survey are time consuming (Klien *et. al.*, 2014) while the collected data are subjective because only an approximate visual inspection is usually performed (Golparvar–Fard *et. al.*, 2009).

BIM can be used in all phases of building lifecycle, that is, planning, design, construction, and operation. The operation phases consist of six BIM purposes that consist of three primary uses and three secondary uses (Rohena, 2011). Lin and Su (2013) emphasized that BIM can be an effective visual tool for facility maintenance management (FMM). The primary uses of BIM in the operation phase are as a record model, for maintenance scheduling, and building system analysis. Meanwhile, the secondary uses of BIM are asset management, space management/tracking, and disaster planning. BIM functionalities of visualization, analysis, and control will provide and support FMM practice (Becerik–Gerber *et. al.*, 2011).

Information is a key to the success of facility management (Lin and Su, 2013). Traditional practices deliver new asset information to FMM teams after the construction phase, and are manually loaded into a computerized maintenance management system (CMMS) after the handover (Foster, 2012). This process is time consuming and can lead to misinformation during the delivery process. In addition, the FMM team is also not involved during the design and construction phase. Thus, they need to extract all information to understand and learn about the completed building. Managing the assets effectively is difficult for the FM team if there is lack of information. The deployment of BIM in physical construction can improve the handling of information and knowledge from the design to the construction and maintenance phases (Akanmu *et. al.*, 2010; Anumba *et. al.*, 2010; Akanmu *et. al.*, 2014).

BIM models can be designed to provide information about the building quickly, and provides a database as a platform for conducting the required analysis and evaluation at all levels, including at the operational phase (Kasim *et. al.*, 2012). Azhar *et. al.* (2012) stated that BIM contains complete information about a building/facility as it evolves through planning, design, and construction. Thus, this information is useful for a facility manager to manage and maintain a facility more efficiently (Azhar *et. al.*, 2012). BIM 3D models increase work efficiency and upgrade maintenance information storing system (Su *et. al.*, 2011). BIM integrated assessment enables maintenance staff to access and review 3D BIM models for updating related maintenance records in a digital format (Lin and Su, 2013). According to Hore *et. al.* (2013), BIM can increase performance, utilization, and financial information in the maintenance phase, as the design and built asset information is still present in a single BIM model. For a facility manager, the use of BIM will facilitate their work by providing all critical information in a single electronic file, and all related information can be accessed easily by using the electronic system (Azhar *et. al.*, 2012). The most important benefit of BIM

in building condition assessment is it enables the generation and management of building data during its lifecycle (Akanmu *et. al.*, 2014).

Yen *et. al.* (2011) asserted that BIM is an ideal tool and platform for developing an inspection and maintenance system. The uses of BIM 3D models will assist the maintenance team in easily and quickly finding the location of defects (Su *et. al.*, 2011). Three compulsory tasks during inspection are completing the inspection checklist, recording defects, and taking photos of defects (Yen *et. al.*, 2011). By using BIM model in facility management, the information about building equipment and systems can be accessed by simply clicking on an object in the model (Azhar *et. al.*, 2012) by the on-site inspector. Then, inspection details can also be keyed into the system on site by using a wireless network. In addition, for the identifying and controlling purposes of the physical components in a building, this integrated approach is also able to provide remote access (Akanmu *et. al.*, 2014). This feature greatly helps accelerate the process of building inspections, and furthermore provides an accurate information and analysis process. Figure 2 depicts the general concept of building inspection.

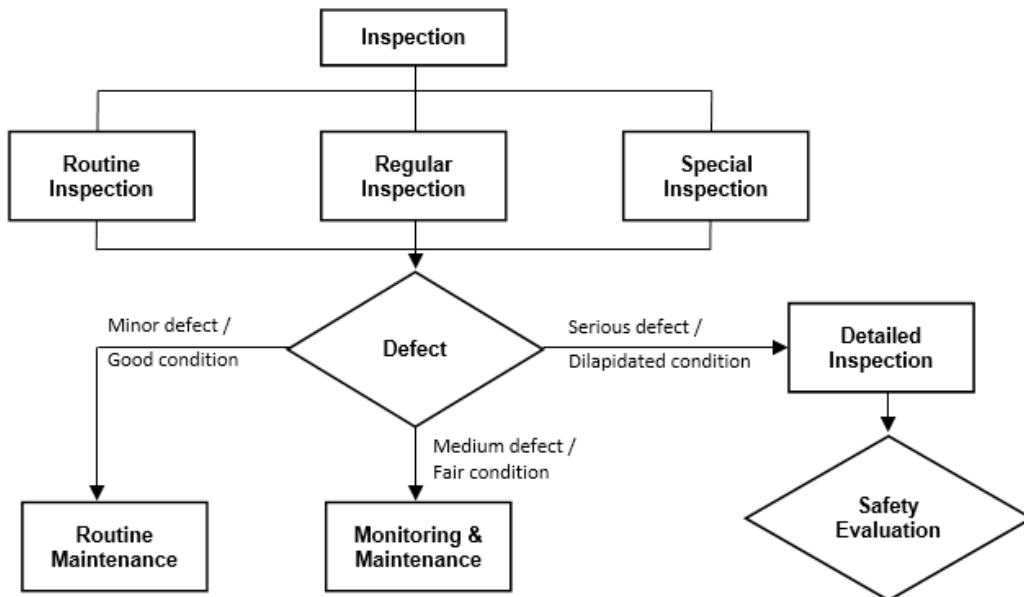


**Figure 2.** General concept of inspection (Yen *et. al.*, 2011)

Based on Figure 2, three types of inspection exist, namely, routine inspection, regular inspection, and special inspection. All these inspections aim to detect any defect that will reduce building and facility performance. Three categories of defect exist, which are minor defects (building/facilities are in good condition), medium defects (building/facilities are in fair condition), and serious defects (building/facilities are in dilapidated condition). Each level of defect requires different maintenance actions according to the severity of defects. For minor defects, routine maintenance is sufficient to maintain the quality and performance of the asset. However, monitoring and maintenance are required for medium defect. When a defect is identified as a serious defect, detailed inspection is required because dilapidated building/facilities may raise safety issues. Then, safety evaluation must be carried out by a specialist to determine further action.

Yen *et. al.* (2011) proposed a structure for BIM-based maintenance management systems that consists of three major components, that is, 3D models, inventory of structure facilities, and a maintenance database.

- i. 3D models - 3D models are fundamental for BIM, and a code or ID for each building component must be generated by creating a naming or numbering principle to facilitate defect plan tagging.
- ii. Inventory of structure facilities - The inventory must include all related drawings and documents including management data, environment data, and photos. Some information can be saved as data fields directly within the 3D model, such as dimension data and design criteria. Other information can be saved in a separate database connected via link, such as documents and photos.
- iii. Maintenance database - A maintenance database includes inspection records and maintenance records that are too complicated. Thus, it must be stored in a separate database and use data ID for reference purposes.

Apart from the three major components, Yen *et. al.* (2011) also designed eight modules to support the inspection tasks, namely, Basic Information Module, Inspection Management Module, Inspection Execution Module, Analysis and Report Module, Maintenance Module, GIS Module, Monitoring Module, and System Preference Module.

## **RESULTS AND DISCUSSION**

Building condition assessment is one of branches of facility management, other than building maintenance. Effective building maintenance work is highly dependent on building condition assessment that provides information on the latest building condition. Failure to conduct effective building condition assessment could also mean failure to carry out maintenance work properly. Therefore conducting the building condition assessment effectively is important. The current technology development has now provided a new platform to conduct building condition assessment via BIM.

Current building condition assessment using traditional systems is conducted manually. Each building defect is recorded on paper during site inspection with some details that describe the defect, including defect photos. Then, the location of the defect is tagged on the building layout plan (usually 2D drawing) to indicate the location of the defect for further action. For analyzing and storing purposes, all defects captured during the inspection will be recorded again into a computerized system. This means that the recording process is done twice, therefore requiring a long time to complete the process. This may cause errors when transferring the information and may affect the result. With the integration of BIM in building condition assessment, the inspection work can be simplified and accelerated. Yen *et. al.* (2011) compared the traditional inspection system and BIM-based inspection system, as shown in Table 1.

**Table 1.** Comparison between the traditional inspection system and the BIM-based inspection system

(Yen *et. al.*, 2011)

	<b>Traditional System</b>	<b>BIM-based System</b>
Structural components	Database-centric system with 2D CAD connection.	3D-CAD-centric system supplemented by a database.
Inspection execution	Record defects on paper in the field, then reproduce to digital form or database record afterward.	Record defects on mobile device with 3D view and location. Result can automatically upload to database.
Defect recording	Plain text with associated photos.	Mark on 3D CAD and link to text and photos.
Inquiry and report	Return with record from database. Can link to 2D CAD and photos.	Return with 3D models and link to records and photos.

### Potential of BIM-based BCA

The integration of BIM into building inspection enables a more efficient, quick, and accurate data recording process compared with the traditional method, because BIM can be developed comprehensively with the combination of designs from different fields (architecture, civil and structure, mechanical, electrical) in one model. By creating a “layer” for each building main part, users can hide unnecessary layers to expose the required layer (CREAM, 2014). This feature enables a building surveyor to see the overall picture of the building, especially hidden components such as plumbing and electrical components. Thus, building surveyors will know exactly what is behind the concrete wall by referring to the virtual model. This may facilitate building surveyors to predict the cause of building defects when they have complete information about a building and its facilities.

### Advantages of BIM-based BCA

The advantages of BIM are the following: the 3D models provide a new interface with strong visualization effect to enhance the overall comprehensiveness; the defects are directly marked on the 3D model to provide a more accurate record; and the inspection execution module is designed to take advantage of the advanced hi-tech mobile devices with wireless communication capability, GPS sensor, and photo shooting lens, to assist inspection in the field (Yen *et. al.*, 2011). Thus, the flow of building condition assessment via BIM can be summarized as follows.

- i. Development of virtual 3D model – FMM team should cooperate with the designers earlier on from the design phase of the BIM model (Wang *et. al.*, 2013). The development of 3D model should be completed with the entire database for operation and maintenance works after the completion of building.
- ii. Coding process – If possible, every building component should be given a special code or serial number. This code must be recorded into the virtual model so that the “bridge” between the virtual model and physical construction can work properly for the transmission of information.
- iii. Inspection works – Building inspection works conducted on site by building surveyors using mobile devices to capture defects. Sensor/scanners can be used to automatically detect the defective component and link it with the virtual model. Then, defect details can be recorded into the BIM model and the location of the defect will automatically be tagged into the model (or at least 2-point coordinates need to be captured for plotting

the defect in its exact location, should this needed to be done manually). The photo of the defect can also be captured using a mobile device and stored into the model or other supporting database, and synchronized at a later stage (where an app, either mobile or personal computer, is the platform of technology).

- iv. Data analysis – Given all defect details are recorded directly into the model, the analysis process should be generated automatically. However, the assessment system must be developed and integrated into the BIM virtual model to provide an accurate and quick data analysis.

### **Necessity of BIM-based BCA**

BIM-based BCA is necessity to shift the way of thinking and working process of traditional methods that are time consuming, complex, and outdated in terms of technology. In addition, the traditional assessment method and analysis process that are conducted manually may cause inaccurate results. This matter can be solved by using BIM-based BCA, which can provide automatic analysis and generate results by using the system. The accurate result will present the actual building condition, wherein determining the best maintenance action or remedy is important. This may provide more efficient facility maintenance processes (Azhar *et. al.*, 2012), increase work efficiency, upgrade maintenance information storing system (Su *et. al.*, 2011), provide easy access information (Azhar *et. al.*, 2012), and create the sustainable generation and management of building data (Akanmu *et. al.*, 2014).

### **Concept of BIM-based BCA**

Based on findings from the literature review, this research has developed a concept for building condition assessment via BIM. This concept was developed for usage on existing buildings that does not have BIM models. BIM is a new technology that has been integrated into the construction industry. Thus, only the latest buildings, especially those built within the last 10 years would probably have BIM models. However, this research believed that only a few buildings were constructed and managed by BIM because of its barriers. Even for buildings that were not constructed using BIM, there is still a possibility to manage its next lifecycle, as the occupancy phase is the longest phase in a building lifecycle. Thus, developing a concept for building condition assessment via BIM for existing buildings is important. Figure 3 depicts the concept of building condition assessment via BIM.

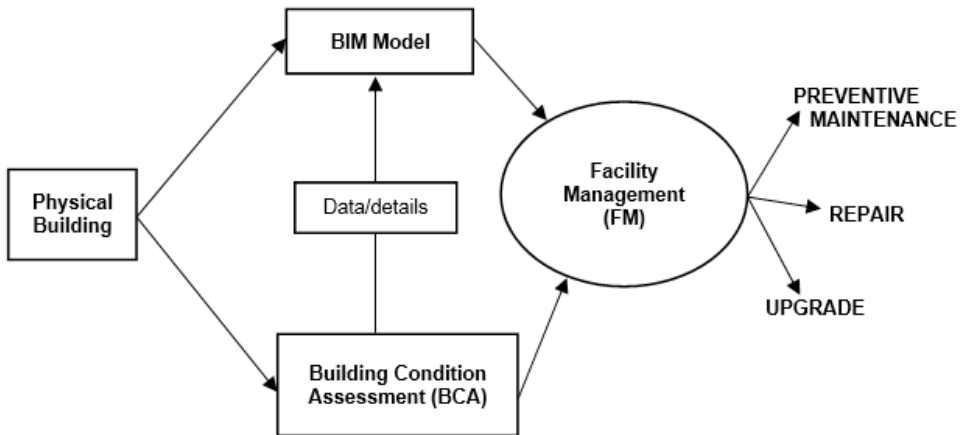


**Figure 3.** Building condition assessment concept via BIM

Based on Figure 3, the development of the BIM model and BCA works should be carried out simultaneously to achieve the good practice of facility management for the existing building. Both BIM model development and BCA should be conducted by two teams that have a good collaboration, integration, and communication, as the simultaneous processes need data and information exchange. BIM model and BCA works will collect the building condition data for the facility management team to plan and execute maintenance works. The data collected will be used to determine the maintenance levels; whether it needs preventive maintenance, repair, or facility upgrade. Thus, the objective is clearly to provide accurate data for a good facility management practice throughout the lifecycle of buildings.

The BIM team will develop the BIM model for physical buildings that include LOD100, LOD200, and LOD500 drawings. LOD 300 and LOD 400 are not required in the building condition assessment process because these LODs are more likely to be used for construction drawings for tendering and scheduling for monitoring purposes during construction. LOD 100 is a 2D drawing that shows every single space and building components. Meanwhile, LOD 200 contains all parametric information about defects. LOD 500 is an as-built model that shows the actual physical building. The model will be used by the building surveyor during the BCA processes.

Three main activities in the BCA process include verification of floor plan, verification of space name, and building inspection. In traditional BCA, the surveyor will start with the building inspection without the first two processes. In BIM-integrated BCA, the surveyor must verify the building model produced by the BIM team. The verification process is composed of the floor plan and space name verification. The surveyor needs to survey the actual physical building to verify the model to ensure that the model conforms to the existing building specification.

Floor plan verification is composed of space configuration and construction details. The critical part in floor plan verification is to verify construction details such as finishes and sizing; physical visual appearance; structural details; mechanical, electrical and plumbing;

and fittings. Then, the surveyor must verify the name for every space by creating a coding system. The coding system must be systematic by providing building level and room number. For example, code L01-R02 can be used for Level 1 and Room number 2. All information in the first two activities should be updated into the BIM model. After that, the building condition assessment process continues with building inspection works, which will be conducted in accordance with the model that is developed and verified. The surveyor will key-in defect data directly into the model, no longer using paper as in the traditional methods.

During the defect capturing and recording process, the critical part is to identify defect locations at least by a two-point coordination, which is composed of horizontal and vertical points. This coordination must be plotted exactly into the model to facilitate further action to be taken by the maintenance team (in detecting the exact location of the defect). Therefore, the surveyor must measure the height and width of the defect from the reference point. Defect ratings are also determined using a formulation system (Condition  $\times$  Priority). From this formulation, total-building ratings can be obtained (Che-Ani *et. al.*, 2011). All information about defects will be keyed-in directly into the model. The information on construction details is for preventive maintenance, while building condition assessment data are for repairing and upgrading works.

## **CONCLUSION**

The application of BIM in the construction industry leaves a great positive effect in developing this sector. The most significant effect of BIM is providing a “bridge” between the virtual model and physical building. This “bridge” facilitates the accurate information transfer between both platforms. Accurate information is very important for related works during a building lifecycle from the start of the construction phase up to the building demolition phase. In addition, this information is critically needed during the longest building life cycle, which is the occupation phase. During the occupation phase, maintenance work needs to be conducted based on the information provided. Accurate information can be provided only by performing the building condition assessment.

The traditional building condition assessment method has often been faced with the problem of a lack of building information because it can only be conducted based on 2D drawings. The hidden details of building components were often unavailable, and previous maintenance history could not be easily retrieved. Therefore, the BIM-integrated building condition assessment is the answer to this problem. BIM model provides all the required information needed to perform a comprehensive building condition assessment. The information is available in the model and can be assessed by simply clicking the related part. However, most completed buildings in Malaysia were not built on BIM models as the technology was just introduced about 10 years ago.

Therefore, this research designed a framework of BIM-integrated building condition assessment for existing buildings. The objective of this framework is to implement a good facility management composed of preventive maintenance, repair works, and upgrade works. To achieve this objective, a BIM model for existing buildings that synchronizes BCA work from two different teams must be developed. The BCA team will verify the model developed

by the BIM team. Then, data from BCA works will be directly recorded into the BIM model for further processes.

## ACKNOWLEDGEMENT

The authors would like to express their heartiest thanks to Universiti Kebangsaan Malaysia [Lestari Physical Development Research Group-LPhyD and Evolutionary and Sustainable Urban Living Research Group-EvoSUL] and Construction Industry Development Board (CIDB) Malaysia for supporting this research. Credit also goes to various organizations that assisted toward the success of this research.

## REFERENCES

- Akanmu, A., Anumba, C. & Messner, J. 2014. Critical review of approaches to integrating virtual models and the physical construction. *International Journal of Construction Management*. 14(4): 267-282. DOI:10.1080/15623599.2014.972021
- Arayici, Y., Khosrowshahi, F., Ponting, A.M., and Mihindu, S. 2009. Towards Implementation of Building Information Modelling in the Construction Industry. *Fifth International Conference on Construction in the 21st Century (CITC-V) "Collaboration and Integration in Engineering, Management and Technology" May 20-22, 2009, Istanbul, Turkey.*
- Azhar, S, Khalfan, M. and Maqsood, T. (2012) 'Building information modelling (BIM): now and beyond', *Australasian Journal of Construction Economics and Building*, **12** (4) 15-28.
- Becerik-Gerber, B., Jazizadeh, F., Li, N., and Calis, G. (2012). "Application Areas and Data Requirements for BIM-Enabled Facilities Management." *J. Constr. Eng. Manage.*, 138(3), 431–442. DOI: 10.1061/(ASCE)CO.1943-7862.0000433.
- Bedrick, J. 2008. Organizing the Development of a Building Information Model. American Institute of Architects. Available at: <http://www.aia.org/groups/aia/documents/pdf/aiab078868.pdf>
- Behringer, A. and Azhar, S. 2012. BIM for Construction Safety: A Case Study. *Journal of Building Information Modelling*. Fall 2102: 20-21.
- BIMForum. 2013. Level of Development Specification. Version: 2013. Available at: <http://www.bimforum.org/lod>. [Retrieved on 5 February 2015].
- Blass, J. 2015. Cloud Computing – A game changer for building engineers? *Building Engineer*. April 2015: 16-17.
- Bynum, P., Issa, R., and Olbina, S. (2013). "Building Information Modelling in Support of Sustainable Design and Construction." *J. Constr. Eng. Manage.*, 139(1), 24–34. DOI: 10.1061/(ASCE)CO.1943-7862.0000560.
- Che-Ani, A.I., Tazilan, A.S.M. & Kosman, K.A. 2011. The development of a condition survey protocol matrix. *Structural Survey*. 29(1): 35-45.
- Cao, D., Wang, G., Li, H., Skitmore, M., Huang, T., and Zhang, W. 2015. Practices and effectiveness of building information modelling in construction projects in China. *Automation in Construction*. 49(A): 113-122. DOI: doi:10.1016/j.autcon.2014.10.014.
- Chandrasekaran, B., Josephson, J.R. and Benjamin, V.R. (1999). What are ontologies, and why do we need them? *Intelligent Systems and Their Applications, IEEE*. 14(1): 20-4.
- Chen, L. and Luo, H. 2014. A BIM-based construction quality management model and its applications. *Automation in Construction*. 46: 64-73. DOI: doi:10.1016/j.

autcon.2014.05.009.

- Chhibber, A. and Batra, S. 2103. Security Analysis of Cloud Computing. *International Journal of Advanced Research in Engineering and Applied Sciences*. 2(3): 49-53.
- Construction Research Institute of Malaysia (CREAM). 2014. *Issue and Challenge in Implementing BIM for SME's in The Construction Industry*. Kuala Lumpur: Construction Research Institute of Malaysia.
- Dawood, I. and Underwood, J. 2010. Research Methodology Explained. PM-05 International Project Management Conference; Advancing Project Management for the 21st Century Concepts, Tools & Techniques for Managing Successful Projects, Heraklion, Crete, Greece, May 29-31, 2010.
- Foster, B. 2012. Using Real-Time CMMS Asset Data Capture during Construction to Improve Facility Management. *Journal of Building Information Modelling*. Fall 2012: 16-17.
- Francom, T. and El Asmar, M. (2014) Principal Component Analysis to Investigate the Effect of BIM Use on AEC Project Changes. *Computing in Civil and Building Engineering* (2014): pp. 159-166. DOI: 10.1061/9780784413616.021
- Golparvar-Fard M, Pena-Mora F, Savarese S. 2009. Application of D4AR \_ A 4-Dimensional augmented reality model for automating construction progress monitoring data collection, processing and communication. *J Inform Technol Constr (ITcon)*, Special Issue Next Generation Construction IT: Technology Foresight, Future Studies, Roadmapping, and Scenario Planning. 14:129-153.
- Haron, A. T. (2013). *Organisational Readiness to Implement Building Information Modelling: A Framework for Design Consultants in Malaysia*. (Doctoral Dissertation, University of Salford Manchester, Salford)
- Ho, S.P., Tserng, H.P and Jan, S.H. 2013. Enhancing Knowledge Sharing Management Using BIM Technology in Construction. *The Scientific World Journal*. 2013: 1-10. DOI: 10.1155/2013/170498.
- Hore, A.V, McAuley, B, West, R. And Rowland, D. (2013) Creating Interactive Facilities Management capabilities through Building Information Modelling as a tool for managing the Irish Public Sector Estates, Proceedings of the CITA BIM Gathering, Dublin, Ireland, 14th – 15th November, pp 17-24.
- Jiao, Y., Wang, Y., Zhang, S., Li, Y., Yang, B. and Yuan, L. 2013. “A cloud approach to unified lifecycle data management in architecture, engineering, construction and facilities management: integrating BIMs and SNS,” *Advanced Engineering Informatics*, vol. 27, no. 2, pp. 173–188, 2013. doi:10.1016/j.aei.2012.11.006.
- Kacprzyk, Z. and Kepa, T. 2014. Building Information Modelling – 4D Modelling Technology on the Example of the Reconstruction Stairwell. *Procedia Engineering* 91 (2014) 226 – 231. doi: 10.1016/j.proeng.2014.12.051.
- Kasim, T., Li, H.J. and Rezgui, Y. 2012. BREEAM: Based Dynamic Sustainable Building Design Assessment. Presented at: *EG-ICE 2012*, Munich, Germany, 4- 6 July 2012.
- Khosrowshahi, F. and Arayici, Y. 2012. Roadmap for implementation of BIM in the UK construction industry. *Engineering, Construction and Architectural Management*. 19(6): 610-635.
- Klien, L., Li, N. and Becerik-Gerber, B. 2012. Imaged-based verification of as-built documentation of operational buildings. *Automation in Construction*. 21: 161–171. DOI: 10.1016/j.autcon.2011.05.023
- Kong, C.W.S. & Li, H. 2009. A qualitative evaluation of implementing virtual prototyping in

- construction. 2009 Second International Conference in Visualization; 15\_17 July 2009, Barcelona, Spain. p. 121-126.
- Lawson, D. 2004. Reorienting economics: on heterodox economics, themata and the uses of mathematics in economics. *Journal of Economic Methodology*. 11(3): 329-340.
- Lin, Y.C. and Su, Y.C. 2013. Developing Mobile- and BIM-Based Integrated Visual Facility Maintenance Management System. *The Scientific World Journal*. 2013: 1-10. DOI: 10.1155/2013/124249
- Mohd Faizal Omar, Ahmad Taufik Nursal, Mohd Nasrun Mohd Nawawi, Ahmad Tarmizi Haron. 2014a. A Preliminary Requirement of Decision Support System for Building Information Modelling Software Selection. *Malaysian Construction Research Journal*. 15(2): 11-28.
- Mohd Faizal Omar, Mohd Nasrun Mohd Nawawi and Ahmad Taufik Nursal. 2014b. Towards the Significance of Decision Aid in Building Information Modelling (BIM) Software Selection Process. *E3S Web of Conferences* 3, 01023 (2014). DOI:10.1051/e3sconf/20140301023
- Mohd Harris Ismail. 2014. Building Information Modelling: A Paradigm Shift in Malaysian Construction Industry. *binATECH*. Issue 2: 34-37.
- Mohd Harris, Adi Irfan Che Ani, Ahmad Tarmizi Haron, and Afifudin Husairi Husain. 2014a. The Way Forward for Building Information Modelling (BIM) for Contractors in Malaysia. *Malaysian Construction Research Journal*. 15(2): 1-9.
- Mohd Harris, Adi Irfan Che Ani, Ahmad Tarmizi Haron, Christopher Preece, and Afifudin Husairi Husain. 2014b. Prioritizing Building Information Modelling (BIM) Initiatives for Malaysia Construction Industry. XXV FIG Congress: Engaging the Challenge, Enhancing the Relevance. 16-21 June 2014. Kuala Lumpur, Malaysia.
- Mohd Nasrun Mohd Nawawi, Ahmad Tarmizi Haron, Zuhairi Abd Hamid, Kamarul Anuar Mohamad Kamar and Yusnizam Baharuddin. 2014. Improving Integrated Practice Through Building Information Modelling-Integrated Project Delivery (BIM-IPD) for Malaysian Industrialised Building System (IBS) Construction Projects. *Malaysian Construction Research Journal*. 15(2): 29-38.
- Navon R. and Sacks R. (2007). Assessing research in automated project performance control (APPC)", *Journal of Automation in Construction*, Vol. 16, No. 4, 474-484.
- Nguyen, T.H. and Kim, J.L. 2011. Building Code Compliance Checking Using BIM Technology. *Proceedings of the 2011 Winter Simulation Conference*: 3400-3405.
- Qi, J., Issa, R., Olbina, S., and Hinze, J. (2014). "Use of Building Information Modelling in Design to Prevent Construction Worker Falls." *Journal of Computing in Civil Engineering*. 28, SPECIAL ISSUE: 2012 International Conference on Computing in Civil Engineering, A4014008. DOI: 10.1061/(ASCE)CP.1943-5487.0000365
- Rohena, R., (2011). *BIM Implementation in Naval Construction*. Master Thesis, Louisiana State University. [Available at: [http://etd.lsu.edu/docs/available/etd-06242011-024451/unrestricted/rohena\\_thesis.pdf](http://etd.lsu.edu/docs/available/etd-06242011-024451/unrestricted/rohena_thesis.pdf)]
- Ruiz, J. M. 2009. *BIM software evaluation model for general contractors*. Master thesis, University of Florida.
- Son, H., Lee, S. and Kim, C. 2015. What drives the adoption of building information modelling in design organizations? An empirical investigation of the antecedents affecting architects' behavioral intentions. *Automation in Construction*. 49 (A): 92-99.
- Su, Y.C., Lee, Y.C., Lin, Y.C. 2011. Enhancing Maintenance Management Using Building Information Modelling in Facilities Management. In: *Proceedings of the 28th International Symposium on Automation and Robotics in Construction (2011)*
- Suermann, P. C. (2009). "Evaluating the impact of building information modelling (BIM) on

- construction.” Ph.D. dissertation, Univ. of Florida, Gainesville, FL.
- Wang, Y., Wang, X., Wang, J., Yung, P. and Jun, G. 2013. “Engagement of Facilities Management in Design Stage through BIM: Framework and a Case Study,” *Advances in Civil Engineering*, vol. 2013, Article ID 189105, 8 pages, 2013. doi:10.1155/2013/189105
- Yen, C.I., Chen, J.H., Huang, P.F. 2011. The Study of BIM-Based MRT Structural Inspection System. 2011 Proceedings of the 28th ISARC, Seoul, Korea. Pages 130-135
- Zhang, S., Teizer, J., Lee, J.K., Eastman, C.M., and Venugopal, M. 2013. Building Information Modelling (BIM) and Safety: Automatic Safety Checking of Construction Models and Schedules. *Automation in Construction*. 29: 183-195. DOI: 10.1016/j.autcon.2012.05.006
- Zhang, S., Sulankivi, K., Kiviniemi, M., Romo, I., Eastman, C.M., and Teizer, J. 2015. BIM-based fall hazard identification and prevention in construction safety planning. *Safety Science*. 72: 31-45. DOI: 10.1016/j.ssci.2014.08.001



# GUIDE TO AUTHORS

## Aims and Scope:

The Malaysian Construction Research Journal (MCRJ) is the journal dedicated to the documentation of R&D achievements and technological development relevant to the construction industry within Malaysia and elsewhere in the world. It is a collation of research papers and other academic publications produced by researchers, practitioners, industrialists, academicians, and all those involved in the construction industry. The papers cover a wide spectrum encompassing building technology, materials science, information technology, environment, quality, economics and many relevant disciplines that can contribute to the enhancement of knowledge in the construction field. The MCRJ aspire to become the premier communication media amongst knowledge professionals in the construction industry and shall hopefully, breach the knowledge gap currently prevalent between and amongst the knowledge producers and the construction practitioners.

Articles submitted will be reviewed and accepted on the understanding that they have not been published elsewhere. The authors have to fill the Declaration of the Authors form and return the form via fax to the secretariat. The length of articles should be between 3,500 and 8,000 words or approximately 8 – 15 printed pages (final version). The manuscripts should be written in English. The original manuscript should be typed one sided, single-spacing, single column with font of 11 point (Times New Roman). Paper size should be of Executive (18.42 cm x 26.67 cm) with 2 cm margins on the left, right and bottom and 3 cm for the top. Authors can submit the manuscript:

- By e-mail to [maria@cidb.gov.my](mailto:maria@cidb.gov.my) / [hazim@cidb.gov.my](mailto:hazim@cidb.gov.my) / [foo@cidb.gov.my](mailto:foo@cidb.gov.my)
- By hardcopy and softcopy in Microsoft-Word format to MCRJ Secretariat:

### **Malaysian Construction Research Journal (MCRJ)**

Construction Research Institute of Malaysia (CREAM)

MAKMAL KERJA RAYA MALAYSIA

1<sup>st</sup> Floor, Block E, Lot 8,

Jalan Chan Sow Lin, 55200 Kuala Lumpur

MALAYSIA

Tel. : (6)03 – 9281 0800

Fax : (6)03 – 9282 4800

Website : [www.cream.my](http://www.cream.my)

**Type of fonts:** All text, drawing, graph must be written using Times New Roman

**Language:** Follow the spelling of the Oxford English Dictionary.

**Size/Page Setup:** Executive (18.42 cm x 26.67 cm)

**Paper title:** Arial, 16.

## CODIFICATION AND APPLICATION OF SEMI-LOOF ELEMENTS FOR COMPLEX STRUCTURES

**Author's name** (full name): Arial, 9pt. should follow below the title.

**Jamalodin Noorzaei<sup>1</sup>, Mohd. Saleh Jaafar, Abdul Waleed Thanoon, Wong Jern Nee**

**Affiliation** (including post codes): Arial, 9pt. Use numbers to indicate affiliations.

*<sup>1</sup>Department of Civil Engineering, Faculty of Engineering, Universiti Putra Malaysia, 43400 UPM, Serdang, Selangor, Malaysia*

**Abstract:** Arial Bold, 9pt. Left and right indent 0.64 cm.

**Abstract:** it should be single paragraph of about 100 – 250 words.

**Keywords:** Times New Roman Bold, 9pt (Italic). Left and right indent 0.64 cm.

**Keywords:** *Cooling tower; Finite element code; Folded plate; Semiloof shell; Semiloof beam*

Body Text: Times New Roman, 11 pt. All paragraph must be differentiate by 0.64 cm tab.

Heading 1: Arial Bold + Upper Case, 11pt.

Heading 2: Arial Bold + Lower Case, 11pt.

Heading 3: Arial Italic + Lower Case, 11pt.

**Units:** All units and abbreviations of dimensions should conform to SI standards.

**Figures:** Figures should be in box with line width 0.5pt. All illustrations and photographs must be numbered consecutively as it appears in the text and accompanied with appropriate captions below them.

**Figures caption:** Arial Bold + Arial, 9pt. should be written below the figures.

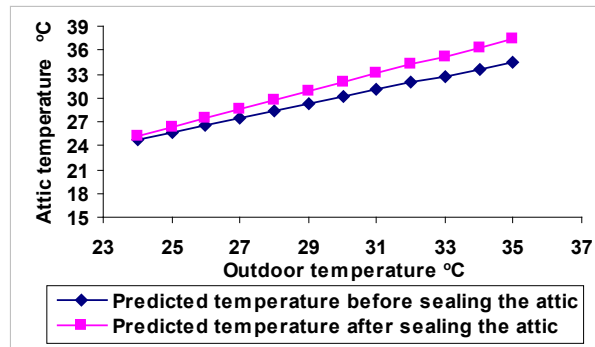


**Figure 8.** Computed attic temperature with sealed and ventilated attic

**Tables:** Arial, 8pt. Table should be incorporated in the text.

**Table caption:** Arial Bold + Arial, 9pt. Caption should be written above the table.

**Table Line:** 0.5pt.

**Table 1.** Recommended/Acceptable Physical water quality criteria

Parameter	Raw Water Quality	Drinking Water Quality
Total coliform (MPN/100ml)	500	0
Turbidity (NTU)	1000	5
Turbidity (NTU)	300	15
pH	5.5-9.0	6.5-9.0

(Source: Twort et al. 1985; MWA,1994)

**Reference:** Times New Roman, 11pt. Left indent 0.64 cm, first line left indent – 0.64 cm. Reference should be cited in the text as follows: “Berdahl and Bretz (1997) found...” or “(Bower et al. 1998)”. References should be listed in alphabetical order, on separate sheets from the text. In the list of References, the titles of periodicals should be given in full, while for books should state the title, place of publication, name of publisher, and indication of edition.

**Journal**

Sze, K. Y. (1994) Simple Semi-Loof Element for Analysing Folded-Plate Structures. *Journal of Engineering Mechanics*, 120(1):120-134.

**Books**

Skumatz, L. A. (1993) Variable Rate for Municipal Solid Waste: Implementation, Experience, Economics and Legislation. Los Angeles: Reason Foundation, 157 pp.

**Thesis**

Wong, A. H. H. (1993) *Susceptibility To Soft Rot Decay In Copper-Chrome-Arsenic Treated and Untreated Malaysian Hardwoods*. Ph.D. Thesis, University of Oxford. 341 pp.

**Chapter in book**

Johan, R. (1999) Fire Management Plan For The Peat Swamp Forest Reserve Of North Selangor and Pahang. In Chin T.Y. and Havmoller, P. (eds) *Sustainable Management of Peat Swamp Forests in Peninsular Malaysia* Vol II: Impacts. Kuala Lumpur: Forestry Department Malaysia, 81-147.

**Proceedings**

Siti Hawa, H., Yong, C. B. and Wan Hamidon W. B. (2004) Butt Joint In Dry Board As Crack Arrester. *Proceeding of 22<sup>nd</sup> Conference of ASEAN Federation of Engineering Organisation (CAFEO 22)*. Myanmar, 55-64.



## Contents

Editorial Advisory Board

Editorial

ANALYSIS OF ROCK BURST EVENT IN DEEP TBM EXCAVATION OF PAHANG-SELANGOR RAW WATER TRANSFER TUNNEL  
Romziah Azit and Mohd Ashraf Mohamad Ismail

PRE-CRACKED RC CONTINUOUS BEAMS STRENGTHENED IN SHEAR USING CFRP STRIPS ORIENTED AT 45°/135°  
Noorwirdawati Ali, Abdul Aziz Abdul Samad, J. Jayaprakash, Noridah Mohamad and Shahiron Shahidan

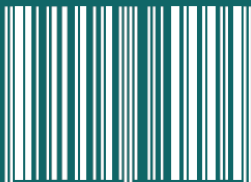
PERFORMANCE OF INNOVATIVE CELLULAR MAT (NEW LIGHTWEIGHT MATERIAL) USING MINI TRIAL EMBANKMENT  
Reventheran Ganasan, Alvin John Lim Meng Siang and Devapriya Chitral Wijeyesekera

EXPERIMENT AND COMPUTATIONAL FLUID DYNAMICS (CFD) SIMULATION OF FLOW CHARACTERISTICS IN DISSOLVED AIR FLOTATION TANK  
Nor Azalina Rosli, Mohamad Fared Murshed and Mohd Nordin Adlan

THE ADOPTION OF PASSIVE COOLING STRATEGY IN DESIGNING PUBLIC ASSEMBLY BUILDING – A DESIGN TYPOLOGY FOR THE TAOIST ACADEMIC CENTRE IN TROPICAL CLIMATE  
Loo Kok Hoo, Benson Lau and Foo Chee Hung

A REVIEW OF BUILDING INFORMATION MODELING (BIM)-BASED BUILDING CONDITION ASSESSMENT CONCEPT  
Adi Irfan Che-Ani, Mohd Harris, Muhammad Farihan Irfan Mohd-Nor, Mohd Zulhanif Abd-Razak and Afifuddin Husairi Hussain

ISSN 1985-3807



9 771985 380005